

INFORMATION TO USERS

This manuscript has been reproduced from the microfilm master. UMI films the text directly from the original or copy submitted. Thus, some thesis and dissertation copies are in typewriter face, while others may be from any type of computer printer.

The quality of this reproduction is dependent upon the quality of the copy submitted. Broken or indistinct print, colored or poor quality illustrations and photographs, print bleedthrough, substandard margins, and improper alignment can adversely affect reproduction.

In the unlikely event that the author did not send UMI a complete manuscript and there are missing pages, these will be noted. Also, if unauthorized copyright material had to be removed, a note will indicate the deletion.

Oversize materials (e.g., maps, drawings, charts) are reproduced by sectioning the original, beginning at the upper left-hand corner and continuing from left to right in equal sections with small overlaps.

Photographs included in the original manuscript have been reproduced xerographically in this copy. Higher quality 6" x 9" black and white photographic prints are available for any photographs or illustrations appearing in this copy for an additional charge. Contact UMI directly to order.

**ProQuest Information and Learning
300 North Zeeb Road, Ann Arbor, MI 48106-1346 USA
800-521-0600**

UMI[®]

NOTE TO USERS

This reproduction is the best copy available.

UMI



Diagenesis of Jauf Sandstone in Hawiyah Area

BY

Khalid Abdulsamad Al-Ramadan

A Thesis Presented to the
DEANSHIP OF GRADUATE STUDIES

KING FAHD UNIVERSITY OF PETROLEUM & MINERALS

DHAHRAN, SAUDI ARABIA

In Partial Fulfillment of the
Requirements for the Degree of

MASTER OF SCIENCE

In

GEOLOGY

DECEMBER 2001

UMI Number: 1409807

UMI[®]

UMI Microform 1409807

Copyright 2002 by ProQuest Information and Learning Company.
All rights reserved. This microform edition is protected against
unauthorized copying under Title 17, United States Code.

ProQuest Information and Learning Company
300 North Zeeb Road
P.O. Box 1346
Ann Arbor, MI 48106-1346

**KING FAHD UNIVERSITY OF PETROLEUM & MINERALS
DHAHRAN, SAUDI ARABIA**

DEANSHIP OF GRADUATE STUDIES

This thesis, written by **Khalid Abdulsamad Al-Ramadan** under the direction of his Thesis advisor and approved by his thesis committee, has been presented to and accepted by the Dean of Graduate Studies, in partial fulfillment of the requirements for the degree of **MASTER OF SCIENCE IN GEOLOGY**.

Thesis Committee



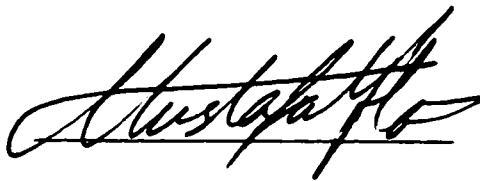
Chairman (Dr. Badrul Imam)



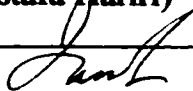
Co-Chairman (Dr. Mahbub Hussain)



Member (Dr. Salih Saner)



Department Chairman
(Dr. Mustafa Hariri)



Dean of Graduate Studies
(Dr. Osama A. Jannadi)

8/12/2001

Date



Dedication

This Thesis is dedicated to the one true love of my life, my wife. Her love, extraordinary support and encouragement have enabled me to accomplish this work. I am equally indebted my family in Saihat for their continuous help during my studies.

ACKNOWLEDGMENTS

Acknowledgments are due to King Fahd University of Petroleum and Minerals for support of this research. I would like to express my sincere gratitude to my committee Chairman, Dr. Badrul Imam, for his patience and guidance during the course of this research work. His good nature and understanding were appreciated more than I can express. I would like to thank my other committee members, Dr. Mahbub Hussain and Dr. Salih Saner for their constructive criticism and valuable insight.

Appreciation and special thanks are due to Chairman Dr. Mustafa Hariri and other faculty and colleagues of the Earth Sciences Department for their support during my graduate studies. Thanks also expressed to Mr. Aziz Ullah Khan, Mr. Abdul-Rashid Issak and Mr. Saeed Al-Jaroodi for their assisting me with thin section, SEM and XRD, respectively.

I am also grateful to the Research Institute for providing the data. Special thanks to Mr. Hassan M. Hassan for his assistance in porosity measurements. Great thanks are also due to Mr. Fadhel Al-Khalifah and Mr. Mushabab Assiri for their aid in printing this work.

Finally, my deep personal appreciation is expressed for my wife, parents and family for their love and concern.

TABLE OF CONTENTS

Acknowledgments	iv
List of Tables	vii
List of Figures	viii
Abstract (English)	xiii
Abstract (Arabic)	xiv
CHAPTER 1: INTRODUCTION	1
1.1. Introductory Statement	1
1.2. Objective and Scope	3
1.3. Samples and Methods	4
CHAPTER 2: STRATIGRAPHY AND SEDIMENTOLOGY OF JAUF FORMATION	12
2.1. Jauf Formation in the Surface	14
2.2. Jauf Formation in the Subsurface	18
2.2.1. Jauf Formation in Hawiyah Area	22
2.2.2. Jauf Formation in Shedgum Area	29
CHAPTER 3: PETROGRAPHY OF THE JAUF FORMATION	30
3.1. Petrographic Characteristics of Subsurface Core Samples	34
3.1.1. Texture	34
3.1.2. Composition and Classification	34
3.1.2.1. The Detrital Components	35
3.1.2.2. Authigenic Component-Cement	44
3.2. Petrographic Characteristics of Surface Samples	62
CHAPTER 4: DIAGENESIS OF JAUF FORMATION	67
4.1. Introduction	67
4.2. Diagenesis in Jauf Sandstone	68
4.2.1. Compaction	69
4.2.2. Cementation	73
4.2.2.1. Early Calcite Cementation	73
4.2.2.2. Pyrite Cementation	75
4.2.2.3. Clay Cementation	75

4.2.2.4. Quartz Cementation	76
4.2.2.5. Late Calcite Cementation	78
4.3. Alteration and Replacement	79
4.4. Dissolution and Secondary Porosity	79
4.4.1. Origin of Secondary Porosity	91
4.4.2. Importance of Secondary Porosity	93
CHAPTER 5: DISCUSSION AND CONCLUSIONS	94
REFERENCES	104

LIST OF TABLES

Table	Page
Table 1: A detail description of cores from Well B	24
Table 2: Percentages of rock components including porosity for Well A	31
Table 3: Percentages of rock components including porosity for Well B	32
Table 4: Percentages of rock components including porosity for field samples	32
Table 5: A comparison of the textural attributes of the surface and subsurface samples	66

LIST OF FIGURES

<u>Figure</u>	<u>Page</u>
Figure 1-1: Base Map showing the location of the studied wells	5
Figure 1-2: Locations of samples in Well A	6
Figure 1-3: Locations of samples in Well B	7
Figure 1-4: Geographic map showing the location of Jawf Area (Bottom) and the geographic location of the three studied outcrops as shown by black triangles (Top)	8
Figure 1-5: The stratigraphic columns showing the lithology and the distribution of the field samples	9
Figure 2-1: Geologic location of the field area map	13
Figure 2-2: Paleozoic outcrop map of Saudi Arabia showing the location of the regional Devonian formations	16
Figure 2-3: Generalized stratigraphic succession of the Jauf Formation in the Al-Jawf region	17
Figure 2-4: Regional Devonian cross-section of B-B' referring to Figure 8	19
Figure 2-5: Structure map of the Ghawar Area that is composed of a series of horst and tilted fault blocks arranged in a general north-south direction	20
Figure 2-6: E-W cross-section of the Ghawar area showing the Devonian formations, referring to Figure 2-5	21
Figure 2-7: Core #1 is dark gray, indistinct cross bedding, depth 14035.9 ft	26
Figure 2-8: Core #2 is dark gray, distinct cross lamination by dark colored, depth 14041.8 ft	26
Figure 2-9: Core #3 is dark gray, massive sandstone with small white specks, depth 14122.6 ft	26
Figure 2-10: Core #4 is gray, friable, massive sandstone with white specks, depth 14132 ft	26
Figure 2-11: Core #5 Light gray, hard and compacted, distinct parallel cross laminations with white specks, depth 14137.1 ft	27

Figure 2-12: Core #6 is Light gray, parallel cross laminations with white specks, depth 14143.9 ft	27
Figure 2-13: Core #7 is White, massive sandstone, depth 14263.4 ft	27
Figure 2-14: Core #8 is Gray, white cross-bedded, thin white lamina and thin beds alternates with gray sand, depth 14289 ft	27
Figure 2-15: Core #9 is Light gray, distinct cross lamination in the upper part and massive in the middle, depth 14312.4 ft	28
Figure 2-16: Core #10 is Light gray, distinct parallel laminations of alternating light and dark lamina, depth 14317 ft	28
Figure 2-17: Core #11 is Light gray, parallel laminations alternating light and dark bands, depth 14323.6ft	28
Figure 2-18: Core #12 is Gray, parallel lamination, depth 14345.7 ft	28
Figure 3-1: Ternary diagram model used for the studied samples	36
Figure 3-2: Ternary diagrams for sandstone samples of matrix less than 15 % (above) and greater than 15 % (below)	37
Figure 3-3: Plagioclase feldspar showing lamellar twinning, Sample # 384, Well A, depth 14384 feet	39
Figure 3-4: K-Feldspar showing crosshatched twining (microcline) and untwined nature, Sample # 361, Well A, depth 14361 feet	39
Figure 3-5: Chert grain showing extremely dense fine grain size, Sample # 6, Well B, depth 14143.9 feet	40
Figure 3-6: Plastic deformation of biotite and shale clast, Sample # 361, Well A, depth 14361 feet	40
Figure 3-7: Muscovite grains, Sample # 459, Well A, depth 14459 feet	42
Figure 3-8: Zircon grain showing very high (third- or fourth-order) interference colors, Sample # 377, Well A, depth 14377 feet	42
Figure 3-9: Organic matter lamina, Sample # 330, Well A, depth 14330 feet	43
Figure 3-10: Carbonaceous materials coating around the grains, Sample # 9, Well B, depth 14 312.4 feet	43

Figure 3-11: High matrix content of 30%, Sample # 361, Well A, depth 14361 feet	45
Figure 3-12: Pervasive poikilotopic calcite cement, Sample # 373.6, Well A, depth 14373.6 feet	47
Figure 3-13: Pervasive poikilotopic calcite cement, Sample # 380, Well A, depth 14380 feet	47
Figure 3-14: Isolated pore filling late calcite cement, Sample # 3, Well B, depth 14122.6 feet	48
Figure 3-15: Replacement of silicate grains is evidenced by the occurrence of remnant within calcite cement. Sample # 3, Well B, depth 14122.6 feet	48
Figure 3-16: Isolated pore filling late calcite cement. Sample # 390.7, Well A, depth 14390.7 feet	49
Figure 3-17: Complete pore linings on the surfaces of grain-to-grain contact (right), partial pore lining (left)	52
Figure 3-18: Illite coating shoeing the bright white high birefringent line around grain surfaces, Sample # 354, Well A, depth 14354feet	52
Figure 3-19: Authigenic illite cement forming fibrous-like form. Sample #487. Well A, depth 14487feet	53
Figure 3-20: Illite occurs as pore bridging cement. Sample #4, Well B, depth 14132 feet	53
Figure 3-21: XRD profile for Sample # 538, Well A. depth 14538	54
Figure 3-22: Pore filling clay plug interstitial pores	54
Figure 3-23: Chlorite cement showing thin brown coating around grain surfaces, Sample #404, Well A, depth 14404 feet	55
Figure 3-24: Overall view of quartz grains coated by chlorite cement with quartz overgrowths in the left hand side of the micrograph, Sample #394, Well A, depth 14394feet	55
Figure 3-25: Closer view of the figure 47 showing the rosettes of chlorite pore filling, Sample #394, Well A, depth 14394feet	56
Figure 3-26: SEM photomicrograph showing authigenic illite /smectite, Sample # 511, well A, depth 14511 feet	58

Figure 3-27: Pyrite cement in Sample #323, Well A, depth 14323feet	58
Figure 3-28: Silica cement in the form of syntaxial quartz overgrowths (white arrows). Clay dust rims (blue arrows) separate cement from detrital grains, Sample # 487, Well A, depth 14487	60
Figure 3-29: well developed authigenic quartz crystal (Q) in region of abundant authigenic chlorite (Ch). Quartz crystals grew into areas of continuous chlorite coating until they were physically blocked, Sample #394, Well A, depth 14394 feet	60
Figure 3-30: An early stage of development of quartz overgrowth referred to as incipient growth, Sample # 4, Well B, depth 14132 feet	61
Figure 3-31: An advanced stage of development of quartz overgrowth referred to as terminated growth, Sample #519, Well A, depth 14519 feet	61
Figure 3-32: Siltstone with high matrix content, Sample # L2-5	63
Figure 3-33: Zircon grain in very fine sandstone, Sample # L1-7	63
Figure 3-34: Very fine-grained sandstone with high matrix content, Sample # L2-2	64
Figure 3-35: Calcite lamina in very fine grain sandstone, Sample # L1-5	64
Figure 3-36: Chlorite coating in fine grain sandstone, Sample # L1-7	65
Figure 4-1: Physical behavior of sediments during compaction	70
Figure 4-2: Point contact between quartz grains, Sample #365, Well A, depth 14365 feet, plane polarized light	70
Figure 4-3: Long contact between quartz grains, Sample #369.8, Well A, depth 14369.8 feet, plane polarized light	71
Figure 4-4: Concavo-convex type of contact, Sample # 373.6, Well A, depth 14373.6 feet, plane polarized light	71
Figure 4-5: Suture contact between two quartz grains, Sample # 6, Well B, depth 14143.9 feet, cross polarized light	72
Figure 4-6: The paragenetic sequence of different types of cement present in the studied sandstones	74
Figure 4-7: Partial dissolution of feldspar grains, Sample #365, Well A, depth 14365,plane polarized light	80

Figure 4-8: Another partial dissolution of feldspar grains, Sample #365, Well A, depth 14365, plane polarized light	80
Figure 4-9: Criteria used for recognition of secondary porosity in the studied samples	82
Figure 4-10: Honeycomb grain, Sample # 394, Well A, depth 14394 feet, plane polarized light	84
Figure 4-11: Close-up photo of the previous Figure, plane polarized light	84
Figure 4-12: Inhomogeneity of packing, Sample # 373.6, Well A, depth 14373.6 feet. plane polarized light	85
Figure 4-13: Oversized pores, Sample # 523, Well A, depth 14523 feet, plane polarized light	85
Figure 4-14: Partial dissolution of feldspar grains, Sample #380, Well A, depth 14380feet, cross polarized light	86
Figure 4-15: Elongate pore, Sample # 365, Well A, depth 14365 feet, plane polarized light	88
Figure 4-16: Corroded grain, Sample # 365, Well A, depth 14365 feet, plane polarized light	88
Figure 4-17: Photomicrograph showing secondary pores evidenced by skeletal grains, Sample # 330, Well A, depth 14330 feet, plane polarized light	90
Figure 5-1: Paragenetic sequence of diagenetic events in the Jauf sandstone	97

THESIS ABSTRACT

Name: Khalid Abdulsamad Al-Ramadan
Title: Diagenesis of Jauf Sandstone in Hawiyah Area
Major Field: Geology
Date: December 2001

Jauf Formation of Lower Devonian age is an important hydrocarbon reservoir in Saudi Arabia. The sandstone reservoirs of Jauf Formation are mostly fine to medium-grained, moderately to well-sorted and texturally mature quartz arenites. Average composition of the framework grains of the sandstone reservoirs of Jauf Formation is 77% quartz, 2 % feldspar and 0.1% rock fragments. Minor framework grains include carbonaceous materials, micas and heavy minerals. Major authigenic cements include calcite; chlorite, illite and quartz while minor amount of pyrite and illite/smectite clay are present.

The diagenetic processes include compaction, cementation and dissolution (secondary pore generation). The degree of compaction is evidenced by long, concavo-convex and sutured contacts. Compaction reduces pore space. Cementations include an early calcite cementation phase followed by clay coatings (chlorite and illite), quartz overgrowths cementation and late calcite cementation. In addition, some minor pyrite cementation has occurred in early stage of burial. Early-calcite cement is poikilotopic and has occupied most of the pore spaces in some samples reducing the primary porosity. Calcite is also present as isolated patches filling pore spaces as late calcite cement. Chlorite pore fillings and grain coatings have reduced both the porosity and permeability to some extent but also have helped to retain initial porosity at depths by retarding the development of quartz overgrowths. Illite cement is most commonly found as hair-like growth coating the grains and bridging pore throats. This reduces the permeability dramatically. Quartz overgrowths have reduced the porosity and permeability significantly. The late-calcite cement does not have a profound effect on the samples. The invasions of acidic fluids have resulted in partial dissolution of calcite cements and feldspar grains creating secondary porosity in many samples.

Master of Science Degree

King Fahd University of Petroleum and Minerals
Dhahran, Saudi Arabia

December 2001

ملخص الرسالة

الاسم	:	خالد عبد الصمد حسن آل رمضان
العنوان	:	النشأة المتأخرة لمكمن الحجر الرملي لمتكون الجوف في منطقة الحوية
التخصص	:	علم طبقات الأرض
التاريخ	:	ديسمبر ٢٠٠١

يعتبر متكون الجوف من العصر الديفوني الأدنى مكمناً مهماً بالنسبة للبتروكيمياوية في المملكة العربية السعودية. المكمن الرملي لمتكون الجوف يمتاز غالباً بأنه ناعم إلى وسطي الحبيبات، معتدل إلى حسن الفرز وهو من النوع الأريني الرملي الناضج النسيج. يتكون متوسط التركيب للحبيبات الهيكلية للمكمن الرملي من ٧٧% كوارتز، ٢% فلسبار و ٠,١% فتات صخري. تتضمن الحبيبات الهيكلية الثانوية من رواسب كربونية، ميكا ومعادن ثقيلة. تحتوي اللوامح، مكانية النشأة، الرنيسية على كلسيت، كلوريت، إليت وكوارتز بينما تظهر كمية بسيطة من البايريت وخليط من الإليت/سميكتيت الطيني.

العمليات المتأخرة النشأة تتضمن الرص، الإلتحام والإتحلال (تكون المسام الثانوية). توضح التماسات الطولية، المقعرة- المحدبة و المتشابكة بين الحبيبات درجة الرص مع زيادة عمق الدفن ويصحب عملية الرص إنخفاض تدريجي في المسامية. تحتوي عملية الإلتحام على طور لاحم الكلسيت المبكر متبوعه بغلاف الطبقة الخارجية الطينية (كلوريت وإليت)، لاحم السيلكا كنمو زائد ثانوي ولاحم الكلسيت المتأخر. بالإضافة إلى ما سبق، هناك بعض لوامح البايريت التي تشكلت في مرحلة مبكرة من عملية الدفن. يظهر لاحم الكلسيت المبكر بشكل بلورات كبيرة تحيط بحبيبات الرمل كلية ويعرف هذا بالنسيج المبرقش مالنا المسافات المسامية في بعض العينات مقللاً من المسامات الأولية. يوجد الكلسيت أيضاً كلاحم بقعي معزول مالنا المسافات المسامية كلاحم متأخر. الكلوريت المالى للمسامات والمغلف للحبيبات قلل من المسامية والنفاذية إلى حد ما ولكنه أيضاً ساعد على حفظ بعض المسامات الأولية بإعاقه عملية تكون النمو الزائد لللاحم السيلكا. يوجد لاحم الأليت في معظم الأحيان كنمو شعري مغلفاً بحبيبات الرمل وكجسراً بين خوائق المسام. لاحم الأليت ساهم في تقليل النفاذية بشكل كبير. النمو الزائد للسيلكا قلل المسامية والنفاذية بصورة كبيرة. أما بالنسبة لتأثير لاحم الكلسيت المتأخر على المسامية والنفاذية فإنه لم يكن له ذلك التأثير العميق على العينات. اكتساح السوائل الحمضية نتج عنه انحلال وذوبان جزئي للوامح الكلسيت وحبيبات الفلسبار مكوناً ما يعرف بالمسامية الثانوية في معظم العينات.

درجة الماجستير في العلوم
جامعة الملك فهد للبترول والمعادن
الظهران، المملكة العربية السعودية
ديسمبر ٢٠٠١

CHAPTER 1

INTRODUCTION

1.1. Introductory Statement

Diagenesis refers to the physical and chemical changes that occur within the rock after it is buried below the surface. Porosity has a major effect on petroleum in-place calculations for a prospect. Permeability had a major effect on the rate at which petroleum can be produced. Porosity can be enhanced or reduced by diagenetic processes, which determine the sandstone reservoir quality. Porosity can be modified by the mechanical compaction, intergranular pressure solution, cementation, framework grain dissolution and cement dissolution (Houseknecht, 1987). In fact, diagenesis of the reservoir rock is the most important control of the ultimate nature and performance of a reservoir and detailed studies of the petrography and diagenetic history of the reservoir rock is an essential part of a successful hydrocarbon exploitation program. Also, diagenesis is important from academic point of view as it deals with the processes that turn sediments into solid rocks (Parker and Sellwood, 1983).

The Jauf Formation is an important hydrocarbon reservoir in the northern part of the Ghawar field in the Shedgum area, eastern Saudi Arabia. The Jauf is also the reservoir for a giant gas condensate field in the Hawiyah area. Recent emphasis of the Kingdom to exploit its natural gas resources and also the recent increase in the oil prices has made Jauf a prime target for gas exploration. The success of exploitation of the Jauf gas and oil resources will depend to a large extent on the better understanding of the Jauf reservoir and its qualities especially the poro-perm properties and the factors that control such properties.

In spite of the economic importance and also the fact that extensive investigations have been carried out on different aspects of the Jauf Formation, only limited work has so far been done on the diagenetic history of this formation. The present thesis research aims at the study of diagenesis and its effect on the reservoir properties as revealed by various techniques applied on both subsurface core samples as well as surface outcrop materials.

1.2. Objective and Scope

This study focuses mainly on the processes of diagenesis in the Jauf Reservoir, and how these processes affect the reservoir porosity. It may be mentioned here that the main emphasis of the study is focused on the subsurface reservoir core samples because these are fresh and unweathered. However, to broaden the scope of the present study, outcrop samples from the field were also studied and compared with subsurface samples.

More specifically, the study aimed of achieving the following:

- Detail quantitative mineralogical analysis on core samples and outcrop samples by petrographic microscopy to determine the composition and to classify the reservoir rock types.
- Detail analyses of individual mineral cement phases using scanning electron microscopy (SEM) and to identify the effect of individual cement and matrix phases on reservoir porosity and permeability.
- Special emphasis has been given to clay minerals in the pores between grains of the samples that have been analyzed. Clay minerals were identified using x-ray diffraction techniques.
- Comment on the origin of the cements.
- Establish diagenetic model, and paragenetic sequence of diagenetic processes

1.3. Samples and Methods

A total of sixty-two (62) samples were collected from two wells (Well A¹ and Well B¹) in the Hawiyah field (Figure 1-1). Well A core samples are from depths of 14323 to 14538 feet while Well B core samples are from 14035 to 14345.7 feet (Figures 1-2 and 1-3).

Field samples were collected from Subbat El Wadi Member of the Jauf Formation exposed in the north of Dawmat Al-Jandal in Jawf area as shown in Figure 1-4. In this area, three outcrops (L1, L2 and L3) have been studied and sandstone samples have been collected. Based on the field data, stratigraphic columns were prepared to show the lithology and the distribution of the field samples (Figure 1-5).

¹. For the purpose of confidentiality, both wells are given letter symbols instead of the real names.

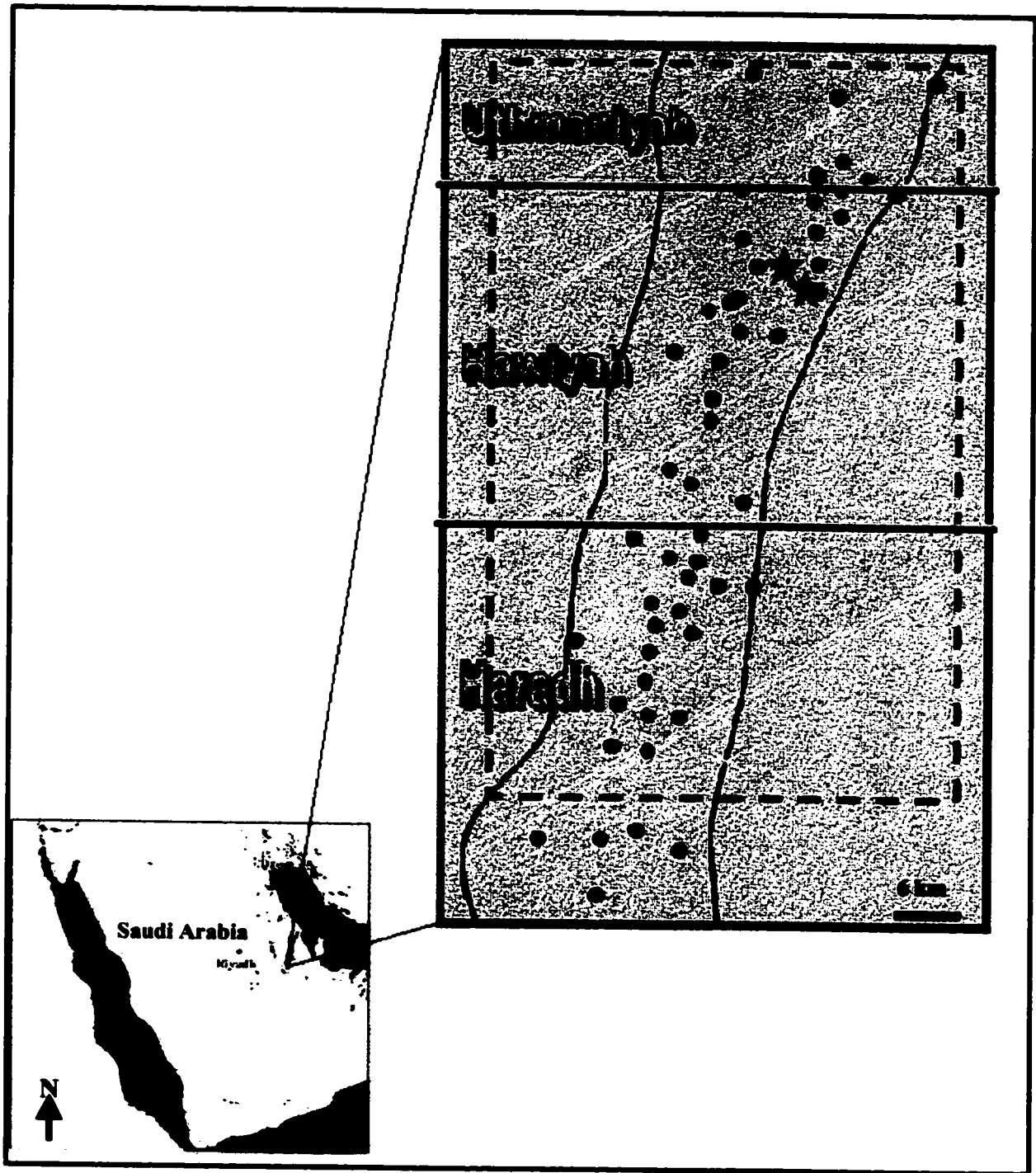


Figure 1-1: Base Map showing the location of the studied wells.

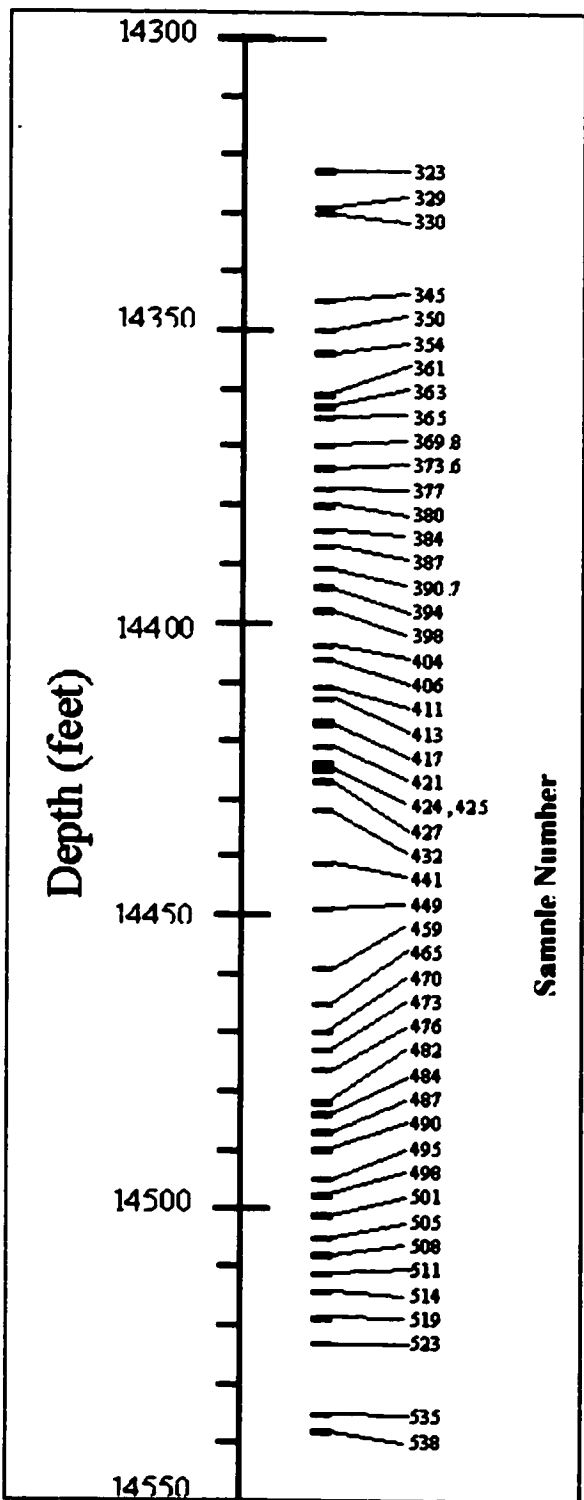


Figure 1-2: Locations of samples in Well A.

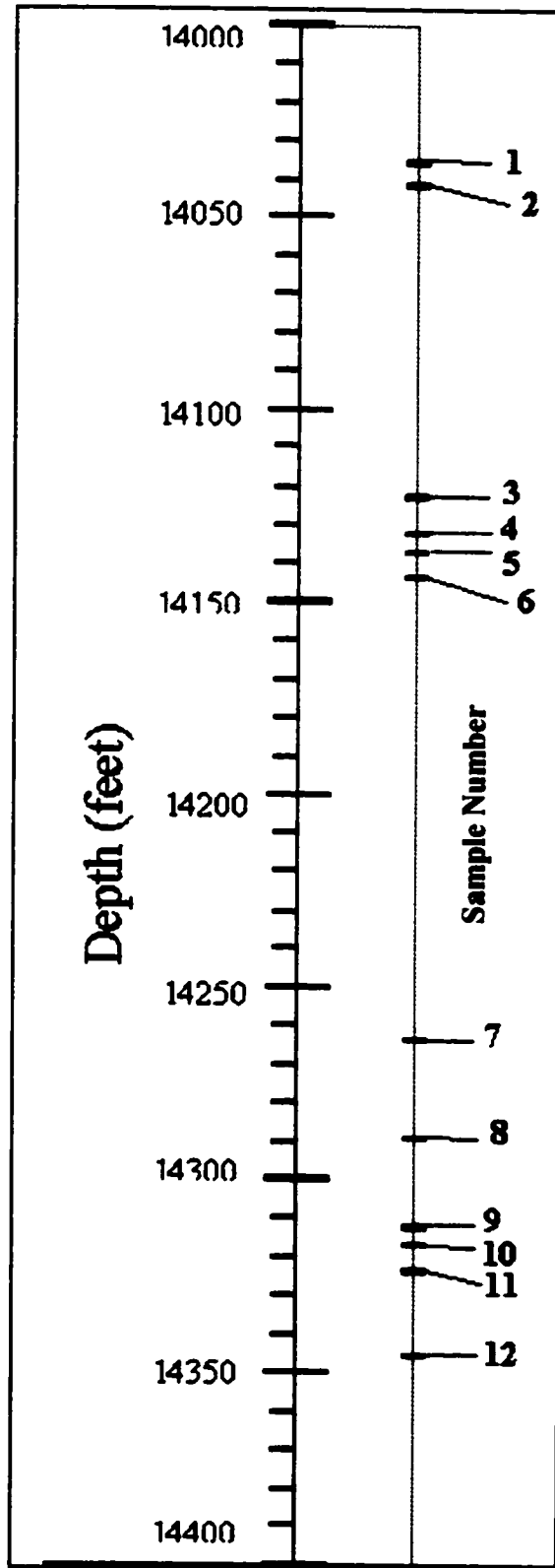


Figure 1-3: Locations of samples in Well B.

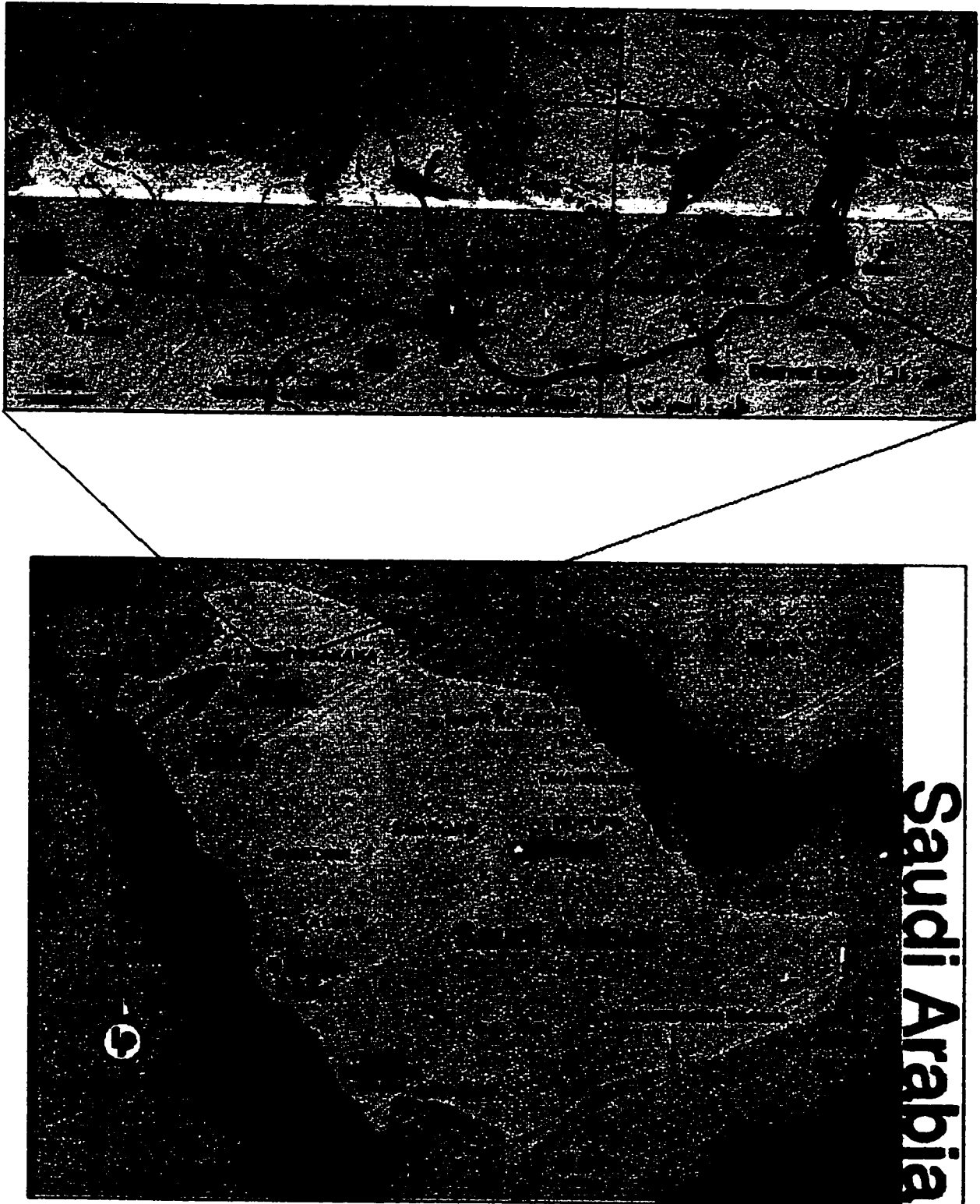


Figure 1-4: Geographic map showing the location of Jawf Area (Bottom) and the geographic location of the three studied outcrops as shown by black triangles (Top).

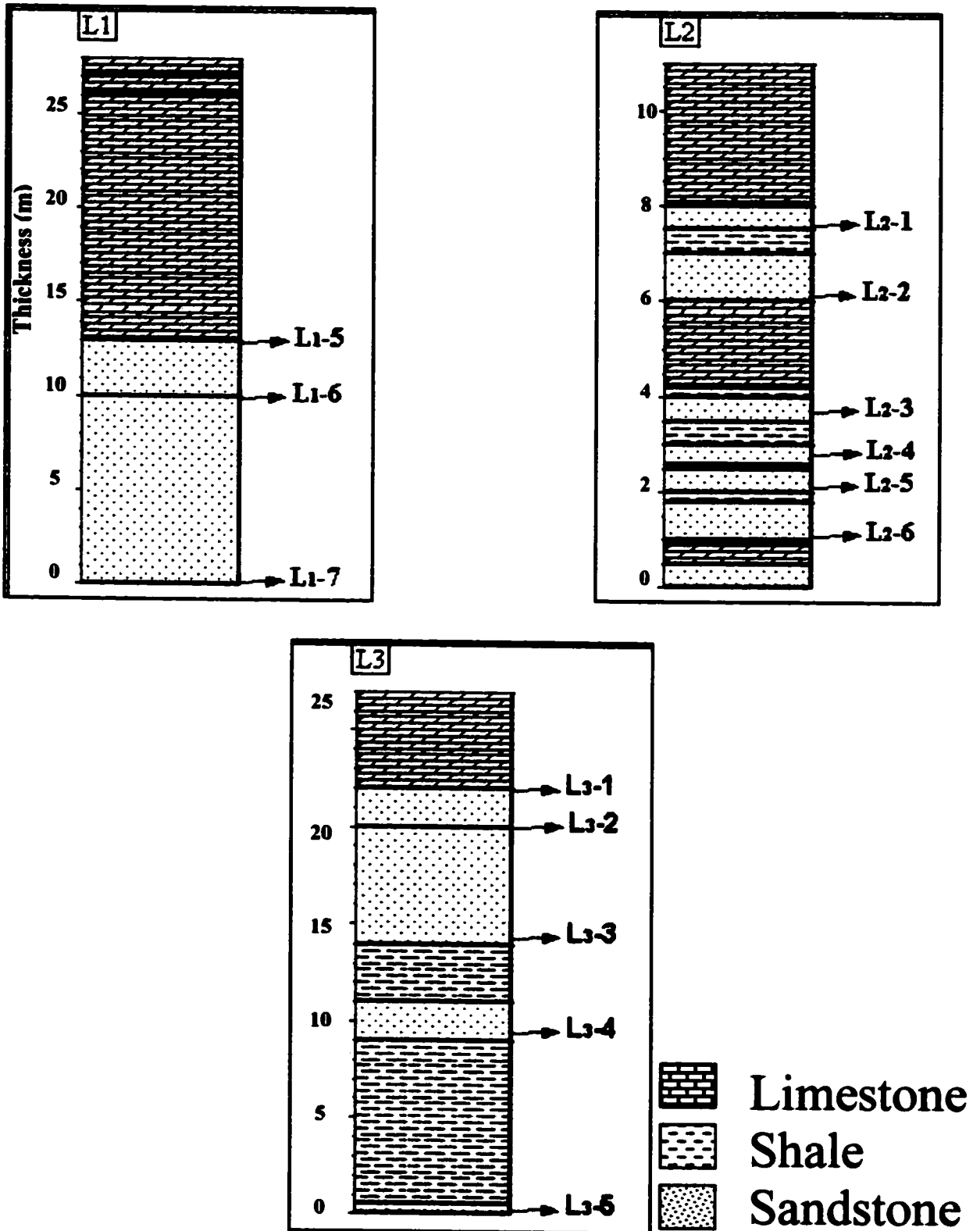


Figure 1-5: The stratigraphic columns showing the lithology and the distribution of the field samples.

The techniques used are as follows:

1. *Thin Section Petrography.*

The samples were impregnated with both red and blue dyed epoxy to facilitate the recognition of porosity using polarizing microscope. 200-point counts as well as comparative visual chart were used for percentage calculation. Leitz polarized microscope (Laborlux 11Pol) fitted with camera were used to study samples under both plane and cross-polarized light.

2. *Scanning Electron Microscopy*

The scanning electron microscope has proven to be valuable for distinguishing diagenetic from detrital features in sedimentary samples. JEOL JSM-5800 LV scanning electron microscope fitted with EDX was used to observe cement morphology and cement-pore relationships. Qualitative energy dispersive X-ray (EDX) analysis was used to study the composition of representative authigenic minerals. Fresh fractured surfaces of the sandstone samples were examined under secondary electron mode with magnification up to X 10,000.

3. *X-Ray Diffraction*

XRD analysis was carried on the separated clay fractions of the sandstones. Following the method outlined by Galeuouse (1971), a piece of each chip was broken in agate mortar. The broken material was soaked in distilled water for a day and was given ultrasound bath for one hour to separate the clay materials from the sandstone. The clay less than 4-micron fractions were collected down by the gravity settling. Oriented mounts of the clay fractions were prepared by filtering the clay suspension through ceramic tile and run in a JEOL X-ray diffractometer using $\text{CuK}\alpha$ radiation at 40 kV and 40 mA, from

2° to 35° 2θ for both air dry and glycolated samples allowed a full identification of clay minerals. Clay minerals were identified from peaks shown in diffractogram defined on both air dry and glycolated samples.

CHAPTER 2

Stratigraphy and Sedimentology of Jauf Formation

In Saudi Arabia, the Devonian rocks are represented by the Tawil, Jauf and Jubah Formations that are dominantly clastic but include some beds of limestone in the Lower Devonian. Jauf Formation is considered to be as Lower Devonian (Powers et al., 1966). The Jauf Formation is named by Berg et al. (1944) after the town of Al-Jawf (lat 29° 49', long 39° 52') near where the entire formation is exposed (Figure 2-1).

According to Wender et al., (1998), the Jauf Formation was deposited over a broad shelf as shallow marine, barrier island and associated channel sandstones, which exhibit unusually high porosities considering the deep burial depths.

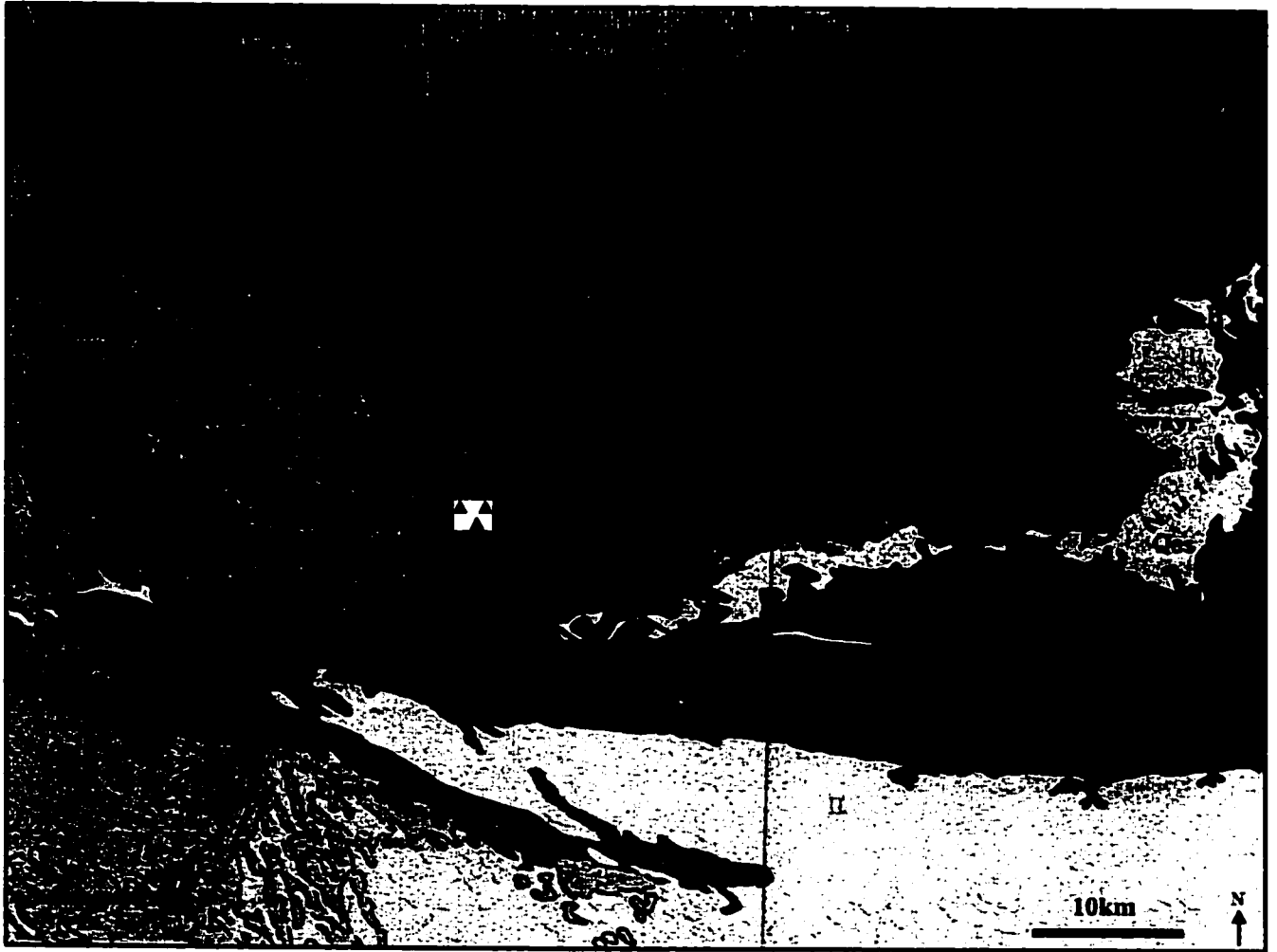


Figure 2-1: Geologic location of the field area map (After Bramkamp et al., 1963).

2.1. Jauf Formation in the Surface

Devonian sedimentary rocks are exposed in the southwestern and northwestern part of Saudi Arabia (Figure 2-2). Jauf exposures are small compared to the other Paleozoic units in the area.

The succession of the Devonian formations in the surface reflects changes in sedimentation from siliciclastic to mixed siliciclastic and carbonates and a return to siliciclastic. The middle part for the succession which is mixed siliciclastic and carbonate units is the Jauf Formation (Al-Hajri et al., 1999).

Jauf exposed in the southwestern part of the country. The type locality of Jauf Formation is about 4 km to the west of Jabal Al-Abd in Al- Jawf region in northwest Saudi Arabia (lat 29° 52'N, long 39° 45'E). The thickness of the type section is about 285 m. In the type section, the lithology of Jauf Formation is fossiliferous limestone and dolomites interbedded with shales, sandy shales, sandstone and sandy siltstone (Al-Laboun 1982).

Jauf Formation is subdivided into four members (Figure 2-3). These are from bottom to top: Sha'ibah Member, Qasr Member, Subbat El Wadi Member and Hammamiyat Member. The Sha'ibah Member is about 35 meters and consists of gray, green and red silty shale with minor limestone and sandstone. The Qasr Member is approximately 20 meters and composes of limestone and dolomite. The Subbat El Wadi Member is approximately 113 meters thick and consists of banded red and gray silty shale with subordinate limestone and sandstone in the upper part. The Hammamiyat Member is about 108 meters thick and composes of cream to pink limestone separated by silty shale layers with subordinate sandstone. The

depositional environment for each member is believed to be a distinct marine environment (Al-Laboun, 1982). The Jubah Formation unconformably overlies the Jauf Formation while the Jauf Formation is unconformably overlying the Tawil Formation, which is Silurian in age (Figure 2-3).

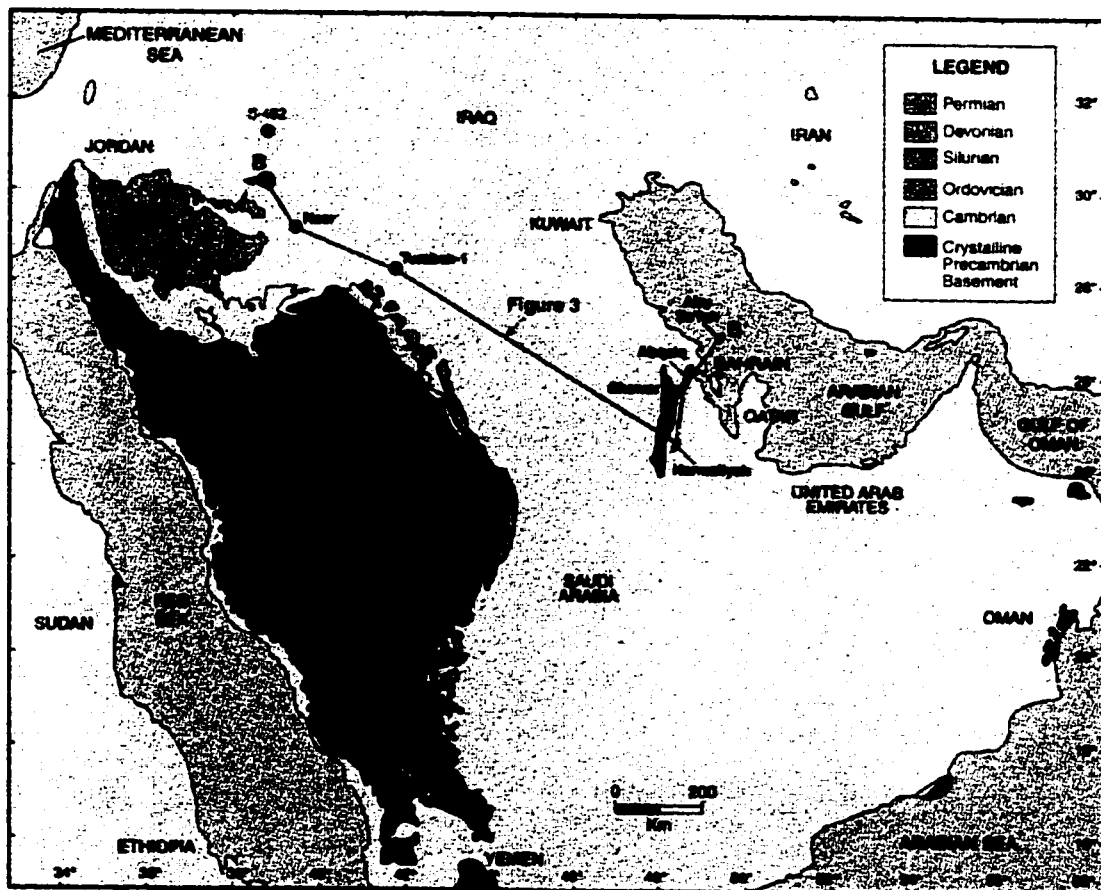


Figure 2-2: Paleozoic outcrop map of Saudi Arabia showing the location of the regional Devonian formations (After Al-Hajri et al., 1999).

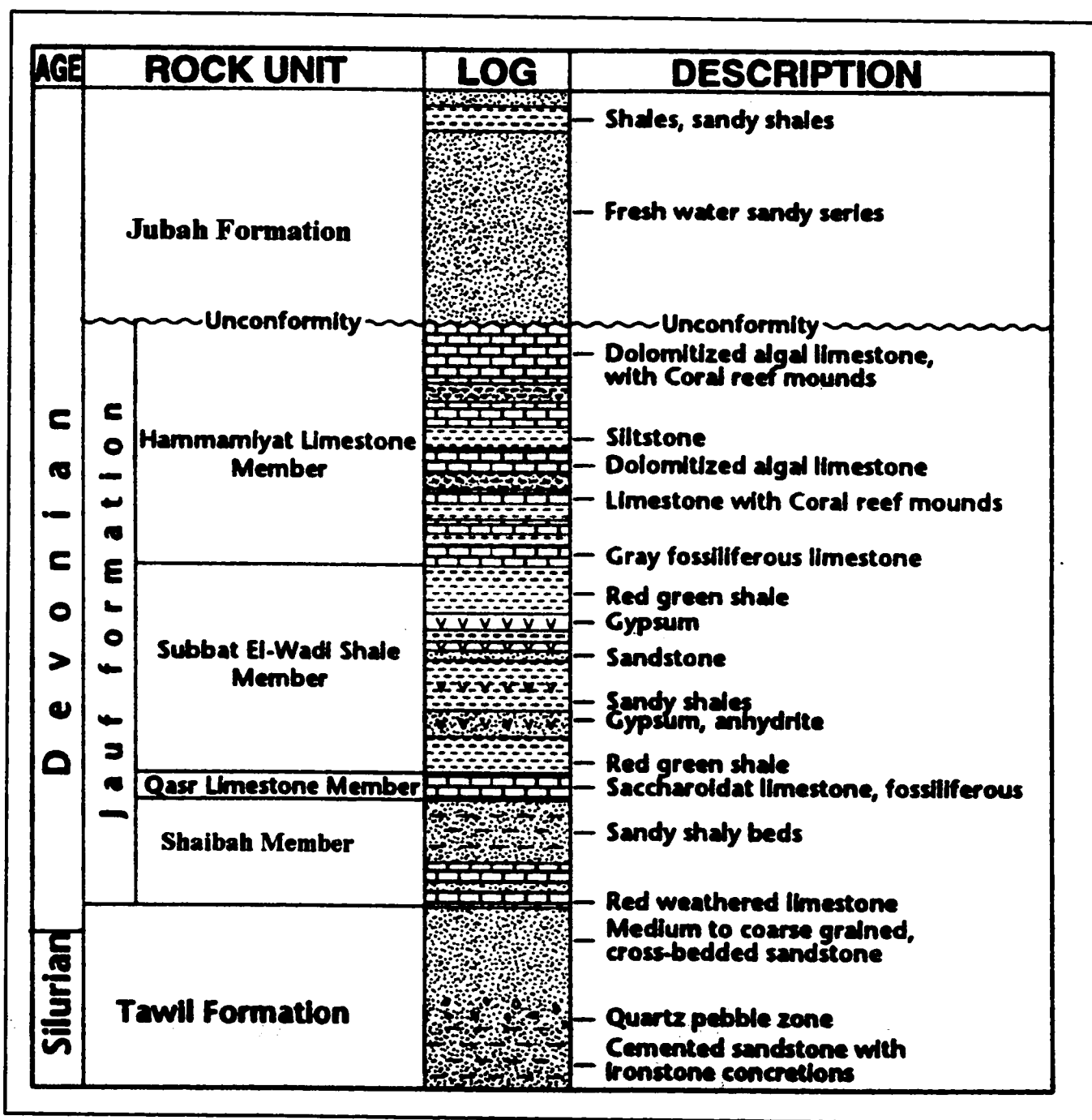


Figure 2-3: Generalized stratigraphic succession of the Jauf Formation in the Al-Jawf region, (Modified after Al-Laboun, 1993).

2.2. Jauf Formation in the Subsurface

Jauf in the subsurface in the Eastern Province has difference in facies in relation to the one in the northwest surface location described earlier. The Jauf Formation in the Eastern Province in the Subsurface is characterized by the absence of shallow marine carbonate members whereas the carbonate members are present in the northwest part (Figure 2-4). This indicate different depositional environment. Figure 2-5 shows a series of horst and grabens and the succession consists entirely of sandstones with some intercalation of silt/shale units that represent continental to marginal marine, fluvio-deltaic depositional system (Hawiyah field in the Ghawar Area). In spite of this, the same classification of the Devonian succession has been extended to the Eastern Province although the formations are less readily differentiated litho-stratigraphically, even with the serve of wireline logs (Al-Hajri et al., 1999).

The Devonian formations are removed from the crest of Ghawar area due to the Hercynian Orogeny (Figure 2-6). Marginal marine sandstones with preserved porosity reaching to 30% characterize the Jauf Formation (Al-Hajri et al., 1999).

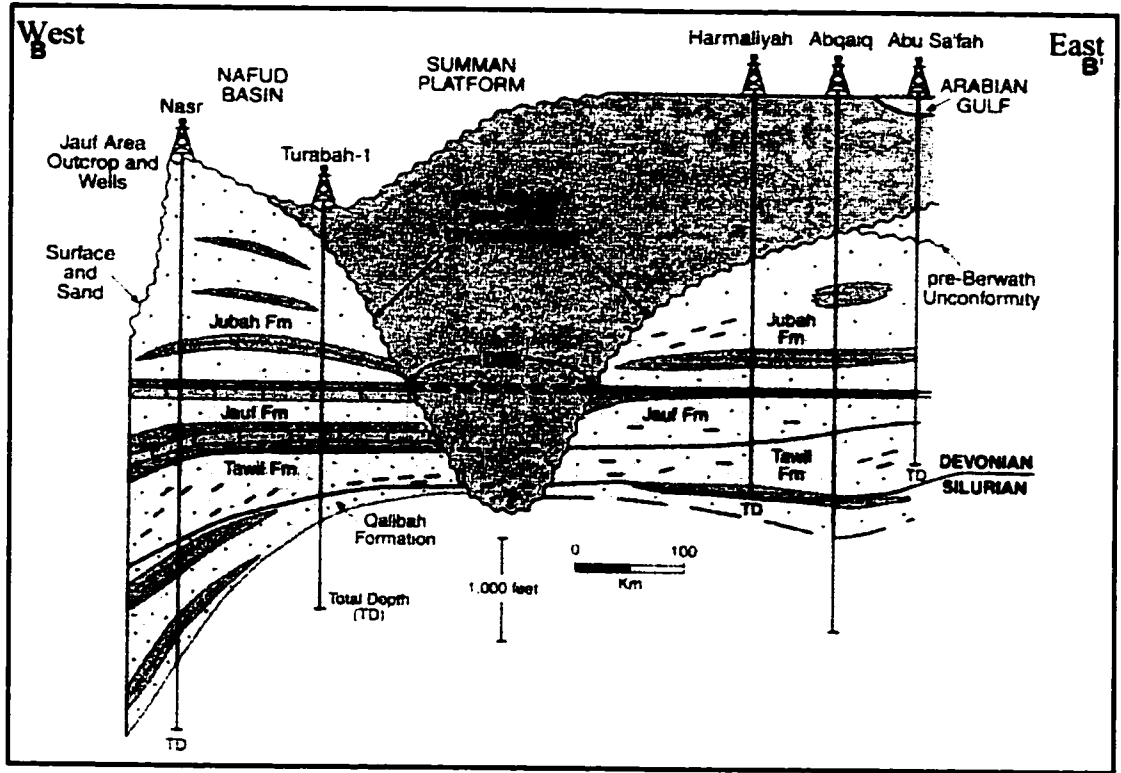


Figure 2-4: Regional Devonian cross-section of B-B' referring to Figure 2-2 (after Al-Hajri et al., 1999).

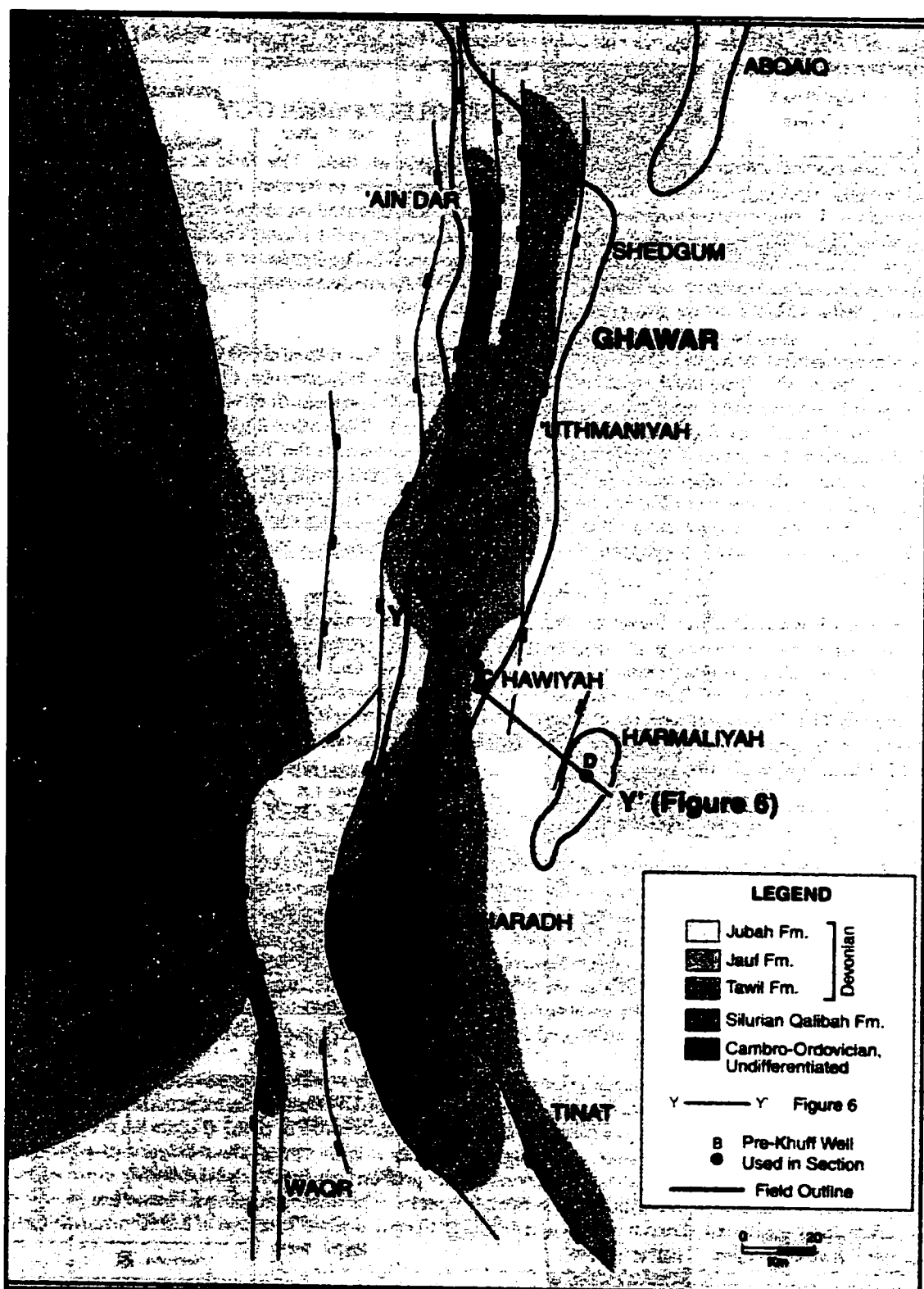


Figure 2-5: Structure map of the Ghawar Area that is composed of a series of horst and tilted fault blocks arranged in a general north-south direction (after Al-Hajri et al., 1999).

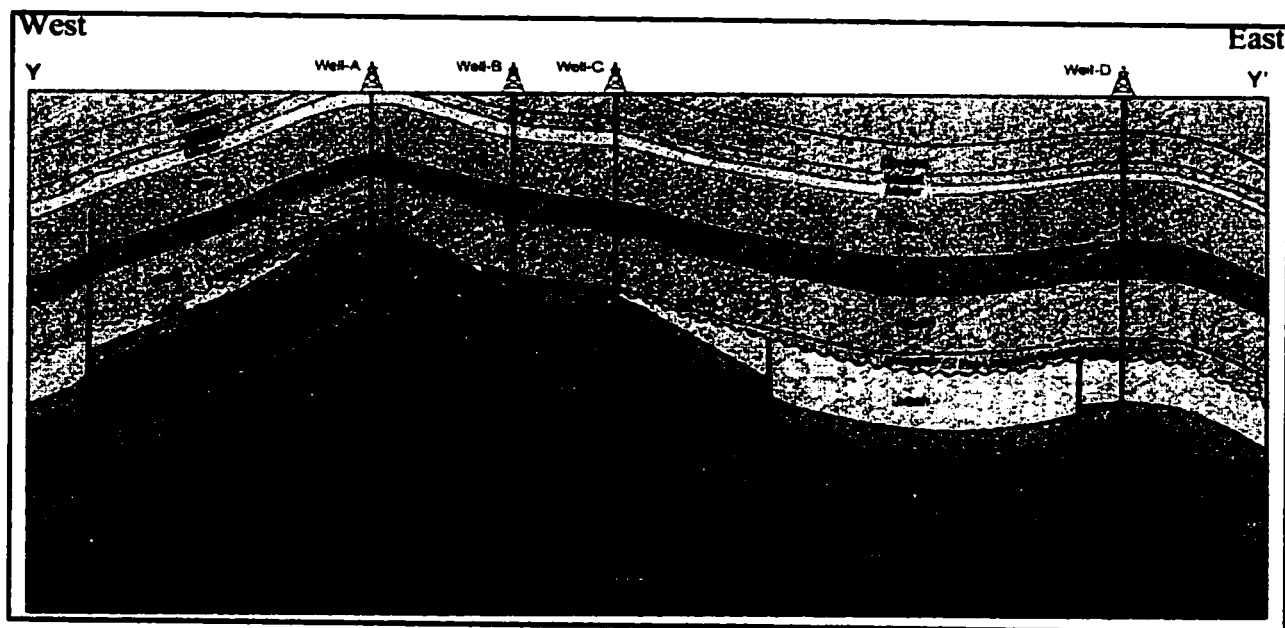


Figure 2-6: E-W cross-section of the Ghawar area showing the Devonian formations, referring to Figure 2-5 (after Al-Hajri et al., 1999).

2.2.1. Jauf Formation in Hawiyah Area

Two wells studied in the Eastern Province including well A and well B. Detailed description of the two wells of the studied formation is shown as follows:

Well A

The subsurface Jauf Formation in Well A is 463 feet thick. Its lithology is mainly sandstone and some shale interlayers. Also, the sandstones are characterized by fine-grained shaly laminae. Jauf Formation in Well A is fining upward sequence in general and this is evidenced by cores analysis. This well is characterized by three zones (Saner, 1998. unpublished report):

1. Black shale zone (14315 to 14376.3 feet): This zone is dominantly marked by black-fossil shale. Also, siltstone and fine sandstone occur. This zone is characterized by heterolithic bedding; ripple cross-laminated siltstone, lenticular bedding and horizontal laminated shale layers. The presence of pyrite and dark color of shale indicate an organic rich anaerobic shallow lagoonal environment, which might be the source rock of some hydrocarbons in the area.
2. Yellowish greenish gray sandstone zone (14376.3-14487 feet): This interval does not have black shale. This upper part of this zone is characterized by horizontal and cross-laminated or massive sandstone and hematitic lamination. Whereas, the lower part is characterized by weavy laminated and bioturbated Sandstone.
3. Massive Quartzitic Sandstone zone (from 14487 feet to 1452.9 feet): The lower 56 feet of this zone is tightly cemented by silica cement. Also, the color of this zone

is reddish due to high hematite content, which is deposited, in a shallow high-energy coastal environment.

The cores available for this study from this well are all chip samples for thin sections.

Well B

The Jauf Formation at well B has a thickness of 310.5 feet. Its general lithology mainly is sandstone. In some intervals of this well, distinct cross lamination and massive sandstone are present. Also, the sandstones are characterized by the presence of small white specks. A detail description of cores from this well is given in Table 1:

Table 1: A detail description of cores from Well B.

Core #	Depth (feet)	Description
1	14035.9	Dark gray, hard and compacted. Fine grain, very well sorted. Indistinct cross bedding (Figure 2-7).
2	14041.8	Dark gray, hard and compacted. Fine to very fine grain, very well sorted. Distinct cross lamination by dark colored, irregular alternating beds. The cross lamination is bi-direction (Figure 2-8).
3	14122.6	Dark gray, hard and compacted. Fine grain, very well sorted. Massive sandstone with small white specks scattered throughout the core (Figure 2-9).
4	14132	Gray, moderately compacted to friable. Fine to very fine grain, well sorted. Massive sandstone with white specks (Figure 2-10).
5	14137.1	Light gray, hard and compacted. Fine to very fine grain, moderately sorted. Distinct parallel cross laminations with white specks. Lamination is due to alternating light and dark bands (Figure 2-11).
6	14143.9	Light gray, hard and moderately compacted. Fine to very fine grain, well sorted. Parallel cross laminations with whit specks. Lamination is due to alternating light and dark bands (Figure 2-12).

7	14263.4	White, hard and compact, medium grain, well sorted. Massive sandstone (Figure 2-13).
8	14289	Gray, hard and compacted. Course to medium grain, moderately sorted. White cross-bedded, thin white lamina and thin beds alternates with gray sand. White specks scattered throughout the core. Local minor deformations (bending) of the white lamina perhaps syndimentary (Figure 2-14).
9	14312.4	Light gray, hard and compact, medium to fine grain, moderately sorted. Distinct cross lamination in the upper part and massive in the middle. Few lithic clastic (green shale) are present. Erosional contact is between the gray sand and white cross bedding sand (Figure 2-15).
10	14317	Light gray, hard and compact. Fine to very fine grain, well sorted. Distinct parallel cross laminations of alternating light and dark lamina (Figure 2-16).
11	14323.6	Light gray, hard and moderately compacted. Fine to very fine grain, moderately sorted. Parallel and cross laminations alternating light and dark bands (Figure 2-17).
12	14345.7	Gray, hard and moderately compacted. Fine grain, well sorted. Parallel lamination (Figure 2-18).

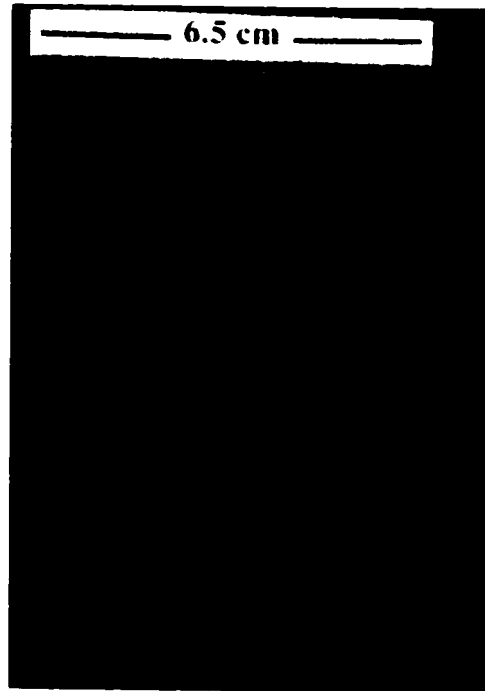


Figure 2-7: Core #1 is dark gray, indistinct cross bedding, depth 14035.9 ft.



Figure 2-9: Core #3 is dark gray, massive sandstone with small white specks, depth 14122.6 ft.



Figure 2-11: Core #5 Light gray, hard and compacted, distinct parallel cross laminations with white specks. depth 14137.1ft.



Figure 2-13: Core #7 is White, massive sandstone, depth 14263.4ft.

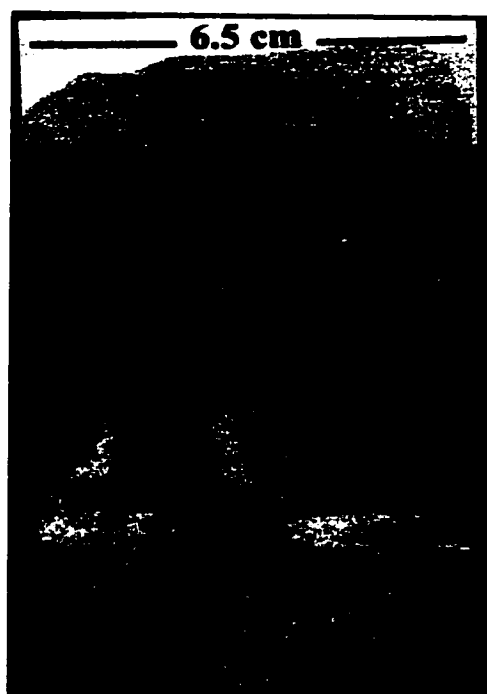


Figure 2-15: Core #9 is Light gray, distinct cross lamination in the upper part and massive in the middle. Few lithic clastic (green shale) are present, depth 14312.4ft.



Figure 2-16: Core #10 is Light gray, distinct parallel laminations of alternating light and dark lamina, depth 14317ft.

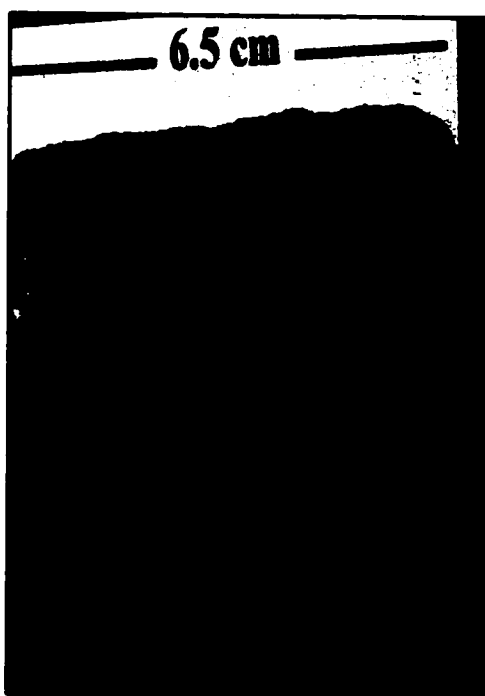


Figure 2-17: Core #11 is Light gray, parallel laminations alternating light and dark bands, depth 14323.6ft.

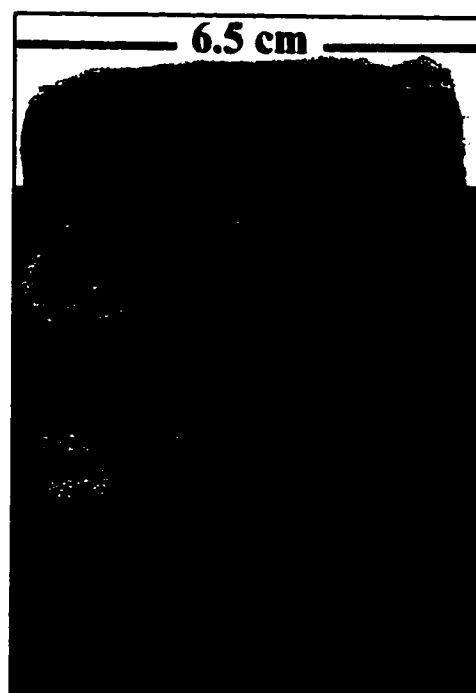


Figure 2-18: Core #12 is Gray, parallel lamination, depth 14345.7 ft.

2.2.2. Jauf Formation in Shedgum Area

In the Shedgum Area subsurface Jauf Formation was studied by Al-Duaiji (1991). In this study, the total thickness of the Jauf Formation sandstone is 423 feet including both the informal units. The upper unit is 226 feet represented by Jauf-A and the lower unit is 197 feet represented by Jauf-B.

Jauf-A is subdivided into six composite units and their lithologies mainly are sandstone with some thin beds of siltstone. The upper units of this reservoir exhibit coarsening upward which indicate an increase in flow regime upward whereas the lower units were probably of fluvial origin, which exhibit a decrease in grain size. Jauf-B is subdivided into three zones and their lithologies are sandstones. The lower two zones are characterized by point-bar sandstone while the upper one is on channel-fill sandstone.

Based on classification of Bott (1964), the Jauf formation sandstones are of graywacke in the Jauf-A whereas in Jauf-B is quartz graywacke. The depositional environment of Jauf Formation in Shedgum area was dominantly nonmarine (Al-Duaiji, 1991).

CHAPTER 3

PETROGRAPHY OF THE JAUF FORMATION

The petrographic analyses of the sandstones of the Jauf Formation were carried out on 62 representative core samples collected from the two wells (Well A and Well B) and 12 outcrop samples collected from the field. Petrographic characteristics influence the reservoir properties of the rocks including the ability of petroleum reservoirs to produce. An understanding of these characteristics can help to better understand the reservoir performance. This chapter will describe the petrographical characteristics of subsurface and surface samples as revealed by thin section petrography, SEM and XRD analyses.

The Jauf Formation at Well A and Well B consists dominantly of sandstone. Textural properties and mineralogical composition of both Well A and Well B samples are presented in Tables 2, and 3, and the result of surface samples are tabulated in Table 4. Following is a summary of the features of the sandstone texture and composition as revealed by the above studies.

Table 2: Percentages of rock components including porosity for Well A.

Sample#	Texture		Grain%							Matrix%	Cement%					Thin section Porosity (Primary and Secondary) (%)
	Grain Size	Grain Sorting	Q	F	L	M	Heavy	Others	Ca		Qtz	I	Cl	Py		
323	F-VF	Well	57	3		1	Tr.		Tr.	30				8		
329	F-M	Moderate	73	3	2		Tr.	3Carb	<1	15			3	Tr.		
330	F-VF	Well	62	3	Tr.		Tr.	9Carb	2	14			4		5	
345	F-M	Well	72	3			Tr.	1Carb	1	5		1	1		15	
350	F-M	Well	60	3	2	1	Tr.		<1.	9		2	3		18	
354	F-VF	Well	62	4			1		1	6		4		1	20	
361	F-VF	Moderate	50	3		5	5		25	5		2		2	2	
365	F-M	Moderate	72	2			2	<1Carb	2			1	4	1	15	
369.8	F-VF	Well	72	3			Tr.		<1	5			2		15	
363	F	W. -M.	65	2		2Mus	Tr.		27					3		
373.6	M	Well	75	1			Tr.		Tr.	4			2		17	
377	F-M	Moderate	65	3		3Mus	Tr.		24					2	2	
380	M-C	Moderate	80	2			Tr.		<1	3		2	2		10	
384	F	Moderate	55	4		2	1		30	5				2		
387	VF-M	Poorly	82	3		1	Tr.		3			Tr.			10	
390.7	M-C	Moderate	90		Tr.		Tr.		2	3			4			
394	M	Moderate	80	2	Tr.		Tr.		Tr.	1					16	
398	F-VF	Moderate	52	5		<1	1	2Carb	35					4		
404	M-C	Moderate	82	3		Tr.	Tr.		1	2	2	Tr.	1		8	
406	F-M	Well	60	5		1	Tr.	2Carb	25					1	4	
411	M-C	Moderate	82	3		1	Tr.		<1	2	1				10	
413	M-C	Moderate	84	3			Tr.		<1			1			11	
417	F-M	Well	82	3			Tr.		<1	2		2			10	
421	F-M	Moderate	82	2		<1	Tr.		1	1		1			12	
424	F-M	Moderate	64	4		1	Tr.		25						5	
425	F-M	Moderate	54	3		Tr.	1		30	2			4		5	
427	F	Well	74	4		1	Tr.		8					4	8	
432	M-C	Moderate	83	3	Tr.	Tr.	Tr.		1	1		1			10	
441	F-C	Poorly	80	2		1	Tr.		11	2					3	
449	F-C	Poorly	73	4		1	1		15						5	
459	VF	Very Well	65	5		4	Tr.		25							
465	F-C	Moderate	80	3			2		7						7	
470	F-C	Moderate	77	2		<1	Tr.		12					1	7	
473	VF-C	Poorly	70				Tr.	3Ch	15	1	2		2	4	2	
476	F-M	Moderate	80			Tr.	Tr.		7	3		2			7	
482	F-M	Moderate	85				Tr.		8	2					4	
484	F-C	Poorly	73				Tr.	3Ch 4Carb	12				5		2	
487	F-M	Moderate	70				Tr.	2Ch	1	2	2		7		15	
490	M-C	Moderate	84				Tr.	2Ch	1	1			1		10	
495	F-M	Moderate	87	1			Tr.	1Carb	<1		1	1			8	
498	F-M	Moderate	92				Tr.		2		1	1			3	
501	F-M	Moderate	85			Tr.	Tr.		3			2		1	8	
505	F-C	Poorly	95				Tr.		2						2	
508	F-C	Poorly	93				Tr.		3			1			2	
511	F-M	Moderate	90				Tr.		<1			2			6	
514	C	Moderate	90				1		1				2		5	
519	F-M	Well	78			1	Tr.		3		8	1			8	
523	M-C	Moderate	90	1		1	Tr.		<1			1			6	
535	F-M	Moderate	87	1			Tr.		2				2		7	
538	F-M	Moderate	85			Tr.	Tr.		<1				6		8	

Table 3: Percentages of rock components including porosity for Well B.

Sample#	Texture		Grain%						Matrix%	Cement%					Thin section Porosity (Primary and Secondary) (%)
	Grain Size	Grain Sorting	Q	F	L	M	Heavy	Others	Ca	Qtz	I	Cl	Py		
1	Fine	Well	72	3			Tr.		4		1		2		17
2	F-M	Well	77	1		<1	Tr.	4Carb	7						9
3	M	Well	83	1				1 Shale	Tr.	5	4				5
4	M	Very Well	74	1			Tr.		Tr.	4	3	2			15
5	M-C	Well	70	1			<1	<1 Carb	4	6	3	2	2		10
6	M	Well	86				Tr.		Tr.	8	3				2
7	F-C	Well	86				Tr.		5	1		3	1		2
8	M-C	Well	94				Tr.		1		2				2
9	M-C	Well	87				Tr.	1 Carb	1		8				2
10	F-M	Well	89				Tr.		Tr.	5	3				2
11	F-M	Well	83				Tr.	1 Carb	2		1				12
12	F-M	Well	90	1			<1		Tr.	3		2			2

Table 4: Percentages of rock components including porosity for field samples.

Sample#	Texture		Grain%						Matrix%	Cement%					Thin section Porosity (Primary and Secondary) (%)
	Grain Size	Grain Sorting	Q	F	L	M	Heavy	Others	Ca	Qtz	I	Cl	Py		
L1-5	M	Well	75	1			Tr.	5Carb	4	3	2				10
L1-6	F-M	Mod-Poor	80	2			1	1 Carb			1		7		8
L1-7	F	Well	81	3			1						6		9
L2-1	VF	Mod	65			13,Bio	<1	2Carb	15						3
L2-2	VF	Well	55	2		3Bio/1Mus		3Carb		35					
L2-3	VF	Well	65	1		5Bio/2Mus		2Carb	25						
L2-4	Silt	Well	63	1		10Bio/3Mus		2Carb	20						
L2-5	Silt	Well	43	2		20Bio/3Mus		2Carb	30						
L2-6	Silt	Well	55			15Bio/2Mus			30						
L3-1	VF	Well	75						25						
L3-2	VF	Well	80						20						
L3-3	Silt	Well	75						25						
L3-4	VF	Well	78	2		1Mica			18						
L3-5	Silt	Well	75						25						

Note in table 2,3 and 4:

F: fine-grained VF: very fine-grained M: medium-grained

C: coarse-grained W.: well M.: moderate

Q: quartz grains including both poly and mono-crystalline types.

F: feldspar grains including both plagioclase and K-feldspar.

L: lithic grains including both chert and shale clasts.

M: mica including both muscovite and biotite.

Ca: calcite

Q_z: quartz cement

I: illite

Cl: chlorite

Py: pyrite

Tr.: trace

Carb: carbonaceous materials

Mus: muscovite

Bio: biotite

Ch: chlorite grains

3.1. Petrographic Characteristics of Subsurface Core Samples

3.1.1. Texture

About 75% of the studied sandstones are fine to medium-grained, 18% medium grained and 8% are very fine-grained (Tables 2 and 3). Approximately 50 % of the studied sandstones are moderately sorted, 37% well-sorted and 13% poorly sorted. The shapes of the grains are mostly subangular to subrounded with some rounded grains. The sandstone samples of the both Well A and Well B are divided into the following three groups on the basis of matrix content and textural maturity. Matrix is defined in this case as detrital particles less than 30 microns in size and includes clay and fine silt (Pettijohn et al., 1987).

1. **Mature:** contain trace to <1% matrix; 31 % of the samples fall in this category.
2. **Submature:** contain 1 to 5 % matrix (average 2 %); 39 % of the samples fall in this category.
3. **Immature:** contain 7 to 35% matrix (average 18 %); 30 % of the samples fall in this category.

3.1.2. Composition and Classification

The detrital mineralogy of the sandstones is dominated by quartz grains with little to trace feldspar and lithic grains. The sandstones contain an average of 77% quartz, 2% feldspar and 0.1% lithic fragments. Sedimentary shale and chert are the lithic fragments observed. A small to trace amount of organic or carbonaceous materials are present in most of the samples. Heavy minerals are typically present as accessory components. The authigenic cement observed include calcite, quartz, illite and chlorite.

Using the QFL Diagram (Pettijohn et al., 1987), the samples were classified according to the percentage of quartz, feldspar and rock fragments (Figure 3-1). The percentages of quartz (Q), feldspar (F) and rock fragments (L) were normalized and the values plotted as points in the QFL ternary diagram. Accordingly, 49 sandstone samples are quartz arenites, 2 samples are subarkosic arenites, 8 samples are feldspar graywackes and 3 are quartzwackes (Figure 3-2). The software that was used for generating ternary diagram is STATISTICA®.

3.1.2.1. The Detrital Components

The detrital components of sandstones comprise the materials that have been carried into the depositional basin from outside by erosion and transportation agents. These are discussed below as: 1) the framework grains and 2) the matrix.

3.1.2.1.1. Framework grains

They are defined as the basic building block materials of the rock. The vast majority of the framework grains are quartz whereas the other framework grains include feldspar, rock fragments, micas (including muscovite and biotite), carbonaceous materials and some heavy minerals. The following is a brief description of individual framework grain types based on petrographic microscopy examinations of the thin sections.

a) Quartz

Detrital quartz represents 55 to 96 % of the total rock components with average of 77.5 % (Table 1 and 2). The quartz grains have been identified by the absence of cleavage, gray birefringence color and clear color. The quartz grains are mostly monocrystalline with a very few percentage of polycrystalline type in most of the samples, and mostly

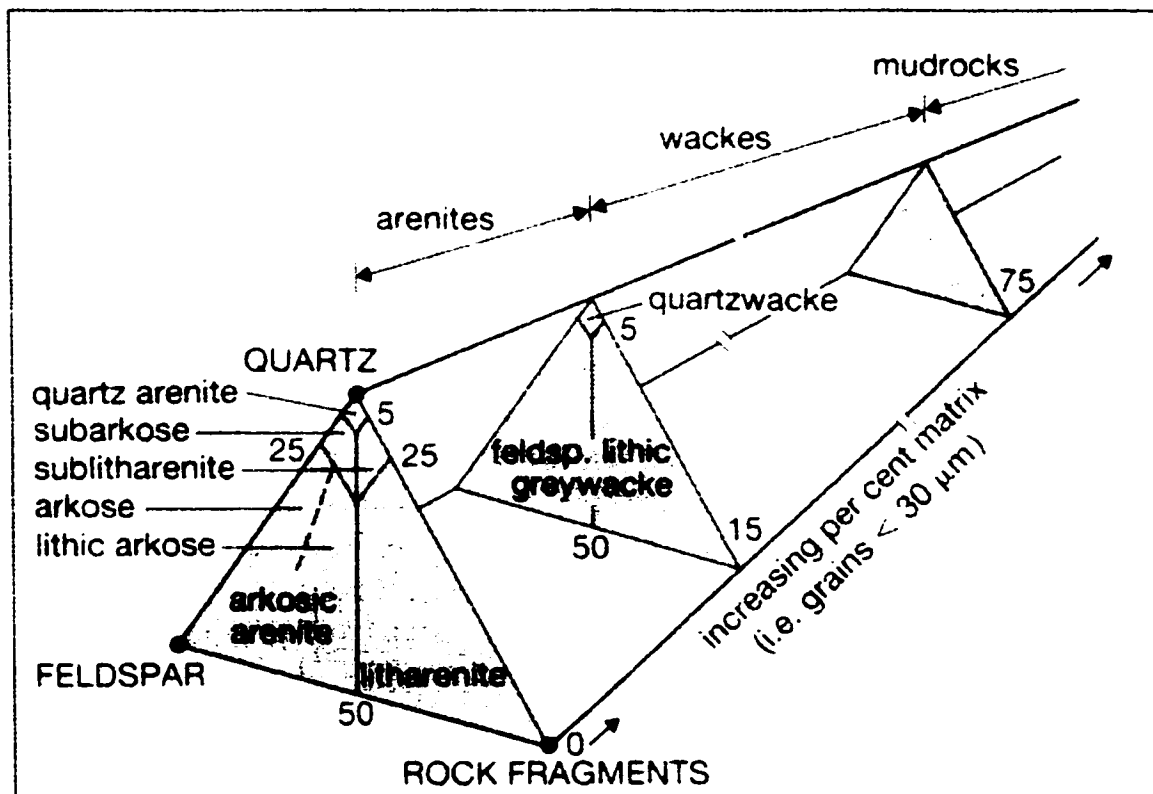


Figure 3-1: Ternary diagram model used for the studied samples (After Pettijohn et al., 1987).

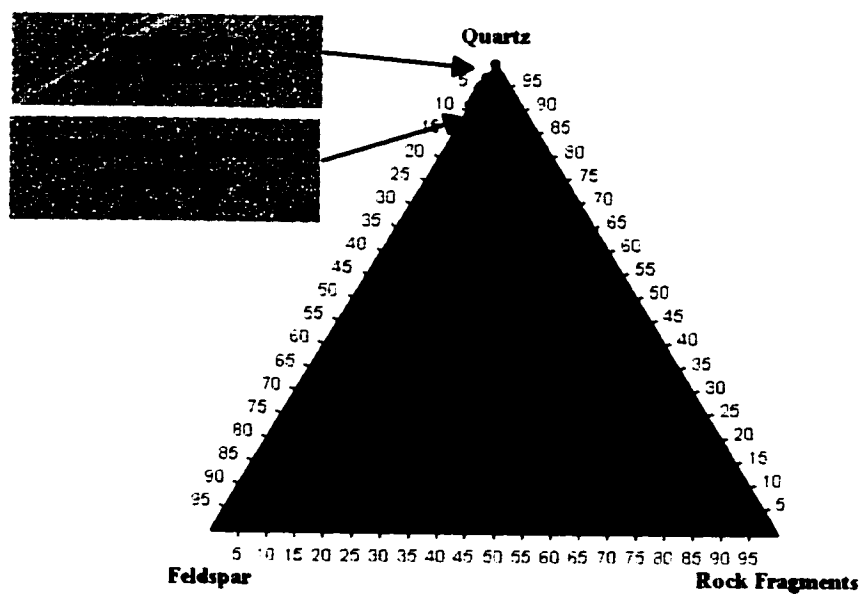
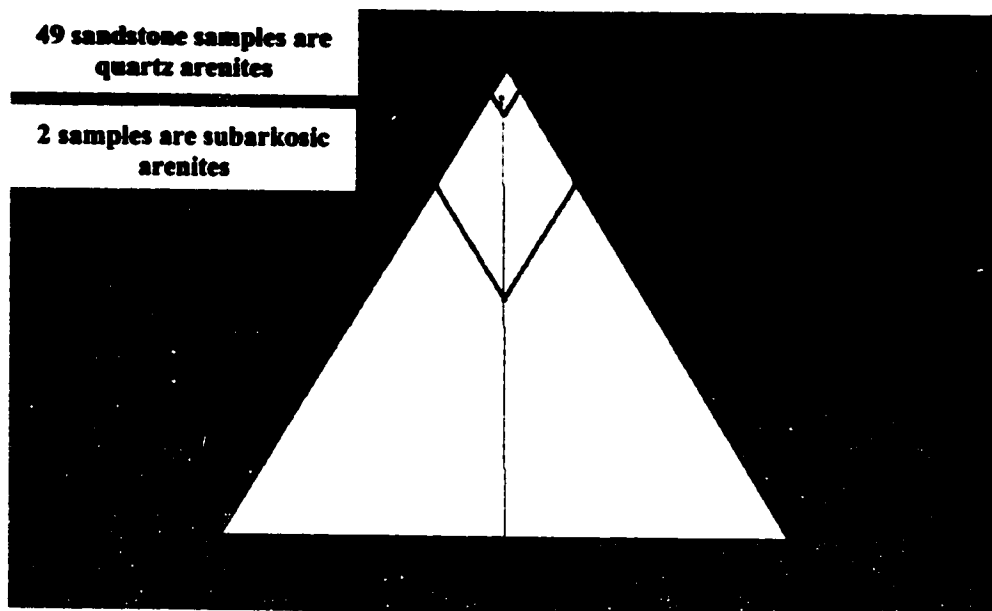


Figure 3-2: Ternary diagrams for sandstone samples of matrix less than 15 % (above) and greater than 15 % (below).

show straight extinction. These indicate igneous source rather than metamorphic (Tucker, 1991).

b) Feldspar

Feldspar including both the K-feldspar and the plagioclase makes up 1 to 6% (average of 2%) of the rock components (Table 2 and 3). Plagioclase feldspar are identified by characteristic lamellar twinning (Figure 3-3) whereas the K-feldspar grains are identified by their crosshatched twinning (microcline) and untwined nature (Figure 3-4). The distinct cleavage and partial weathering (cloudy) of the grains distinguish feldspar from quartz grains. One important feature of feldspar grains is that these are commonly partially dissolved which have major implication in post-burial secondary porosity generation (See Chapter 4). Identification of these partially dissolved skeletal feldspar grains are facilitated by colored epoxy resin.

c) Rock Fragments

The rock fragments constitute trace to 0.1% of the total rock components (Table 2 and 3). The only two kinds of rock fragment in all the samples are chert and shale clast. Chert is microcrystalline quartz grained. Some chert contains siliceous skeletons of microorganisms known as radiolarians, which can be seen in thin section (Figure 3-5). Chert can be recognized in thin section by its extremely dense fine grain size.

Shale fragments are mostly soft and the only other type of lithic grain in the samples. Shale shows evidence of plastic deformation under high compaction (Figure 3-6). Shale fragments in sandstone with moderate to deeply buried are often squashed away from their original grain shapes. Most of the shale fragments are easily identified by their dirty or cloudy look under plain polarized light.



Figure 3-3: Plagioclase feldspar (PF) showing lamellar twinning, Sample # 384, Well A, depth 14384 feet, cross polarized light.



Figure 3-4: K-Feldspar (KF) showing crosshatched twinning (microcline) and untwinned nature, Sample # 361, Well A, depth 14361 feet, cross polarized light.

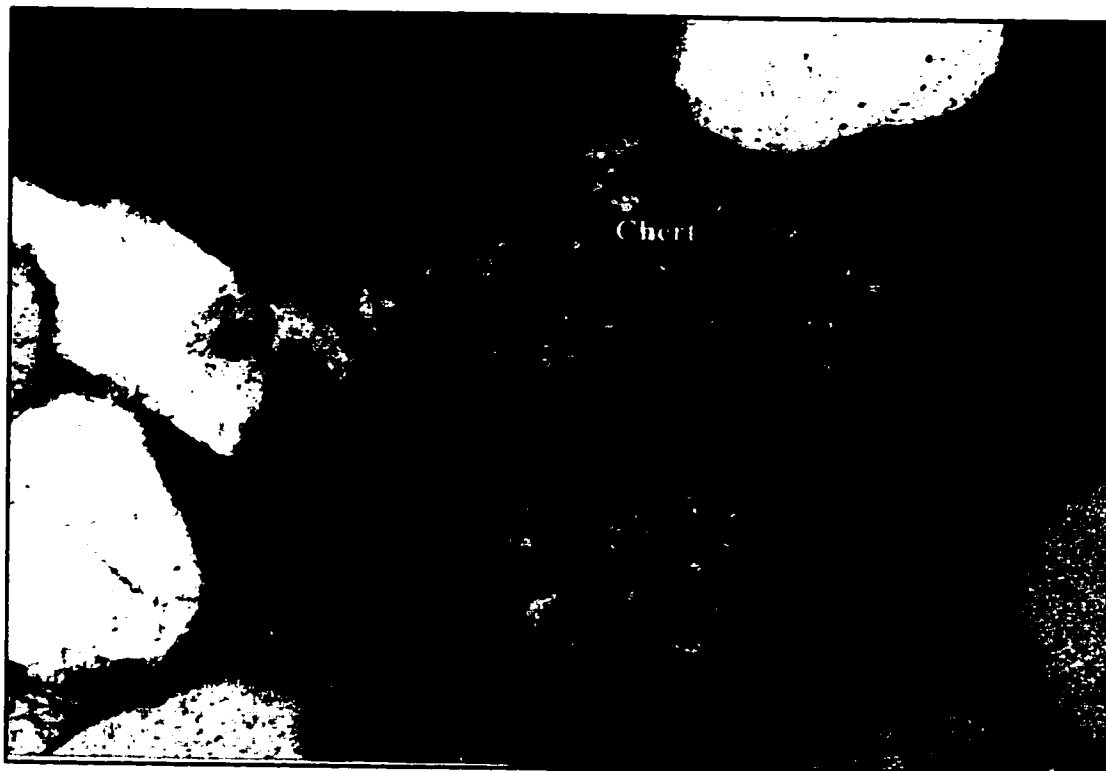


Figure 3-5: Chert grain showing extremely dense fine grain size, Sample # 6, Well B, depth 14143.9 feet, cross polarized light.

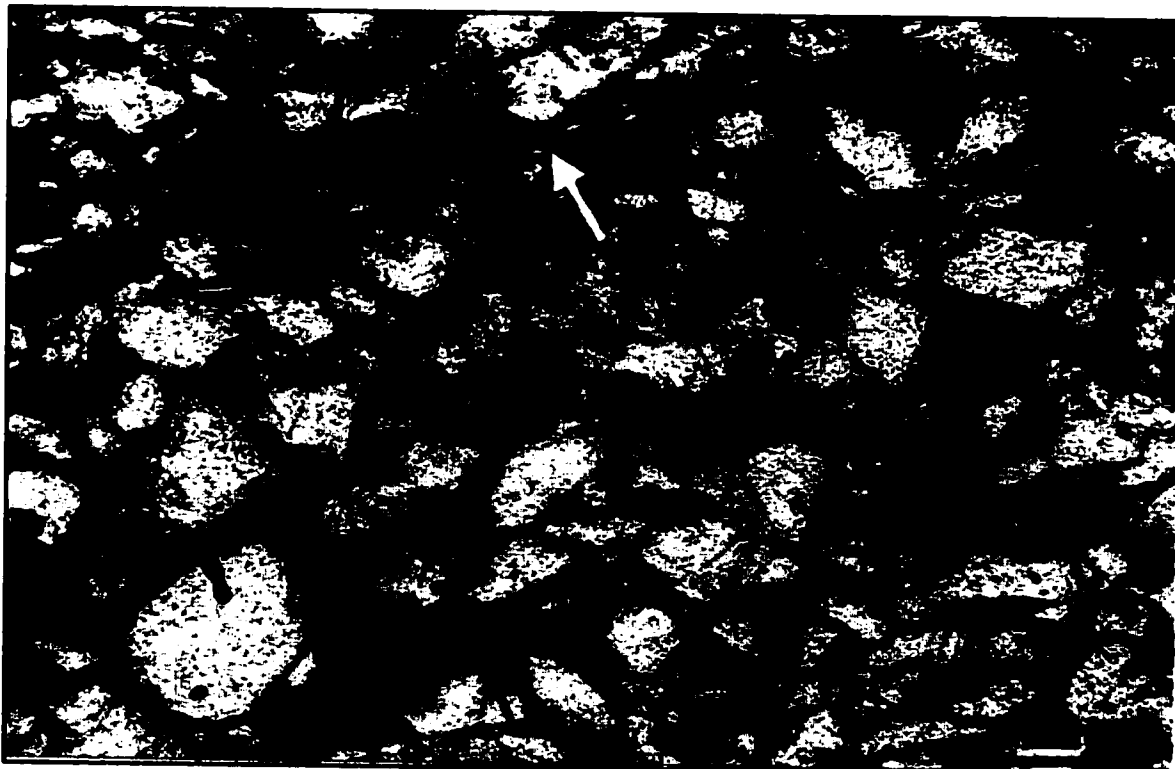


Figure 3-6: Plastic deformation of biotite and shale clast, Sample # 361, Well A, depth 14361 feet, plane polarized light.

d) Micas

Biotite, muscovite and chlorite are minor component in the samples. The micas are flaky and tabular grains and tend to align themselves parallel to the bedding plane. The micas are distinguished on the basis of their color as white muscovite, brown biotite and green chlorite. Micas are more common in fine-grained sandstones than those of the coarser ones. Flaky biotite constitutes trace to 5 % with average of 0.05% of the rock components (Figure 3-6). Muscovite and chlorite, together, comprise trace to 1% of the rock components (Figure 3-7).

e) Heavy Minerals

Though the heavy minerals represent 1 % or less of the total rock component, these are of some varieties. Both opaque and non-opaque heavy minerals were identified. The non-opaque heavy minerals include epidote and zircon (Figure 3-8). The black opaque includes pyrite and may also include magnetite and ilmenite, which can not be distinguished in polarized microscopy. Pyrites are authigenic and are discussed later in cement section.

f) Carbonaceous Grains

Carbonaceous materials represent average of 2% of the sandstone components and occur as black opaque to translucent grains. They are distinguished from others opaque heavies by their irregular grain shape and brownish edges. In instances, organic matters are concentrated as pronounced lamina (Figure 3-9). In some samples carbonaceous matters occurs as coating around grains (Figure 3-10).

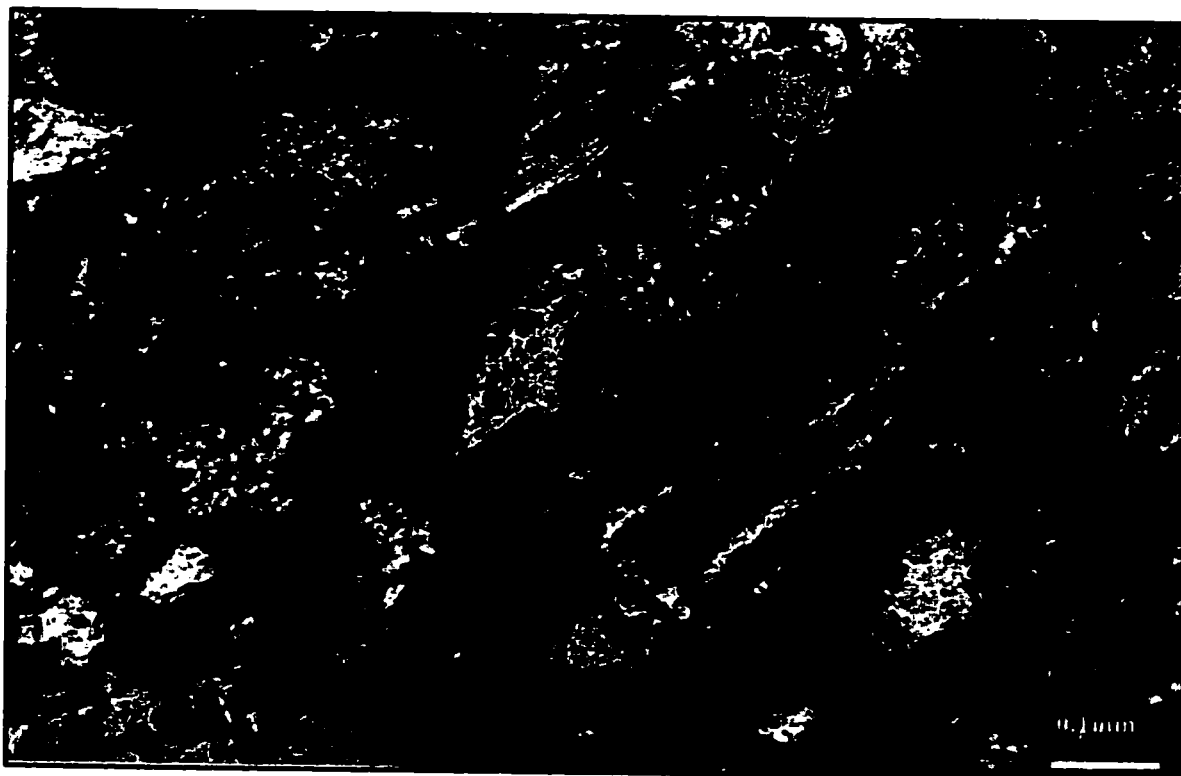


Figure 3-7: Muscovite (M) grains, Sample # 459, Well A, depth 14459 feet, cross polarized light.

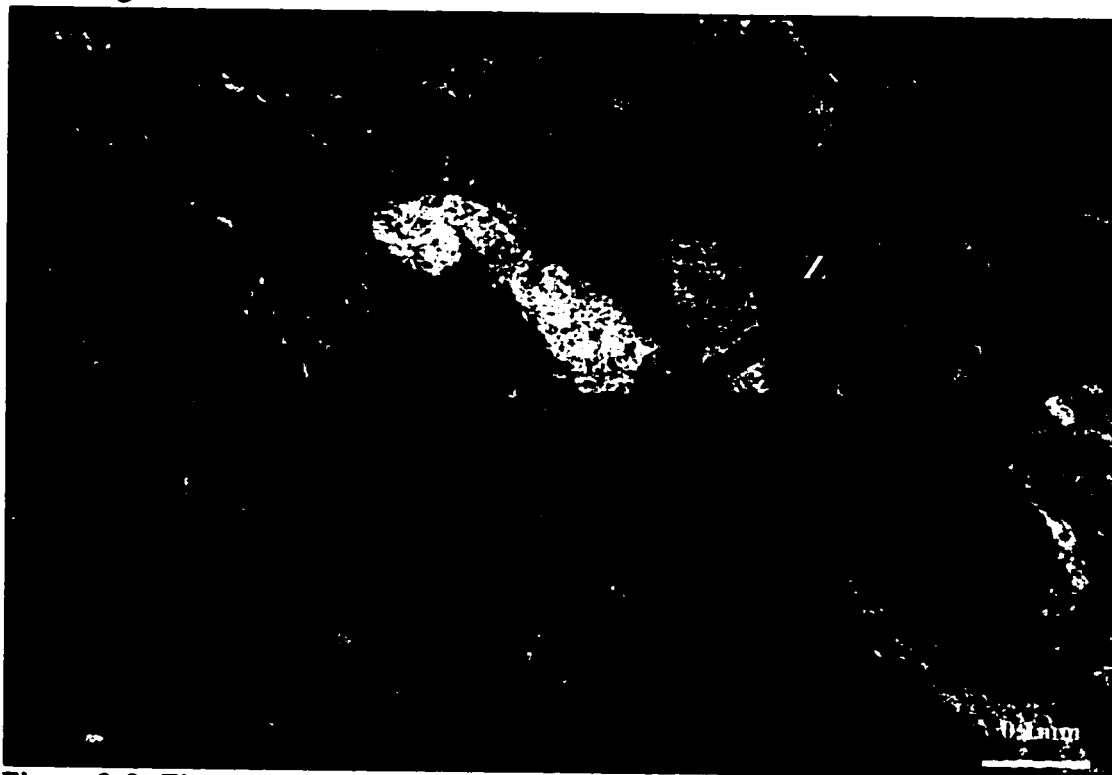


Figure 3-8: Zircon grain (Z) showing very high (third- or fourth-order) interference colors, Sample # 377, Well A, depth 14377 feet, cross polarized light.

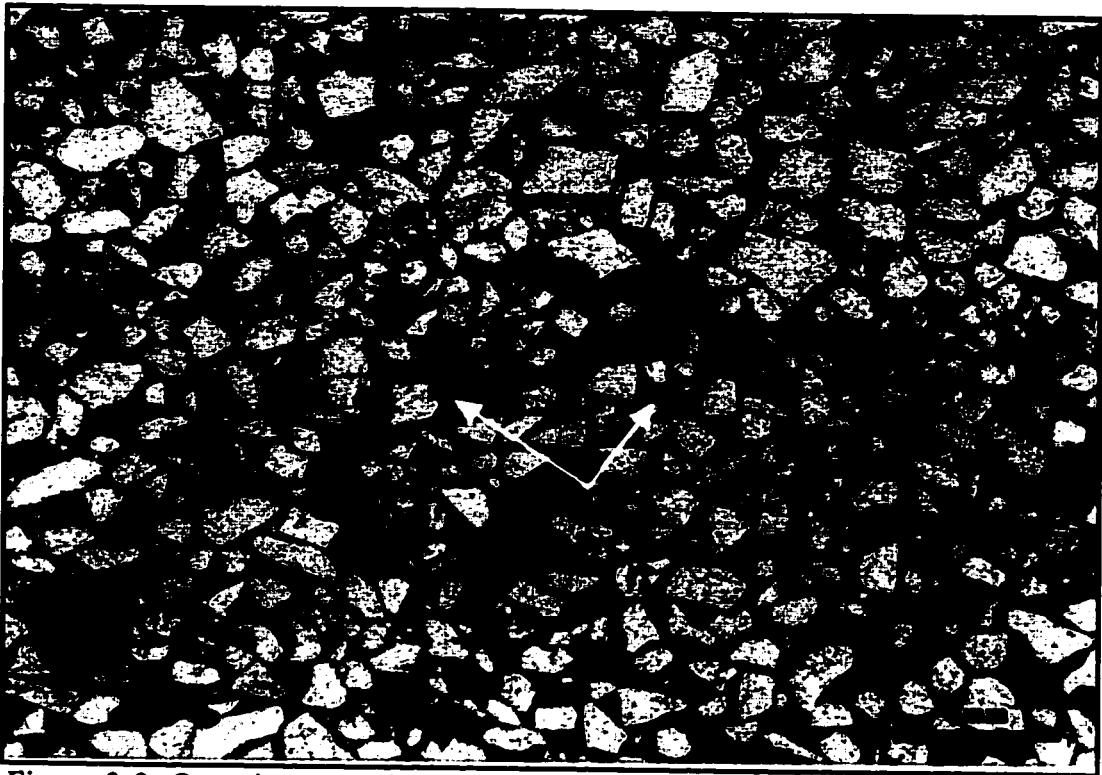


Figure 3-9: Organic matter lamina, Sample # 330, Well A, depth 14330 feet, plane polarized light.

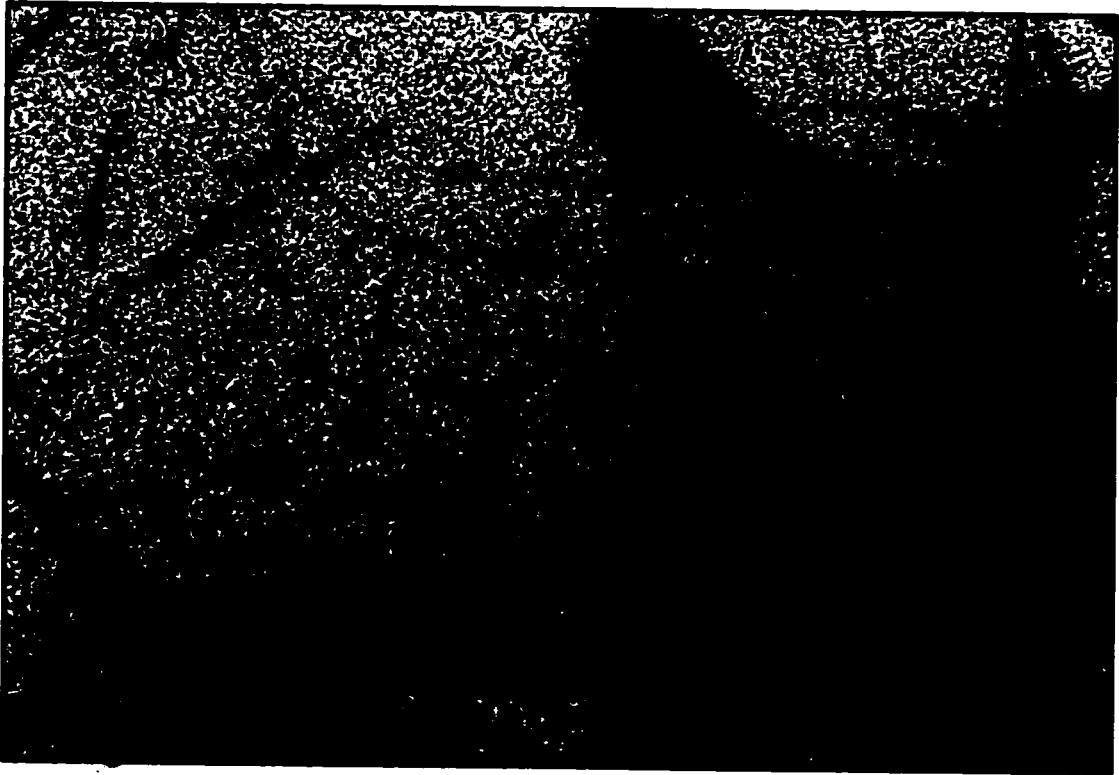


Figure 3-10: Carbonaceous materials coating (arrow) around the grains, Sample # 9, Well B, depth 14 312.4 feet, plane polarized light.

g) Matrix

Matrix is the fine-grained material (silt and clay particles) that is found in the pore space between larger sediment grains. The matrix is derived partly as detrital clay and silt and partly from the alteration products of unstable mineral grains that alter to clays and other minerals during diagenesis. Based on petrographic microscopy, Jauf Formation sandstones are relatively immature to mature comprising matrix content of <1 % to 35% with average of 6% (Figure 3-11). The mineralogical composition of matrix is mostly clay minerals.

3.1.2.2. Authigenic Component-Cement

Cement is defined as any chemically precipitated material formed after deposition and occurring in the interstices of rocks.

The sandstones of the Jauf Formation in Well A and B have a number of pore-filling, grain-replacing and grain-coating cements. Important cements in these sandstones are calcite, illite, chlorite and quartz. Among the minor to trace cement are pyrite, mixed illite-smectite. These were studied under petrographic microscopy, SEM and XRD techniques and are described below:

3.1.2.2.1. Calcite

Calcite is one of the most common and important cement in the Jauf Formation Sandstone in Well A and Well B. Highly cemented sandstones contain 16 to 30 % calcite cement. Calcite is distinguished in thin section by its variable relief on rotation of the stage. It appears to "twinkle" when the stage is rotated. Calcite cement can be seen in thin-section in two modes: i) poikilotopic and ii) isolated patches. The poikilotopic calcites are large calcite crystals enclosing several framework grains. In some cases the

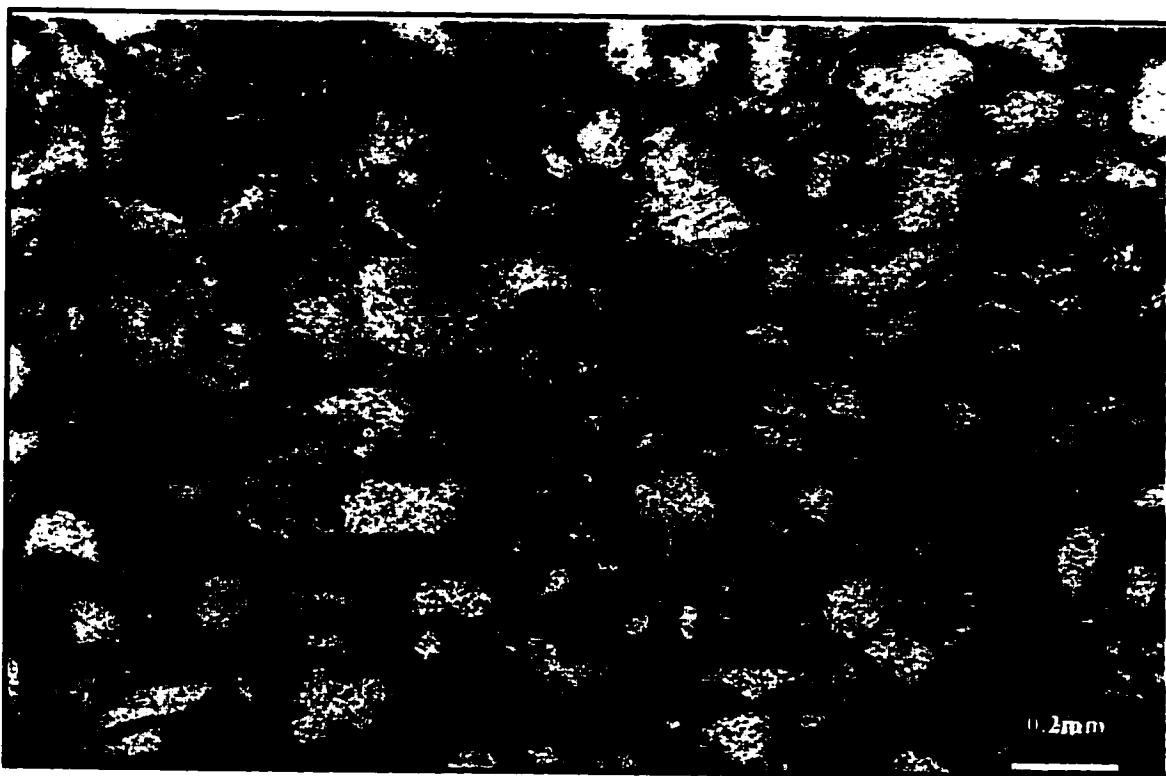


Figure 3-11: High matrix content of 30 %, sample # 361, Well A, depth 14361 feet, plane polarized light.

poikilotopic calcite occupies the total pore space and completely destroy the porosity. More commonly, however, the poikilotopic calcite occurs in patches within the sandstones.

In the studied samples, a typical example of poikilotopic calcite cemented sandstone is shown by sample 373.6 and 380 with calcite cement constituting 17% and 10% respectively (Figure 3-12 and 3-13). There is little grain-to-grain contact and the grains are 'floating' in calcite groundmass. There is no sign of mica bending or any evidence of a degree of compaction in the sandstones. From the above it appears that the calcite cementation must have been taken place at a very early stage of burial i.e. at a shallow depth when only minimum degree of compaction affected the rock.

More commonly, calcite cement occurs as isolated pore-filling and grain-replacing mode (Figure 3-14). In these cases calcite cement generally comprises 1 to about 5 % of the rock components. These sandstones have evidences of advanced stage of compaction (mica bending, sutured contacts, long contact and etc) and calcite cements appear to have formed after the compaction.

The late calcite cement replaces detrital grains preferably quartz and feldspar. Due to extensive replacement it is common to find detrital grains with corroded boundaries. Also, extensive replacement of silicate grains is evidenced by the occurrence of remnant or skeletal grains within calcite cement (Figure 3-15 and Figure 3-16).

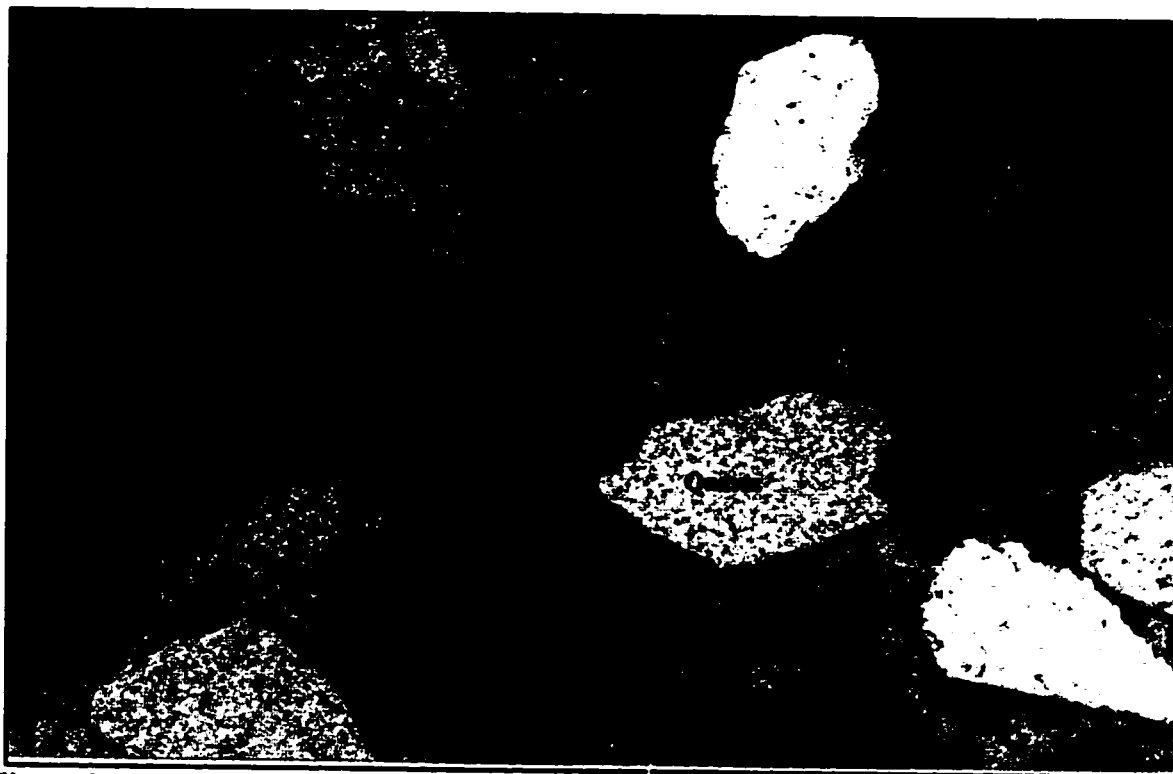


Figure 3-12: Pervasive poikilotopic calcite cement (PC), sample # 373.6, Well A, depth 14373.6 feet, cross polarized light.

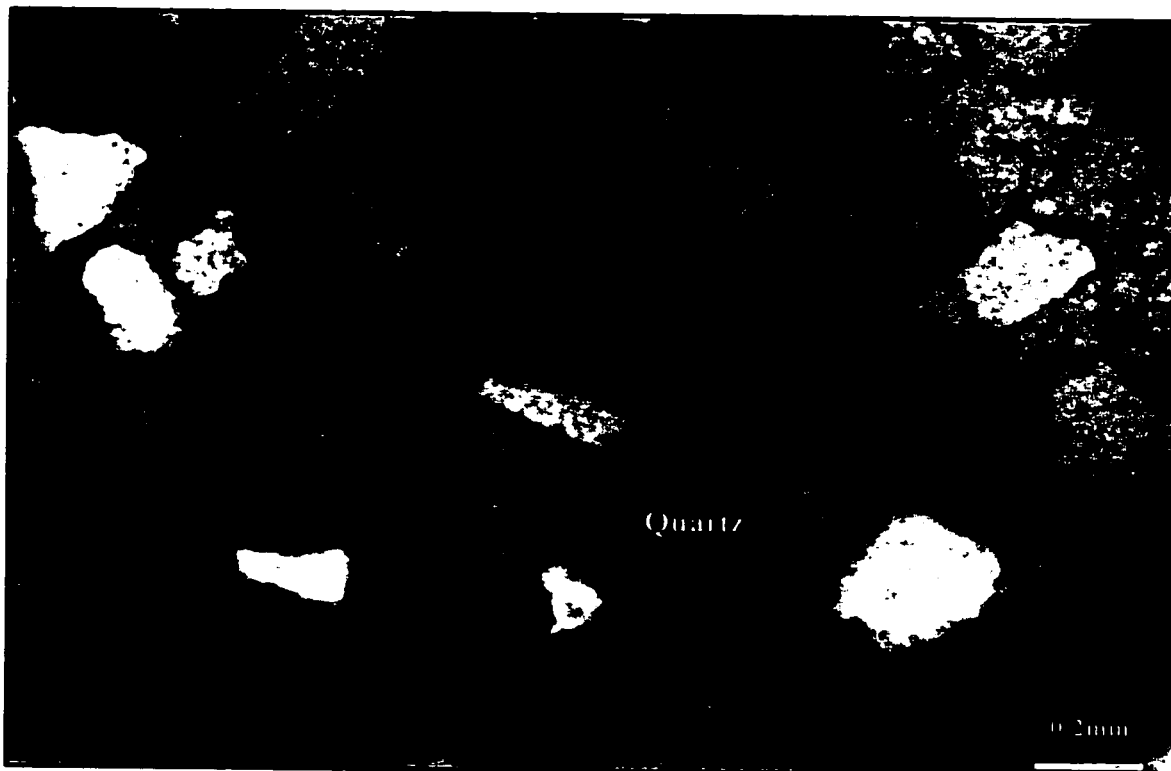


Figure 3-13: Pervasive poikilotopic calcite cement (PC), sample # 380, Well A, depth 14380 feet, cross polarized light.

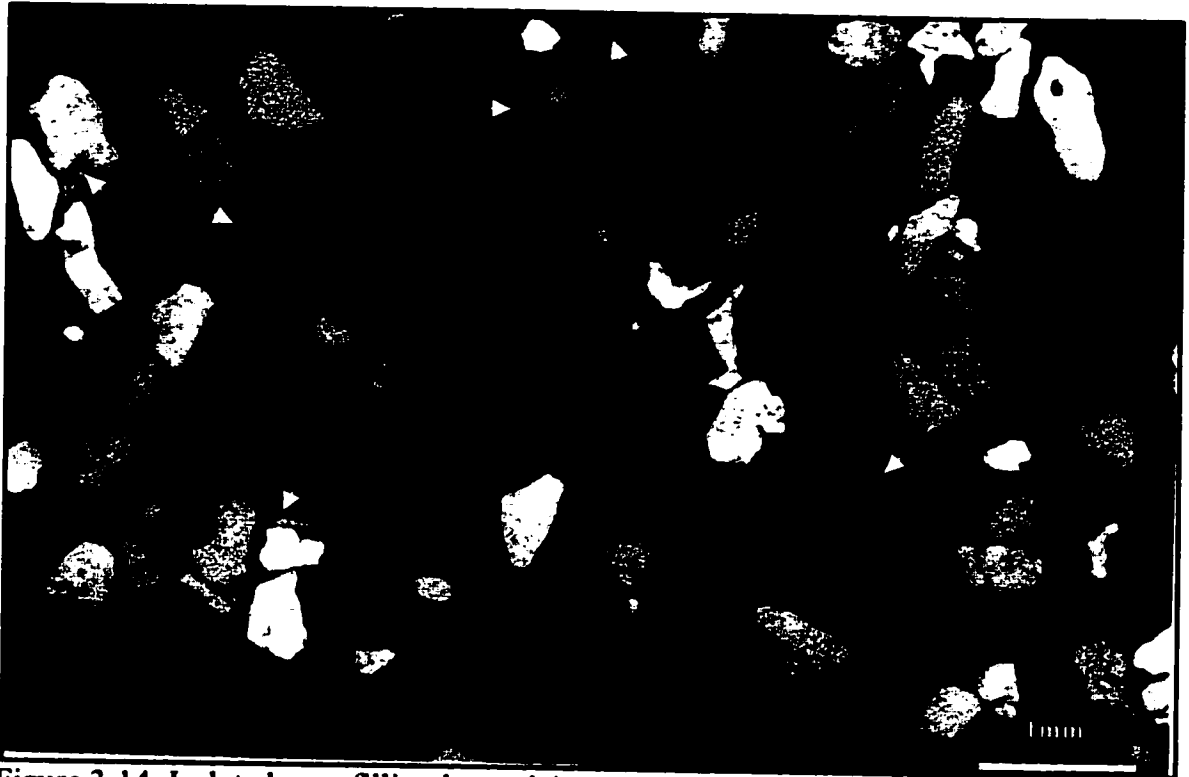


Figure 3-14: Isolated pore filling late calcite cement, sample # 3, Well B, depth 14122.6 feet, cross polarized light.



Figure 3-15: Replacement of silicate grains is evidenced by the occurrence of remnant within calcite cement. Sample # 3, Well B, depth 14122.6 feet, cross polarized light.



Figure 3-16: Isolated pore filling late calcite cement (IC), sample # 390.7, Well A, depth 14390.7 feet, cross polarized light.

3.1.2.1.2.2. Clay Cements

Clay minerals can precipitate in pores as well as form detrital matrix. Clay mineral cements typically form rims around grains, but can also fill (occlude) the porosity. The different clay minerals (e.g., smectite, illite, kaolinite, chlorite) each grow under specific physical and chemical conditions. Authigenic clay minerals that form at shallow depths may alter to other clay minerals as the temperature increases and pore fluids change composition with burial. The manner in which clays are distributed in the pore space has an important bearing on its effect on permeability. Pore-lining and pore-filling clays will greatly reduce the permeability while the replacement or fracture-filling clays will have less effect. The clay minerals have different morphology that makes them easy to identify (Wilson and Pittman, 1977). Characterizing the clay minerals present in reservoir sandstone can be an important aspect in the understanding of petroleum reservoir quality (Eslinger and Pevear, 1988).

In the presently studied samples illite, chlorite and illite/smectite mixed layers clay are identified, and these occur in the above order of abundance. Clay minerals are identified by thin section petrography, SEM and XRD techniques as described below.

a) Illite Cement

Illite is a hydrous group of clay minerals. Illite is fibrous and occupies more of the pore space for a given mass of clay. Fibrous or flaky Illite often bridging the pores also offers a high resistance to fluid flow through the sandstones (Wilson and Pittman, 1977).

In the present study, illite is the most important clay mineral in most of the samples and occurs as pore-linings deposited on the surfaces of grain-to-grain contact (Figure 3-17). The illite fine coatings form dust lines between quartz grain and quartz

cement. In thin section, illite is recognized by bright white high birefringent line around grain surfaces (Figure 3-18). Illite is well represented in SEM as fibrous, lath-like habit, which testify the authigenic origin of the illite cement (Figure 3-19). In some rare instances illite occurs as pore bridging cement providing additional evidences in of the authigenic origin of the illite cement (Figure 3-20). In the XRD profiles, illite is represented by a series of basal 001, 002 and 003 reflections at 9.97-10.1 A°, 4.98-5.01 A° and 3.32-3.34 A°, respectively, that are not affected by glycolation (Figures 3-21).

b) Chlorite Cement

Chlorite is a platy, pale green mineral of the mica group of sheet silicates and is considered to be a type of clay mineral found in sedimentary and low-grade metamorphic rocks. Chlorite is a common cementing minerals in the studied samples and occurs in two forms i.e. i) grain coating or lining mode and ii) pore-filling mode. Pore-filling clay plug interstitial pores and the individual flakes, or aggregates of flakes, exhibit no apparent alignment relative to the detrital grain surfaces as shown in Figure 3-22.

Chlorite rims, the most common form, are very thin and are visible in thin section as brown coating around grain surfaces (Figure 3-23). Under SEM, the chlorite coatings are seen as delicate platelet crystals standing more or less perpendicular to the grain surfaces (Figure 3-24). The delicacy and position of the platelets with respect to the grains testify the authigenic origin of chlorite cement. The absence of silt component (monomineralic nature) is a reliable criterion that testifies the authigenic origin of clay cement in sandstone. The pore-filing chlorites are seen as rosettes or crystal aggregates within the pores (Figure 3-25).

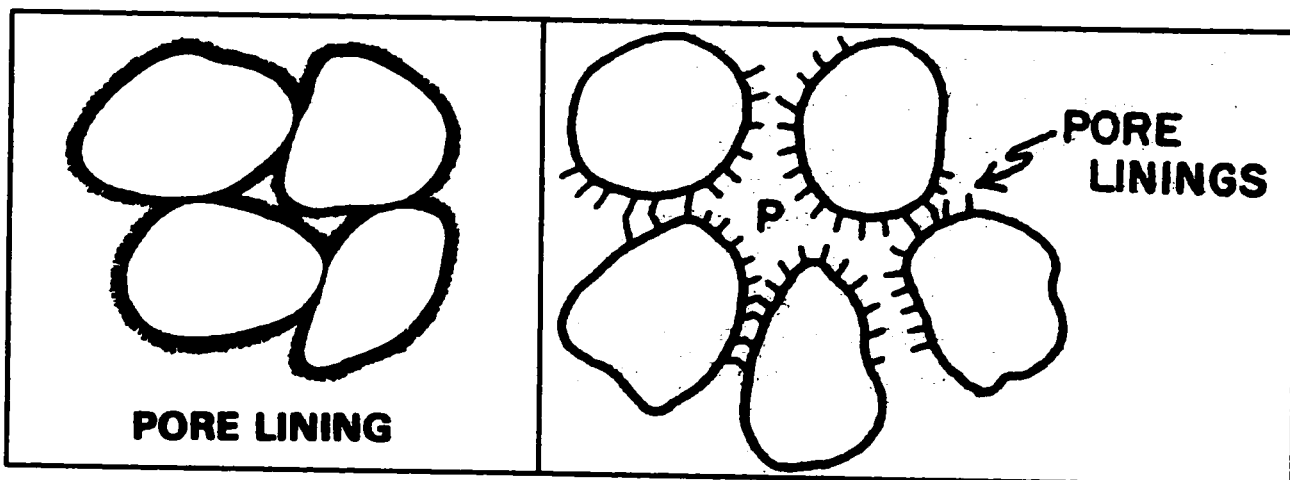


Figure 3-17: Complete pore linings on the surfaces of grain-to-grain contact (right); partial pore lining (left).



Figure 3-18: Illite coating showing the bright white high birefringent line around grain surfaces, Sample # 354, Well A, depth 14354feet, cross polarized light.

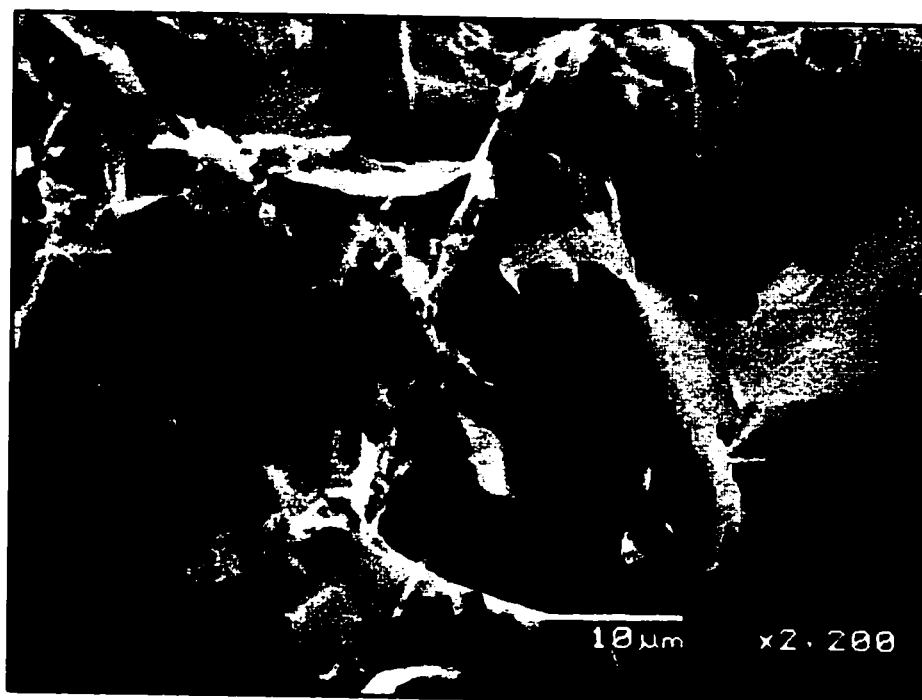


Figure 3-19: Authigenic illite cement forming fibrous-like form, sample #487, Well A, depth 14487 feet.

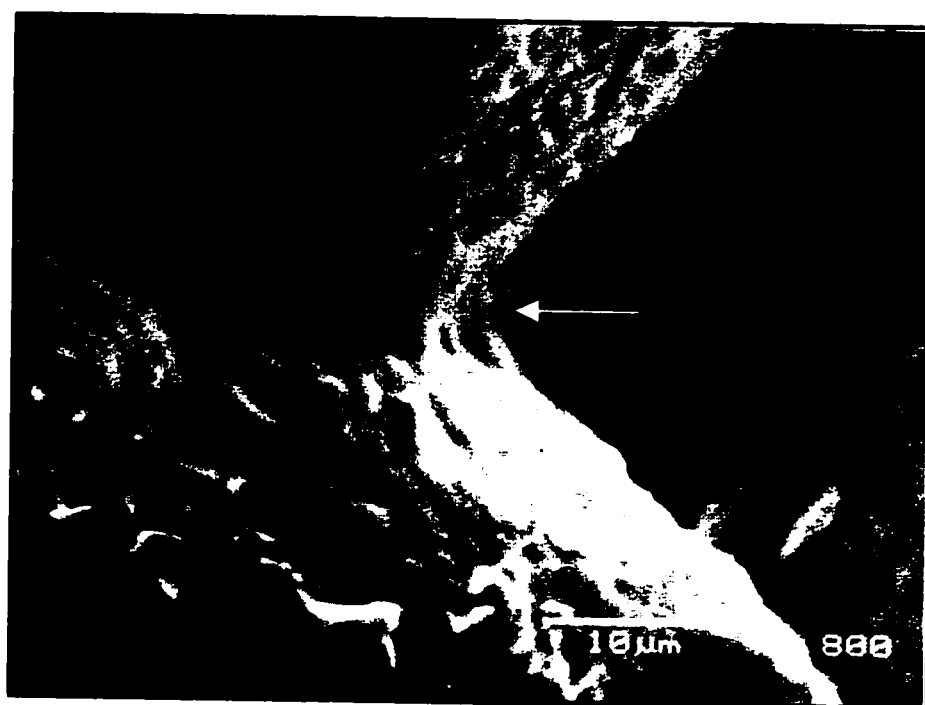


Figure 3-20: Illite occurs as pore-bridging cement, sample #4, Well B, depth 14132 feet.

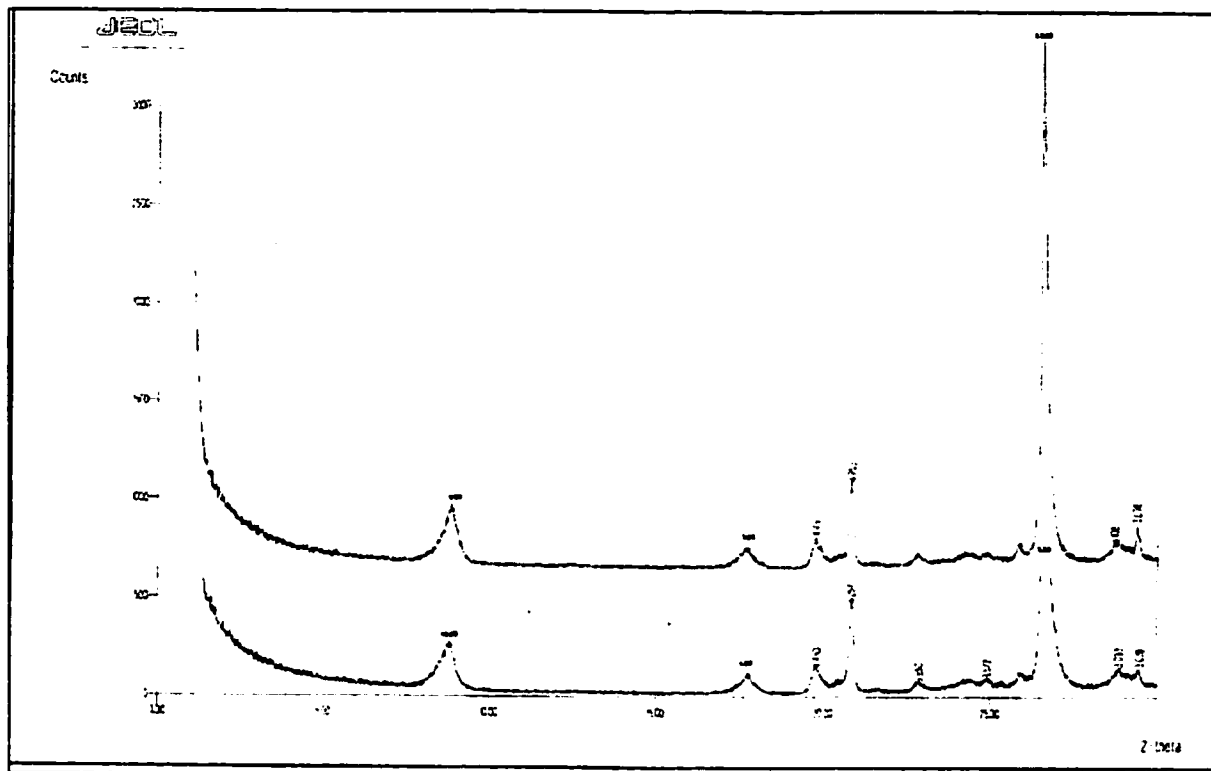


Figure 3-21: XRD profile of sample # 538 showing illite represented by a series of basal 001, 002 and 003 reflections at 10.1 Å, 4.98 Å and 3.34 Å respectively that are not affected by glycolation.

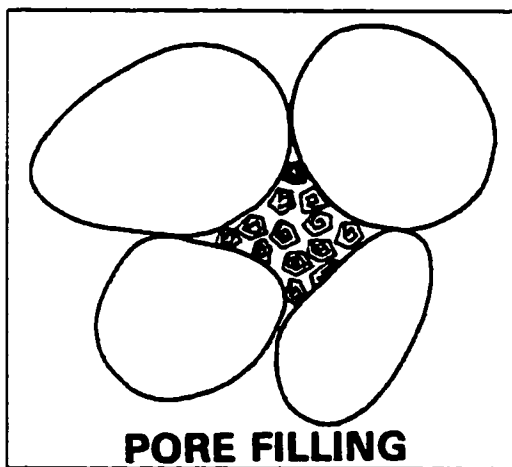


Figure 3-22: Pore-filling clay plug interstitial pores.

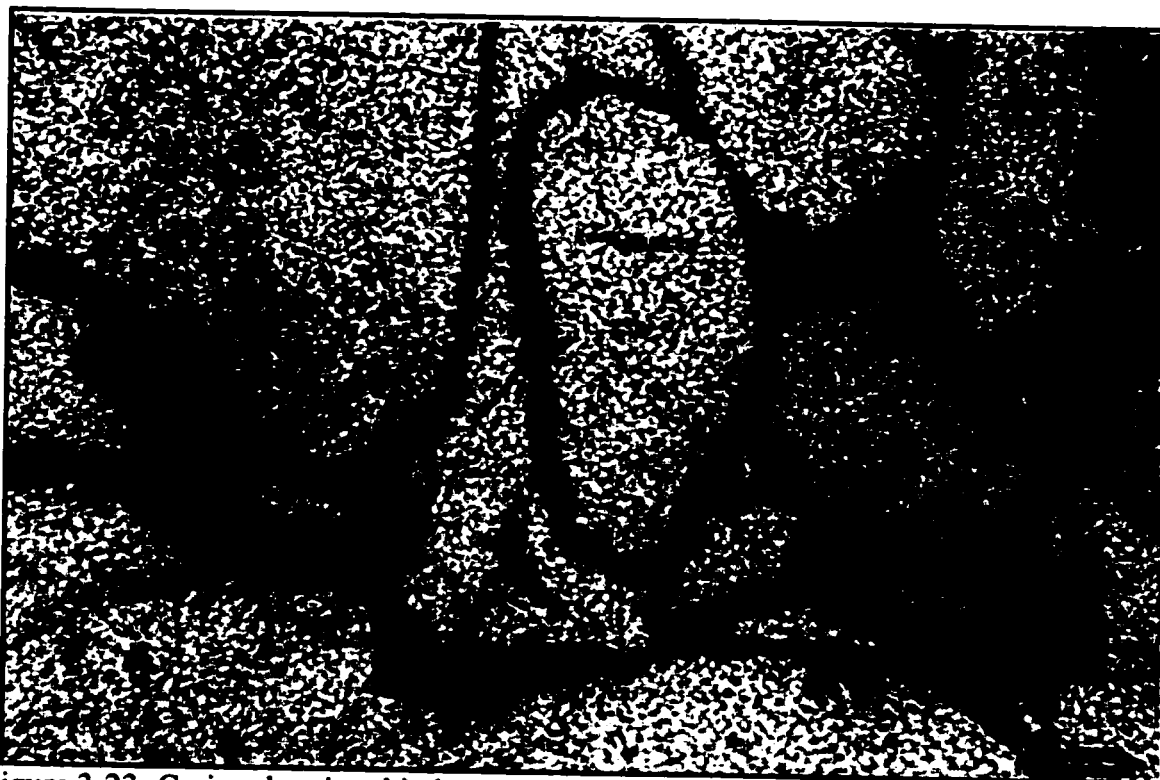


Figure 3-23: Grains showing thin brown coating of chlorite (arrow), Sample #404, Well A, depth 14404 feet, plane polarized light.



Figure 3-24: Overall view of quartz grains coated by chlorite cement with quartz overgrowths (arrows) in the left hand side of the micrograph, sample #394, Well A, depth 14394 feet.

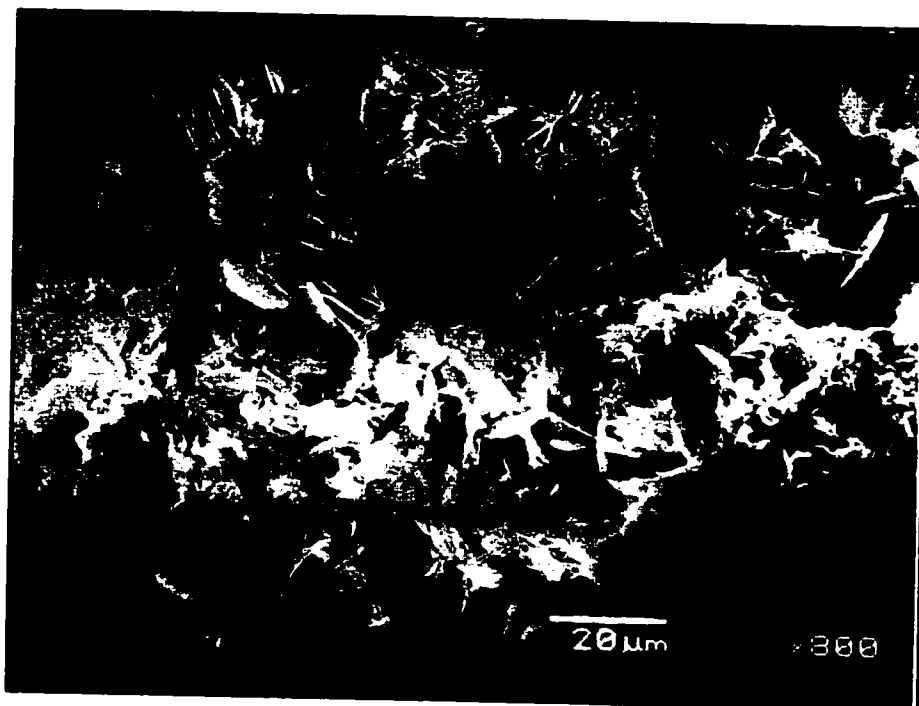


Figure 3-25: Closer view of the Figure 3-24 showing the rosettes of chlorite pore filling, sample #394, Well A, depth 14394feet.

C) Illite/Smectite

Occasional presence of mixed layers illite-smectite mixed layer (I/S) forms complete but thin coatings around detrital grains and are seen in thin-section as brownish color and moderately high birefringence of clay film. Under the SEM, I/S show corn flake with short lath like morphology and occurs as pore-filling masses as well as grain coatings (Figure 3-26).

3.1.2.2.3. Pyrite

Pyrite (FeS_2) can precipitate from fluids rich in sulfur under reducing conditions. Pyrite occurs as opaque, black individual cubic crystals and framboidal aggregates along grains boundaries. Framboidal pyrite is a common mineral texture found in sediments forming a cluster (look like a colony of pyrite) of fine-grained aggregates of euhedral to subhedral pyrite grains.

Pyrite occurs in small quantities in most of the samples and is especially abundant in shaly samples (Figure 3-27). The morphology of the pyrite crystals is distinctive and could easily be recognized in the thin-section microscopy as opaque in reflected light. Pyrite cements comprise 1% to 4% of the rock components and the amount of pyrite does not affect the reservoir quality in the sandstones. Pyrite is commonly associated with carbonaceous grain-rich sandstones.

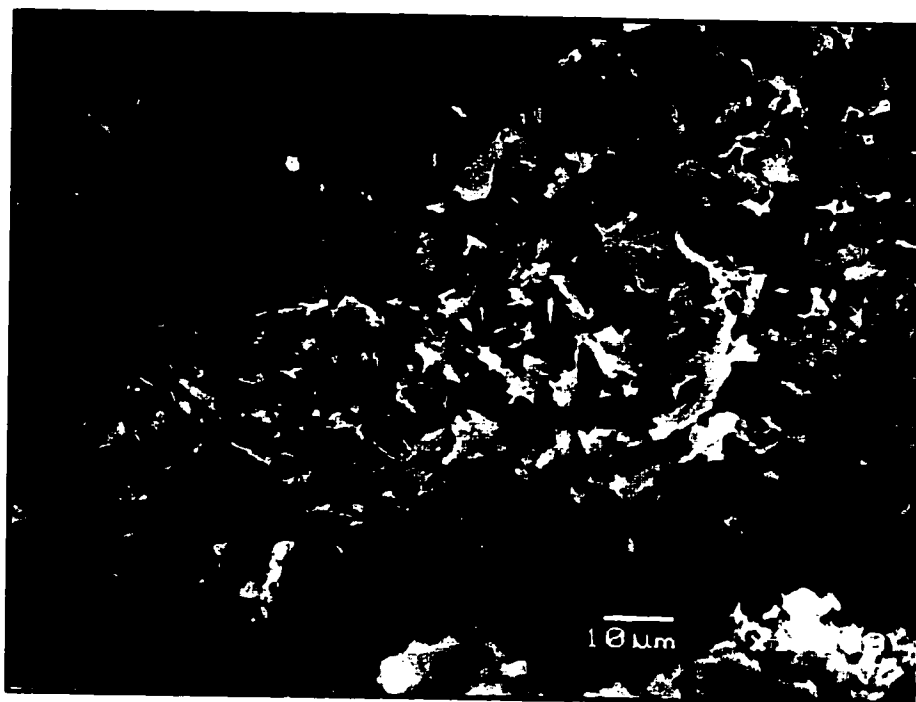


Figure 3-26: SEM image showing authigenic illite /smectite, sample # 511, well A, depth 14511 feet.

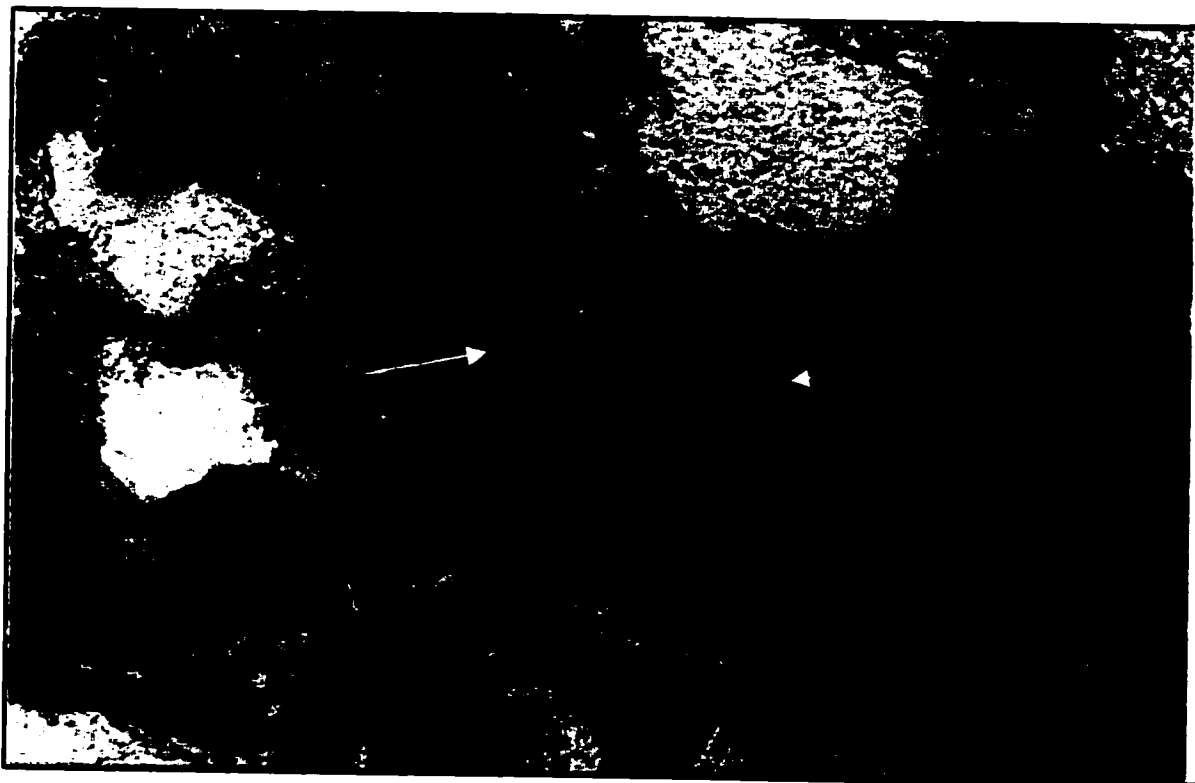


Figure 3-27: Pyrite cement (arrows) in sample #323, Well A, depth 14323feet, cross polarized light.

3.1.2.2.4. Quartz Overgrowth

Quartz cement in siliciclastic sequences is commonly a major diagenetic phase that affects hydrocarbon reservoir quality. Quartz cement occurs as overgrowths on detrital grains (Pittman, 1979). Identification of quartz cement is often difficult because it occurs in optical continuity with the detrital grain. Quartz cements have been distinguished by the following criteria (1) the presence of lines of impurities or dust rims on the surfaces of original quartz grains (Figure 3-28); (2) euhedral forms where the overgrowths have developed in open pore spaces specially seen clearly in SEM (Figure 3-29).

Distribution of quartz cement in Jauf Formation sandstones was determined by standard thin-section petrography, and scanning electron microscopy (SEM) with energy dispersive X-ray Spectrometer (EDX). Quartz cement is more commonly observed in SEM than thin section. This is because of the absence of the dust rims on the surfaces of quartz grains. Quartz overgrowth cement is important cement in Jauf Formation and generally ranges from zero to 4% although there are two samples (Samples # 519 and 9), which contain 8% quartz cement. Quartz overgrowths grew into the primary pores, largely filling them. Two forms of quartz overgrowths have been observed as follows: 1) an early stage of development referred to as incipient growth (Figure 3-30) and 2) an advanced stage of development referred to as terminated growth (Figure 3-31).

Quartz cement appears to be more common in quartz-rich samples and samples with concavo-convex and sutured contacts. It is presumably because pressure solution is contributing to the formation of quartz overgrowth.



Figure 3-28: Silica cement in the form of syntaxial quartz overgrowths (White arrows). Clay dust rims (Blue arrows) separate cement from detrital grains, sample # 487, Well A, depth 14487, cross polarized light.

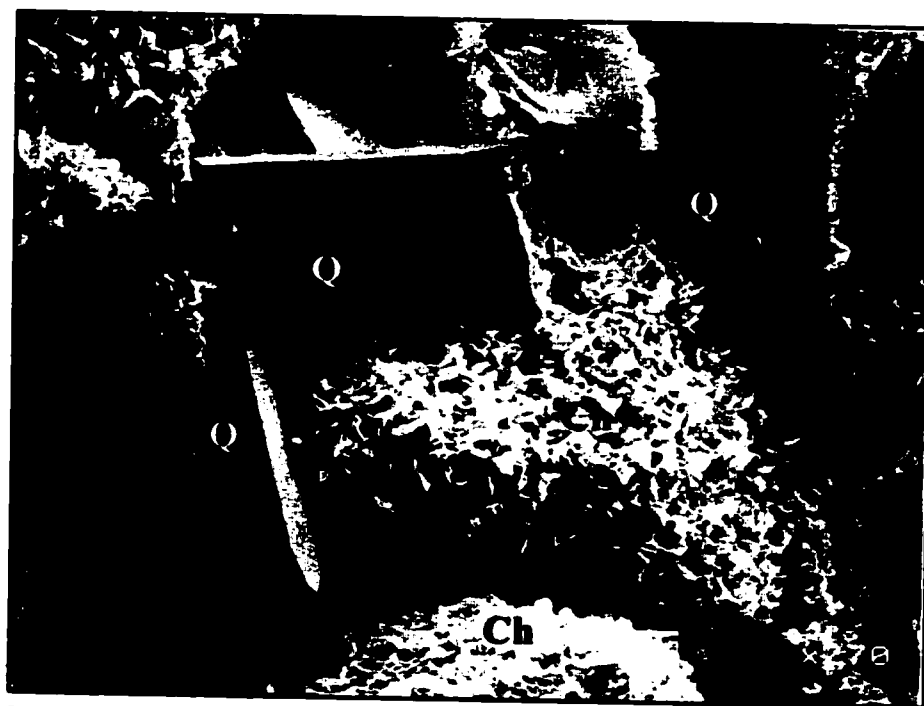


Figure 3-29: Well developed authigenic quartz crystal (Q) in region of abundant authigenic chlorite (Ch). Quartz crystals grew into areas of continuous chlorite coating until they were physically blocked, sample #394, Well A, depth 14394feet.

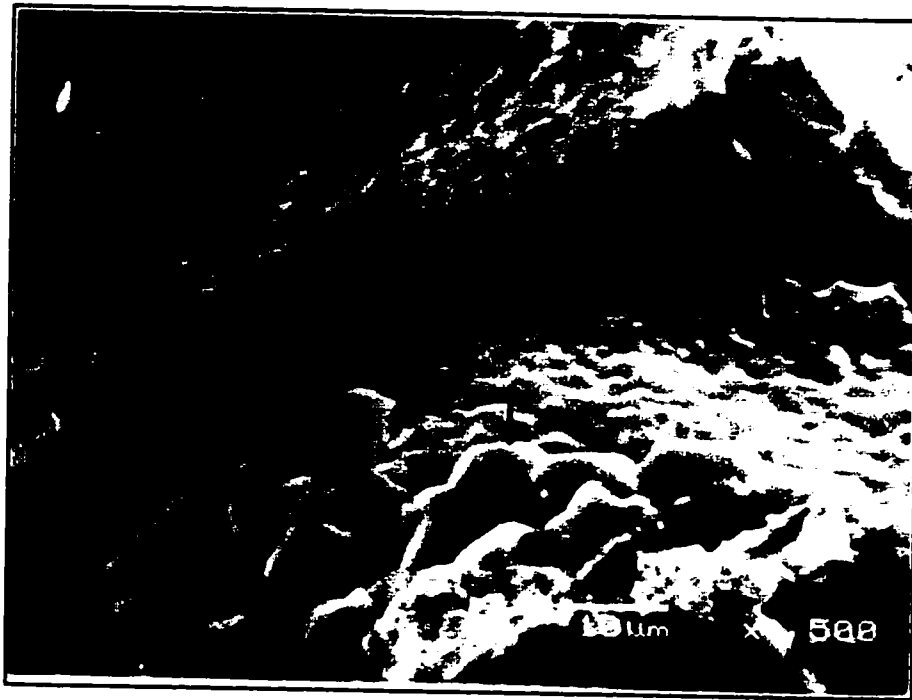


Figure 3-30: An early stage of development of quartz overgrowth referred to as incipient growth (arrows), sample # 4, Well B, depth 14132 feet.

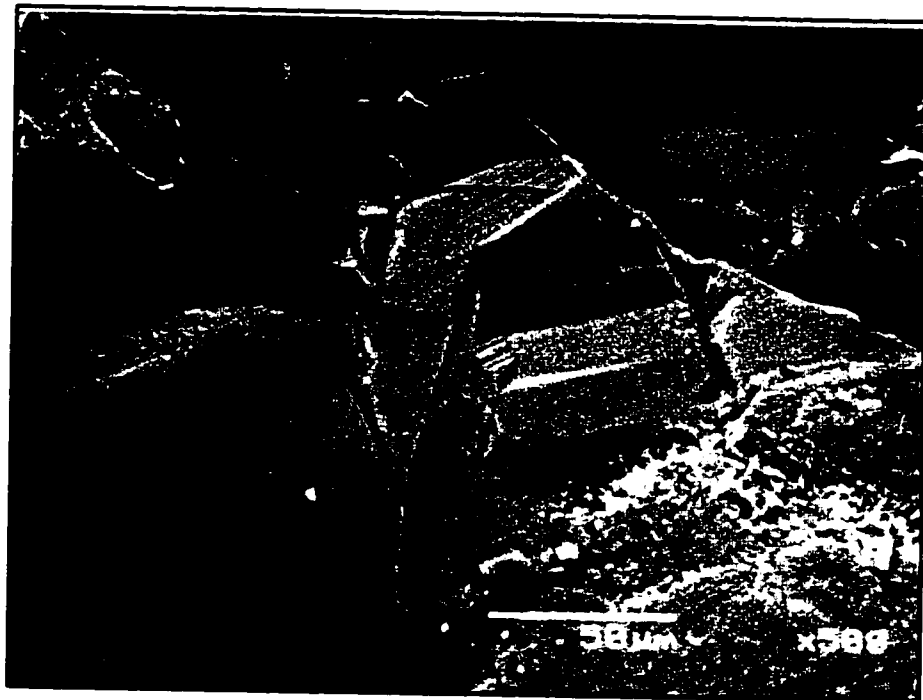


Figure 3-31: An advanced stage of development of quartz overgrowth referred to as terminated growth, sample #519, Well A, depth 14519 feet.

3.2. Petrographic Characteristics of Surface Samples

The Jauf Formation from the three studied outcrops consists of both very fine-grained sandstones and siltstone (Figure 3-32). The average composition percentages of the field samples are presented in Table 4.

The detrital mineralogy of the sandstones and siltstone is dominated by very fine quartz grains with little to trace feldspar. The field samples contain an average of 70% quartz, 1% feldspar and 0 % lithic fragments. A small to trace amount of organic or carbonaceous materials are present in most of the samples (average 1 %). Heavy minerals are rarely present as accessory components (Figure 3-33).

Based on petrographic microscopy, sandstone samples in the field is immature comprising matrix content of 15% to 30% with average of 18 % (Figure 3-34). The mineralogical composition of matrix is mostly clay minerals.

Micas are major component in the samples especially biotite and muscovite. Micas are more common in very fine-grain sandstones and siltstone. Flaky biotite constitutes 1 to 20 % with average of 5% of the rock components. Muscovite comprises 1 to 3 % with average of 1 % of the rock components.

The types of cement present in the field samples are chlorite, calcite (Figure 3-35) and quartz in the above order of abundance (Table 4). Chlorite cement occurs as grain coating in Samples L1-6 and L1-7 (Figure 3-36).

A comparison of the textural attributes of the surface sample and subsurface samples is shown in Table 5.

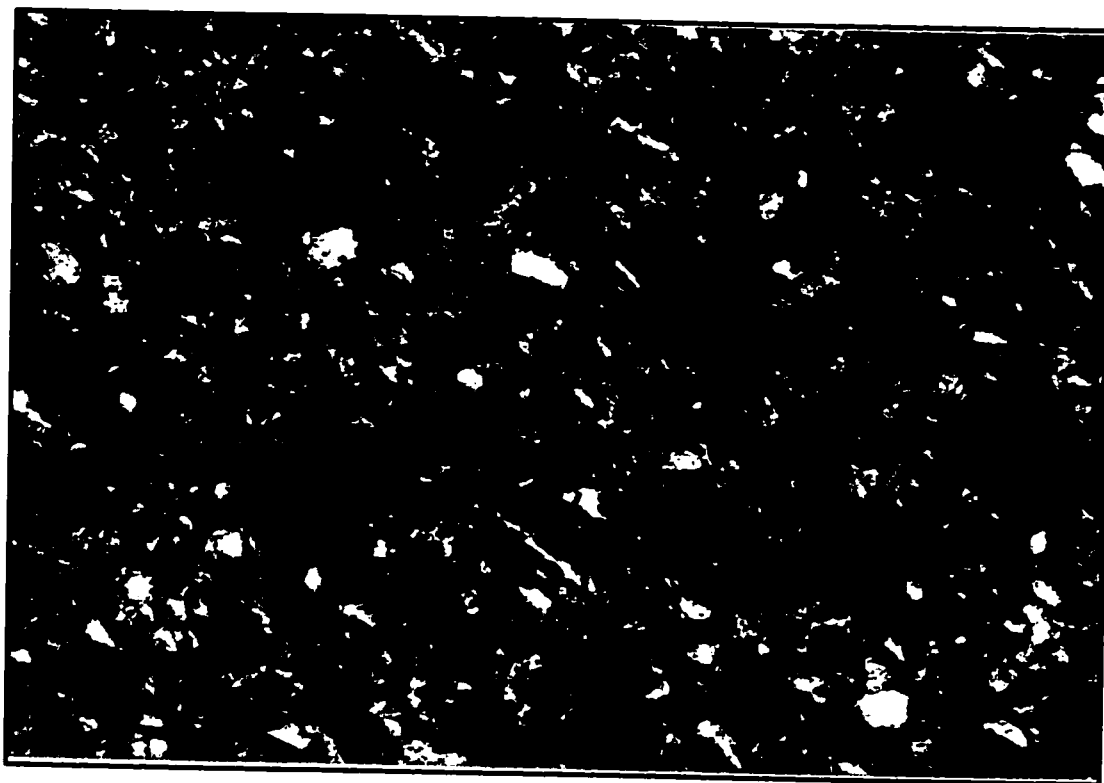


Figure 3-32: Siltstone with high matrix content, Sample # L2-5, cross polarized light.

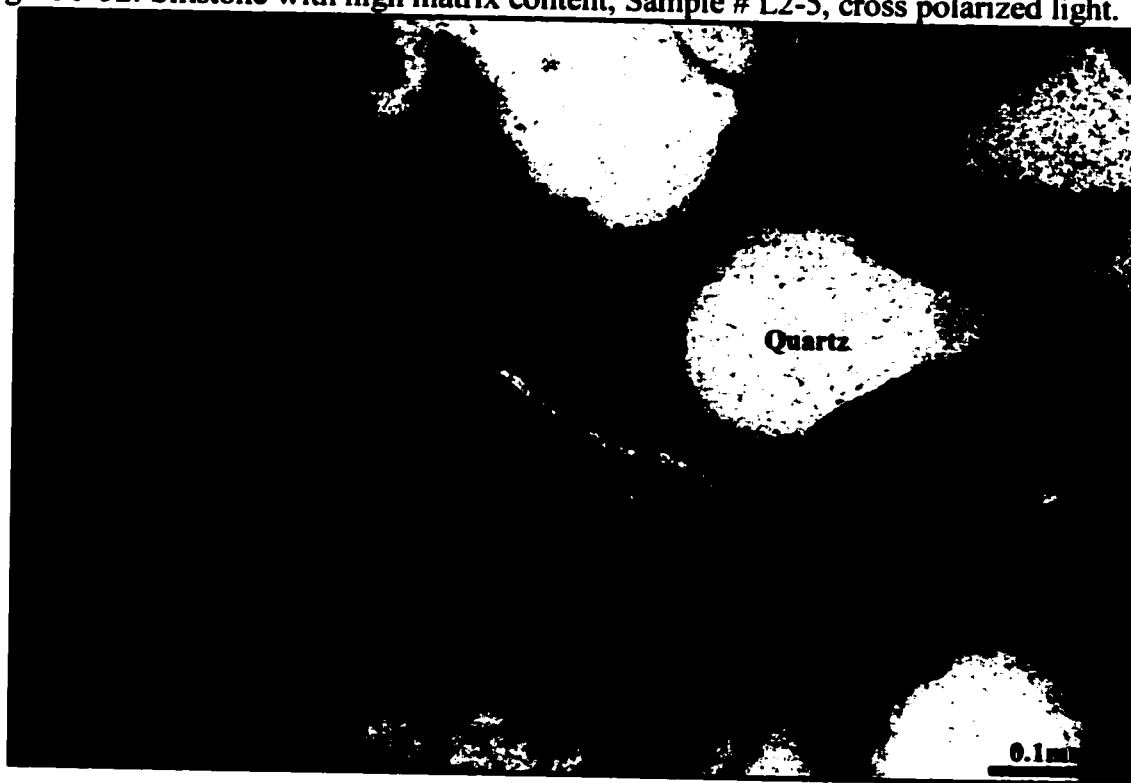


Figure 3-33: Zircon grain (Z) in very fine sandstone, Sample # L1-7, cross polarized light.

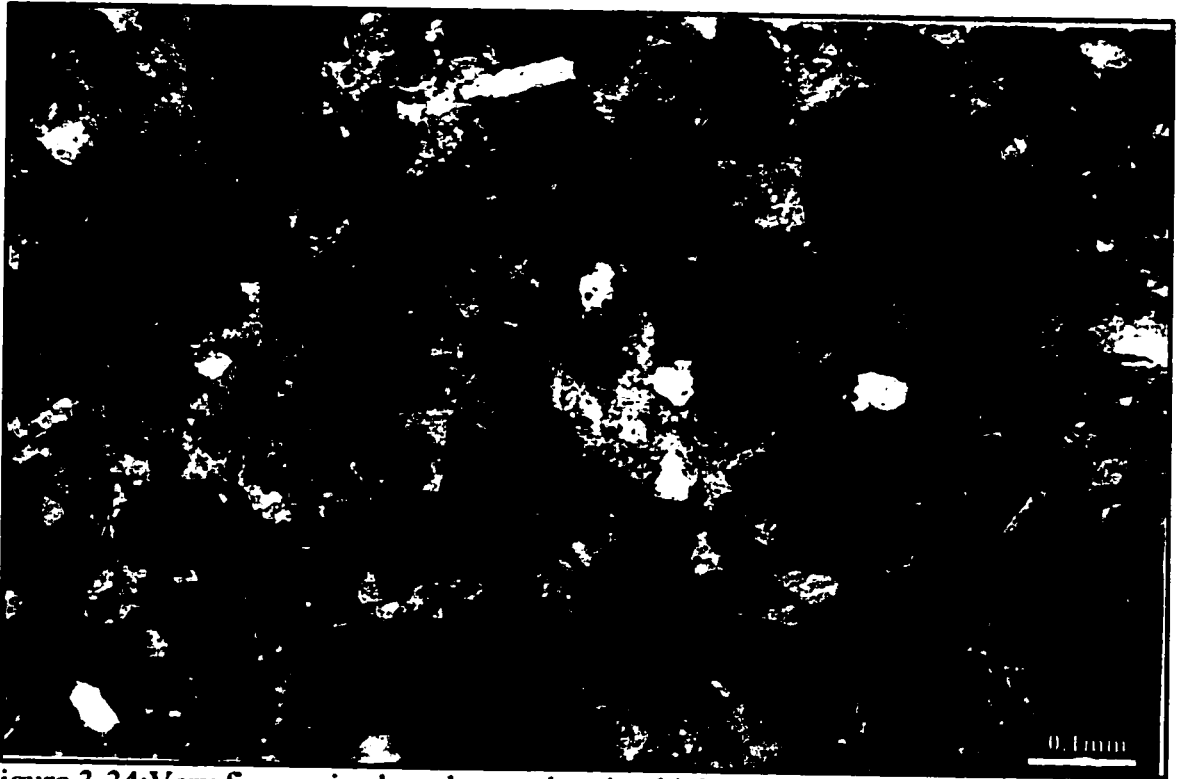


Figure 3-34: Very fine-grained sandstone showing high matrix content, Sample # L2-2, cross polarized light.

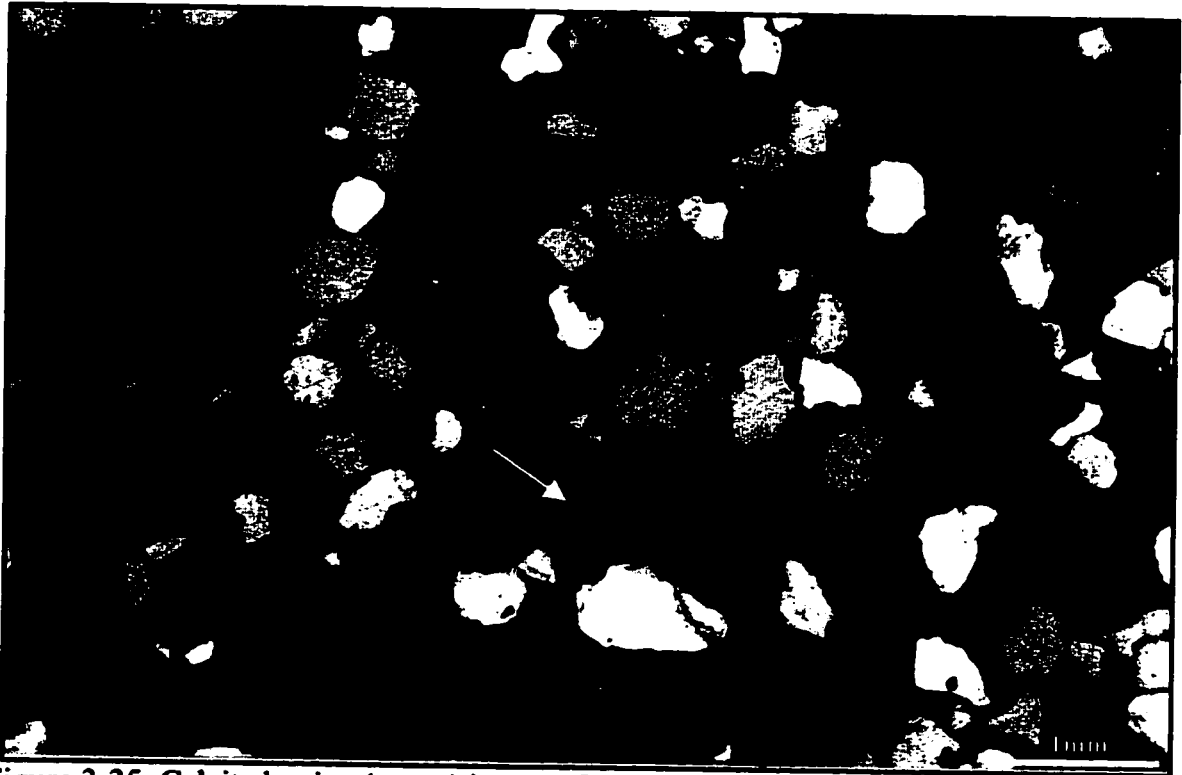


Figure 3-35: Calcite lamina (arrow) in very fine grain sandstone, Sample # L1-5, cross polarized light.

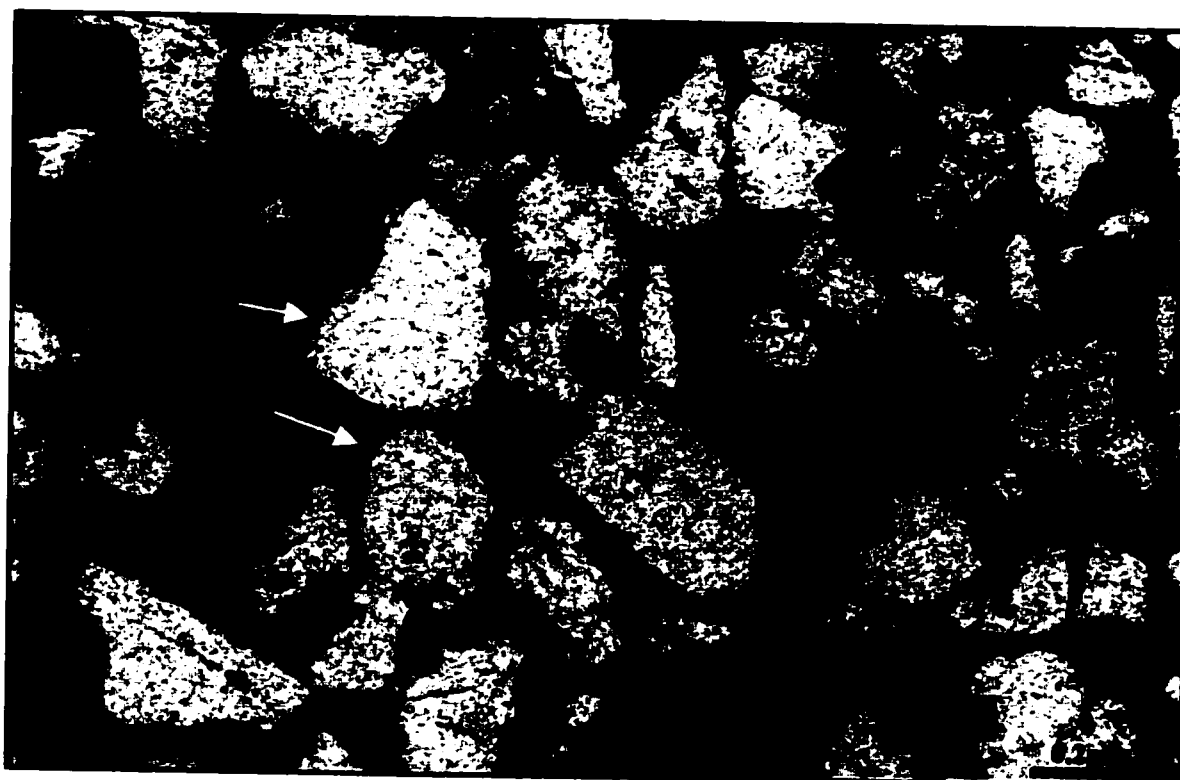


Figure 3-36: Chlorite coating (arrow) in fine grain sandstone, Sample # L1-7, plane polarized light.

Table 5: A comparison of the textural attributes of the surface and subsurface samples

	Attributes	Subsurface			Surface		
		Minimum	Maximum.	Average	Minimum	Maximum	Average
Composition	Quartz	55	96	77.5	43	85	69
	Feldspar	1	6	2	1	3	1
	Lithic Grains	0	0.1	Trace	0	0	0
Texture	Grain Size	75% fine to medium-grained 18% medium-grained 8% very fine-grained			42.8% very fine-grained 35.7% silt 21.4% fine-medium-grained		
	Grain Sorting	50% moderately-sorted 37% well-sorted 13% poorly-sorted			85.7% well-sorted 14.2% moderately-sorted		
	Matrix	<1	35	6	4	30	17
Cements	Calcite	1	30	2.5	3	35	2.7
	Quartz	1	8	0.7	1	2	0.2
	Illite	Trace	4	0.6	0	0	0
	Chlorite	1	7	1	6	8	1
	Pyrite	Trace	8	0.5	0	0	0
	Porosity	2	20	7	3	10	2

CHAPTER 4

DIAGENESIS OF JAUF FORMATION

4.1. Introduction

Diagenesis is the process that is responsible for alteration of freshly deposited sediments. In a very broad sense, diagenesis refers to all processes, physical, physico-chemical and chemical that take place in sediment after deposition and burial up to the beginning of metamorphism. The average of physical and chemical conditions included in diagenesis is 0-200 C° temperature, 1-2000 kg/cm² pressure and water salinities from fresh to brines twice as concentrated as the Dead Sea (340g/l) (Blatt, 1979). Depending upon the geothermal gradient the depth to which diagenesis zone extends below the surface may be up to 10,000 m or even more. The main processes of diagenesis include compaction, cementation, alteration and dissolution.

Since Walther (1893), diagenetic studies have been concerned with an extraordinary variety of chemical and physical interactions, each of which has the potential to significantly affect the final composition and texture of a sedimentary rock.

Larsen and Chilingar (1978), Hayes (1979), Blatt (1979) and McDonald and Surdam (1984) provide a variety of papers that indicate the scope and importance of diagenesis.

Hayes (1979) presented four truths about sandstone diagenesis. First, initial porosity of sandstone when deposited ranges from 35-40 % and permeability of several Darcys but during diagenesis, a dramatic reduction of original porosity and permeability take place. Second, a very large percentage of porosity is not primary porosity but it is secondary, created by the dissolution of detrital grains and authigenic cements. Third, the flow paths of diagenetic fluids through a basin, and the timing of fluid migration are the keys to predict subsurface distribution of sandstone porosity. And finally, the preburial, prediagenetic factors of provenance, depositional environments, and tectonic setting influence sand composition and texture that control mineral reactions and fluid flow rates.

4.2. Diagenesis in Jauf Sandstone

Diagenesis of Jauf Formation sandstone is documented under the following headings:

1. Compaction and pressure solution
2. Cementation
3. Alteration and replacement
4. Dissolution and secondary porosity.

4.2.1. Compaction

Compaction begins immediately after deposition and it takes place in response to overburden pressure in early burial level. As additional sediment accumulates the vertical stress on the sediment increases. This result in increased closed packing. Degree of compaction may be shown by the types of grain contacts. There are four kinds of grain contact in the samples (Figure 4-1): 1) point contact: initial stage of compaction is shown by point contact (Figure 4-2). This is followed by further compaction and result in 2) long contact which was observed in most of the samples investigated (Figure 4-3). With increasing compaction, the physical pressure lead to physico-chemical process of pressure solution. Pressure solution involves dissolution of grain at the point of contact by increased compactional pressure. It can be recognized by 3) concavo-convex contact (Figure 4-4) and 4) sutured contact (Figure 4-5). Pressure solution has played a profound effect on Jauf Formation sandstones as the dissolution of silica at highly stressed quartz grain contacts followed by precipitation of silica ions immediately adjacent to the contact (Figure 4-5). This movement of mass is believed to have reduced both intergranular porosity and permeability in sandstones.

Most samples show high degree of compaction as shown by long, concavo-convex and sutured contacts. However, there are some samples, which show apparent low degree of compaction as shown by point contact. But this does not actually indicate low compaction, because, these are formed by dissolution of rock components (See section 4.4).

Further evidence of compaction is grain deformation. Framework grains in Jauf sandstone are grouped into two types: 1) rigid (hard) grains such as quartz, feldspar and

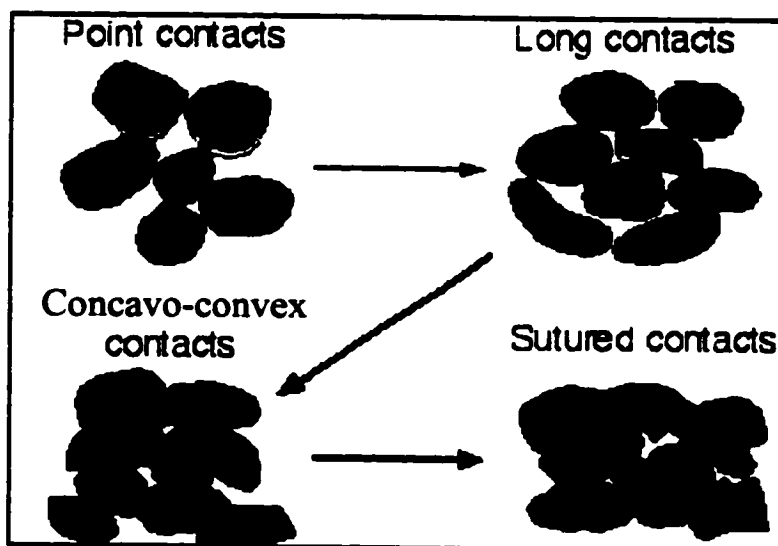


Figure 4-1: Physical behavior of sediments during compaction.

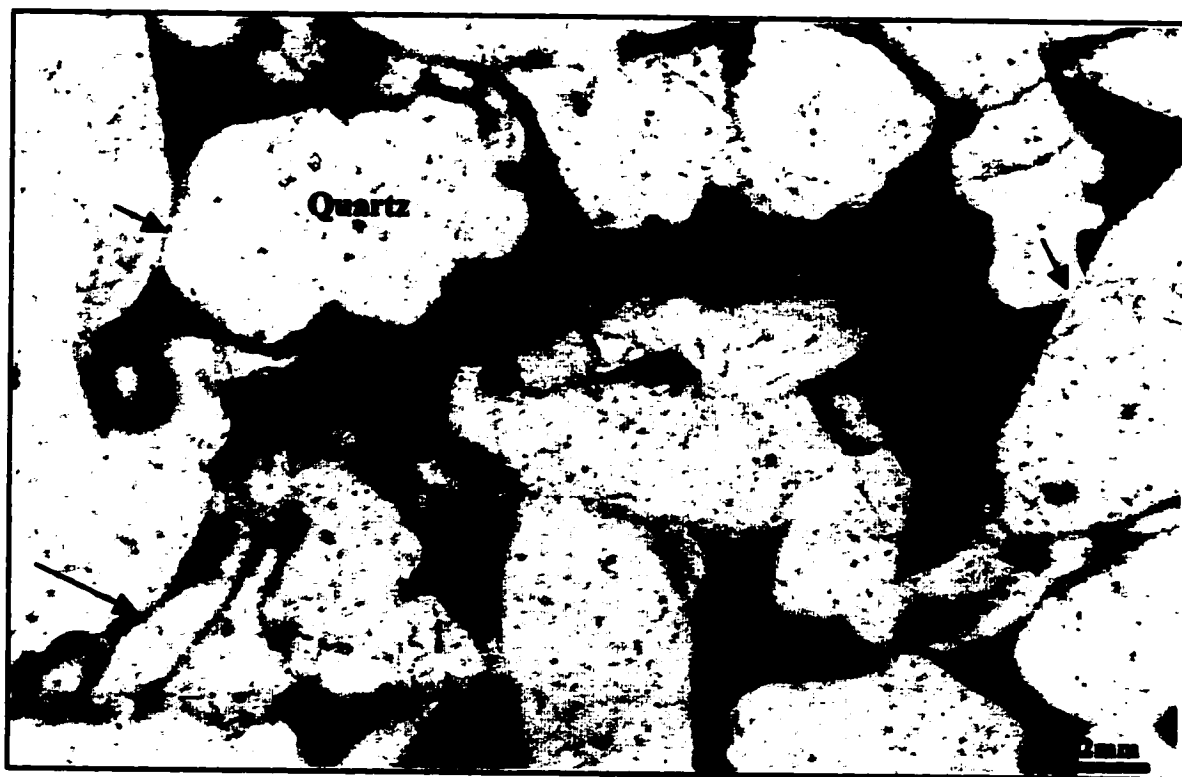


Figure 4-2: Point contact between quartz grains, sample #365, Well A, depth 14365 feet, plane polarized light.

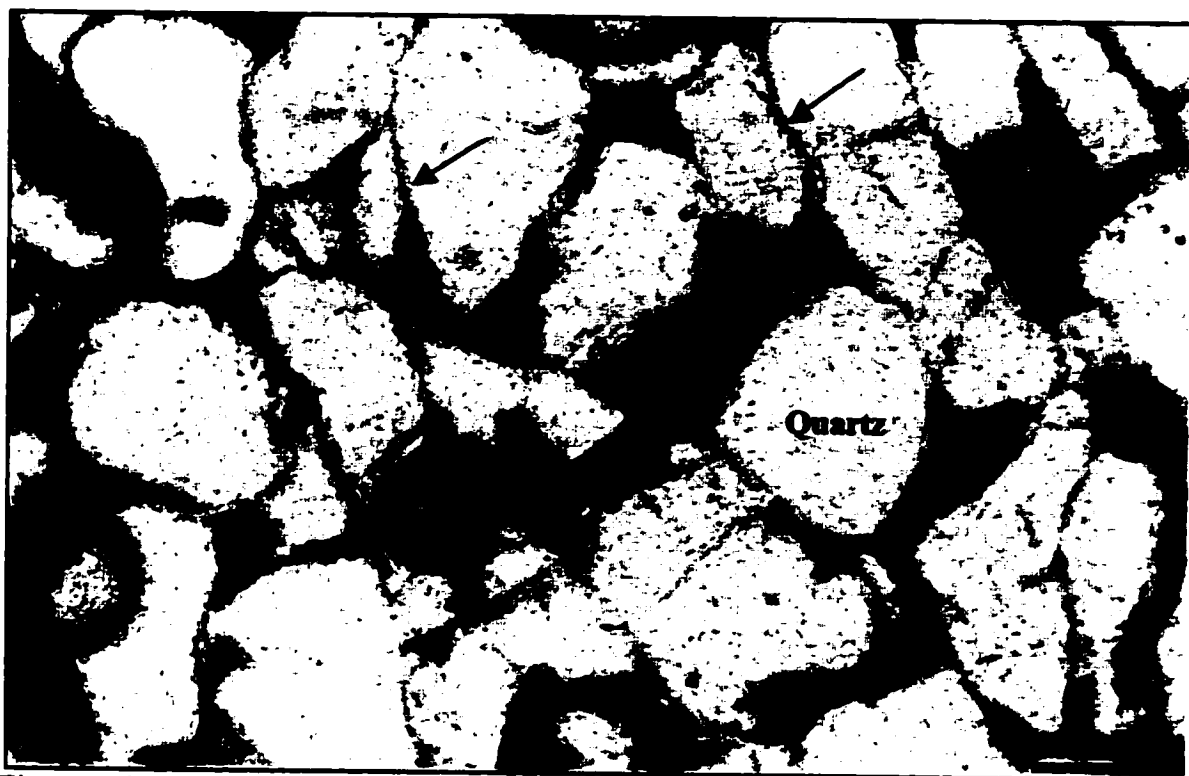


Figure 4-3: Long contact between quartz grains, sample #369.8, Well A, depth 14369.8 feet, plane polarized light.

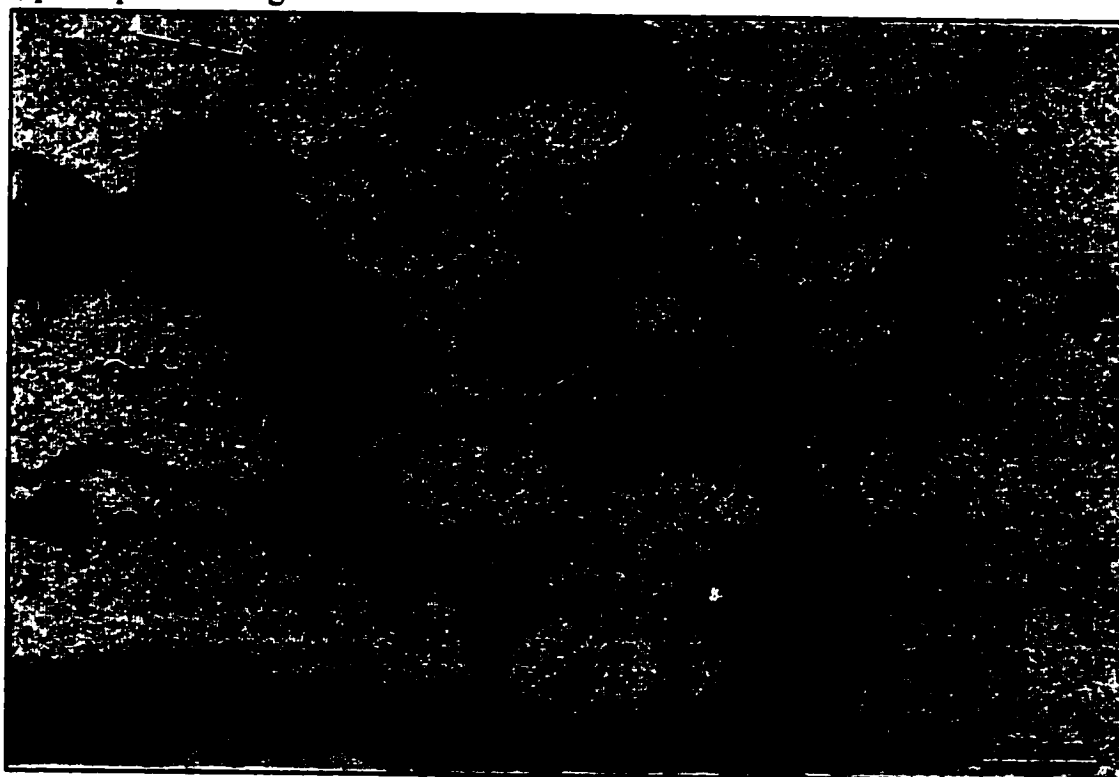


Figure 4-4: Concavo-convex type of contact, sample # 373.6, Well A, depth 14373.6 feet, plane polarized light.

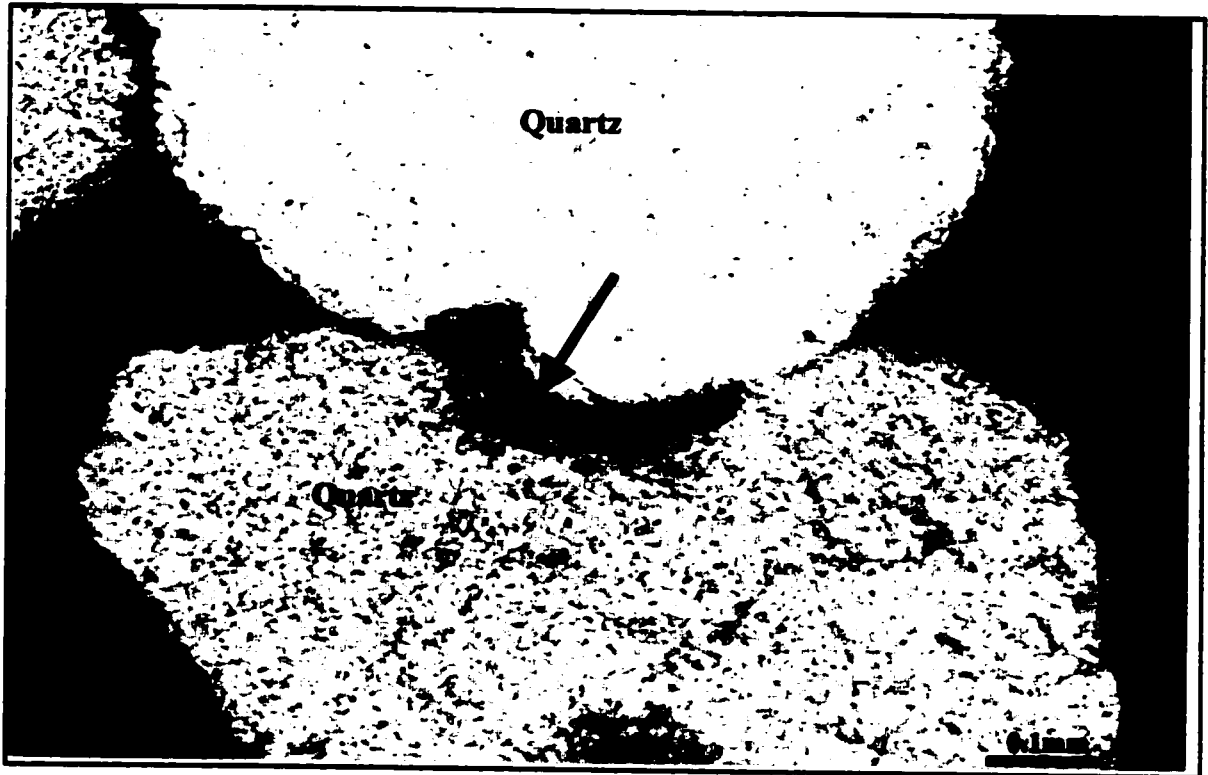


Figure 4-5: Suture contact between two quartz grains, sample # 6, Well B, depth 14143.9 feet, cross polarized light.

chert; 2) labile (soft) grains such as shale, siltstone and schist. Labile grains are subjected to plastic deformation under increasing overburden pressure. These grains may be squeezed in between rigid grains, lose their original grain boundaries and shape and enter into the adjacent pore spaces creating “pseudomatrix” (Figure 3-6 in Chapter 3).

4.2.2. Cementation

Cementation is the occlusion of intergranular volume of rocks by the precipitation of authigenic minerals. The importance of understanding the ways in which porosity and permeability are affected by cementation and clay mineral alteration is vital both for the search for recoverable oil reserves in sandstone and for the reservoir engineering after the oil has been found.

Several major phases of cementation has been recognized in the Jauf sandstone. These include an early calcite cementation phase followed by clay coatings (chlorite and illite), quartz overgrowths cementation and late calcite cementation. In addition, some minor pyrite cementation has occurred in early stage of burial.

The sequence of the above cementation events is determined by the mutual textural relationships of the cements with each other. The paragenetic sequence thus determined is shown in Figure 4-6.

4.2.2.1. Early Calcite Cementation

Early calcite cementation is one of the major diagenetic events in some of the Jauf Formation sandstones. Early calcite is documented as poikilotopic in nature which enclose several grains in a loosely pack arrangement (Figures 3-7 and 3-8 in Chapter 3). Some of the sandstones may contain greater than 20% poikilotopic calcite. The high percentage of calcite cement and apparent loose packing of framework grains suggest that

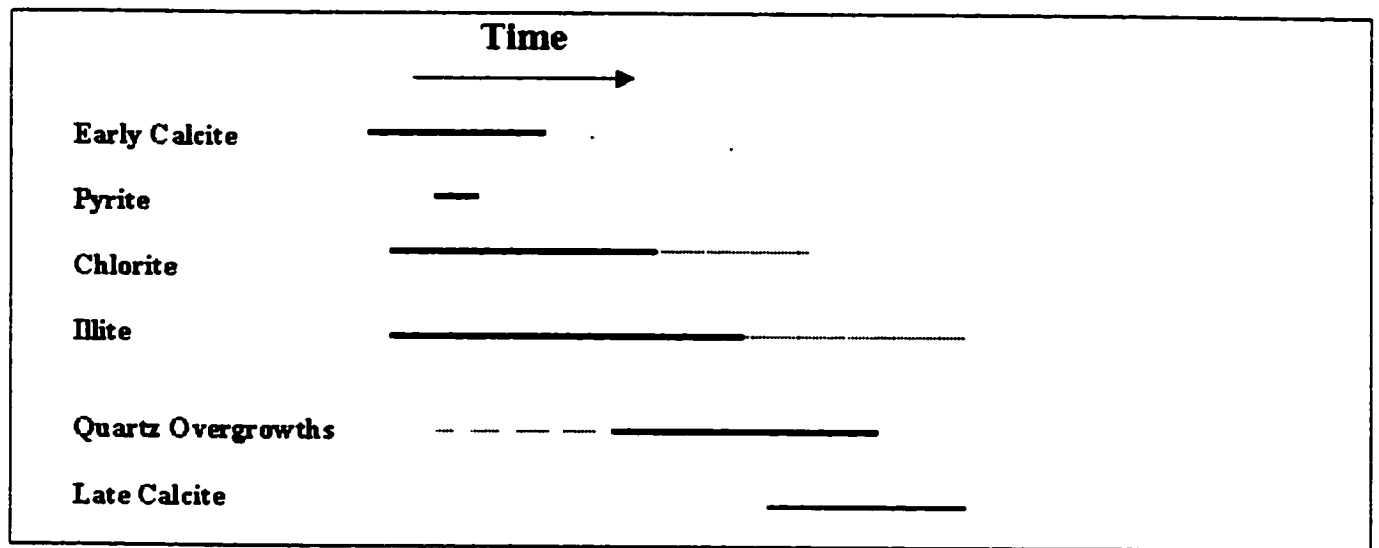


Figure 4-6: The paragenetic sequence of different types of cement present in the studied sandstones.

calcite cementation occurred very early in the burial history before compaction took place.

Generation of early poikilotopic calcite is probably related to total dissolution and reprecipitation of calcitic shell materials in the sandstones. It is interesting to note that there is no shell remains in the samples. Such calcitic shell debris may be deposited in a shelf or marginal marine environment.

4.2.2.2. Pyrite Cementation

Pyrite forms as an important early diagenetic mineral by reaction between iron-bearing minerals and H_2S produced from sulphate in the seawater by sulfate-reducing bacteria (Larsen and Chilingar, 1978). Pyrite occurs as a minor phase in only a few samples. This diagenetic event is not an important diagenetic event in the Jauf sandstone except for few samples.

4.2.2.3. Clay Cementation

Clay cementation is a common and important diagenetic event in the Jauf Formation Sandstones. These include illite cementation as well as chlorite cementation. Both are early-cement phase. Illite cement pre-dates quartz overgrowth cementation as evidenced by illite coating dust line between grain and quartz cement. Similarly, chlorite coating is also considered early cementation event (Figure 3-11 and 3-12 in Chapter 3). The pore-filling illites that bridge the pore throats are generated at the same time with illite coat. This is evidenced from the close association of both coatings and pore-bridging or pore-filling illite. Like illite, chlorite is also an early-coating cement in the Jauf sandstone. Occasionally, the chlorite coating is very thick preventing quartz overgrowths.

The different clay minerals (e.g., illite and chlorite) each grow under specific physical and chemical conditions. Authigenic clay minerals that form at shallow depth may alter to other clay minerals as the temperature increases and pore fluids change composition with burial. Authigenic clays develop subsequent to burial and include both new and regenerated forms.

4.2.2.4. Quartz Cementation

Quartz cementation is one of the most dominant diagenetic processes observed in the Jauf Formation Sandstone. There is a relationship between sandstone compositions to quartz cementation. Higher the percentage of quartz, the higher is the quartz cementation. This is probably because quartz cement is originated at least partially from quartz grains dissolution under pressure solution.

In the present study the quartz cement is usually found as overgrowths on the surface of detrital quartz grains. These overgrowths grow in crystallographic (and optical) continuity with the original quartz grains. The overgrowth cement grows outward from the original grain until it runs into cement growing outward from an adjacent grain.

Major factors that control quartz precipitation have been extensively studied (Pittman, 1979), and include such variables as temperature, framework grain composition, quartz grain surface area, solubility, and availability of fluids. In most sedimentary basins, it forms at temperatures between 60 and 145°C and many different sources of silica have been proposed. Various workers in numerous basins have proposed several silica sources for quartz cement including:

- Pressure solution (Blatt, 1979; Pittman, 1979; Bjorlykke and Egeberg, 1993): This is likely to be one of the major sources of quartz cement in the samples because there are many concavo-convex and sutured contacts.
- Volcanic activity in sea water (Pittman, 1979): This is unlikely to be one of the sources because of the absence of volcanic ash beds or evidence of other volcanic material associated with Jauf sandstone.
- Clay diagenesis (Hayes, 1979, Pittman, 1979, Cugatay et al. 1996): This could be a possible source of silica resulting from releasing the silica from clay diagenesis (e.g. smectite to illite) in the adjacent shale units.
- Dissolution of unstable silicates: This is a possible source of silica especially from the dissolution of feldspar grains.
- Dissolution of biogenic silica (opal-a) from diatoms, sponge spicules, and radiolaria, phytoliths, etc (Pittman, 1979): This is unlikely to be the source because there is no evidence of any biogenic silica in Jauf sandstone.

4.2.2.5. Late Calcite Cementation

Late calcite cementation is a common diagenetic event. Late phase cement that takes place as small patches scattered between the grains and as isolated calcite cement.

Sources of CaCO_3 for cement could be:

1. Pressure Solution: This is not possible source for calcite cement because of the absence of carbonate grains that are susceptible to compaction.
2. Dissolution of calcareous shells: local dissolution and reprecipitation of shell particles within the sandstone could also be an obvious source of late calcite cement. Though there is no evidence of shell remnants but the shells may have completely dissolved away.
3. Migration of water from adjacent limestone: This is unlikely to be one of the sources because of the absence of limestone units in the adjacent or nearby places of the studied formation.
4. Migration of water from adjacent shale: In the absence of limestone in the sandstone units, the source of calcite cement could be the transport of CaCO_3 nutrients from the underlying shale bed. The late cementation of calcite near the sand-shale boundary support the idea of shale derived water as a source of the cement.

4.3 Alteration and Replacement

Diagenetic alterations of minerals are common in Jauf sandstone. Biotite alters to chlorite, muscovite to illite and so on. Replacement of silicate minerals like quartz and feldspar by calcite is a very common diagenetic feature in Jauf sandstone. Calcite replaced by quartz grain is very common. A more advanced stage of replacement process removes almost all of the replaced grain leaving only a remnant grain. In Jauf sandstone, this can be evidenced by the presence of small irregular-shaped quartz grains within large calcite cement.

4.4. Dissolution and Secondary Porosity

Dissolution of rock components including grains and cement materials is a common diagenetic feature in the Jauf Formation Sandstones. Dissolution results from chemical interaction between the minerals and aqueous solutions that fill the interstitial pores. The rock components that are commonly seen to have dissolved in the studied samples include: 1) feldspar grains and 2) calcite cement. Calcite is soluble in acidic water; therefore calcite-cemented sandstones often have their cement partially dissolved. Dissolution of the calcite cement and feldspar grains has resulted in secondary porosity, which are seen extensively in the samples.

1. Dissolution of feldspar: the evidences of feldspar grain dissolution are very common in the Jauf Formation Sandstone. These include i) skeletal grains (honeycombed grains), which are commonly surrounded by a clay rim, which outlines the dissolved portion, and ii) oversized pores (Figure 4-7 and Figure 4-8).

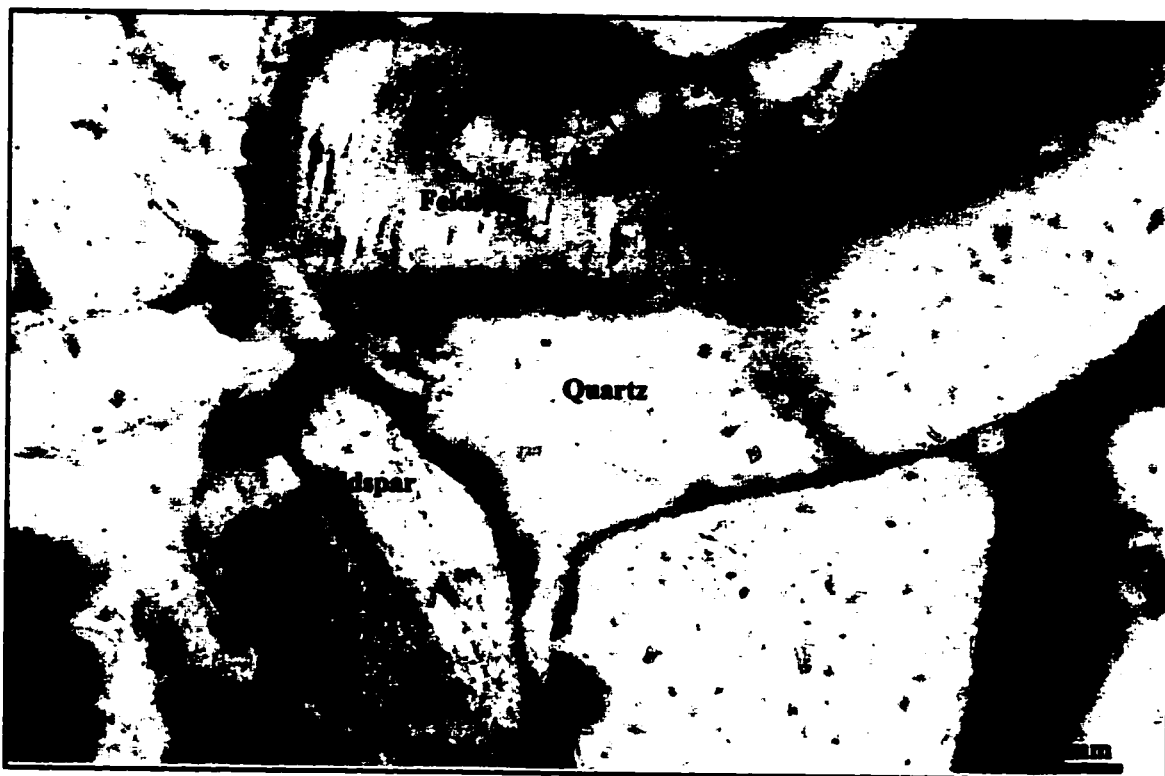


Figure 4-7: Partial dissolution of feldspar grains (arrows), sample #365, Well A, depth 14365, plane polarized light.



Figure 4-8: Another partial dissolution of feldspar grains, sample #365, Well A, depth 14365, plane polarized light.

2. Dissolution of calcite cement: the evidences of calcite cement dissolution include
 - i) inhomogeneity of packing, ii) partial dissolution and iv) elongate pore (All the criteria will be discussed later in the following section).

Secondary Porosity

The subject of secondary porosity was given little consideration in the published literature prior to 1975 (Schmidt and McDonald, 1979). Proshlyakov (1960) was probably the first author to convincingly report significant amounts of sandstone porosity that formed in the subsurface in the presence of saline formation water. Savkevic published the first detailed discussion in 1971 of the possible processes, which create secondary porosity in the subsurface (Schmidt and McDonald, 1979).

The occurrences of secondary porosity have been described in the literature by several workers (Pittman, 1979; Hayes, 1979). The porosity of many major hydrocarbon reservoirs is almost totally secondary (Hayes, 1979). The importance of secondary porosity in reservoir rocks was explained by Schmidt and McDonald (1979) and they were among the pioneers who discuss the secondary porosity. There have been extensive studies of secondary porosity in reservoirs including theories on their origin in deep reservoirs.

Extensive dissolution of feldspar grains and calcite cements has created large volume of secondary porosity in Jauf sandstone. The secondary porosity has clearly identified and observed in thin section studies in colored dyed impregnated samples. The secondary porosity in the studied samples were recognized on the basis of the following six petrographic criteria as outlined by Schmidt and McDonald in 1979 (Figure 4-9):

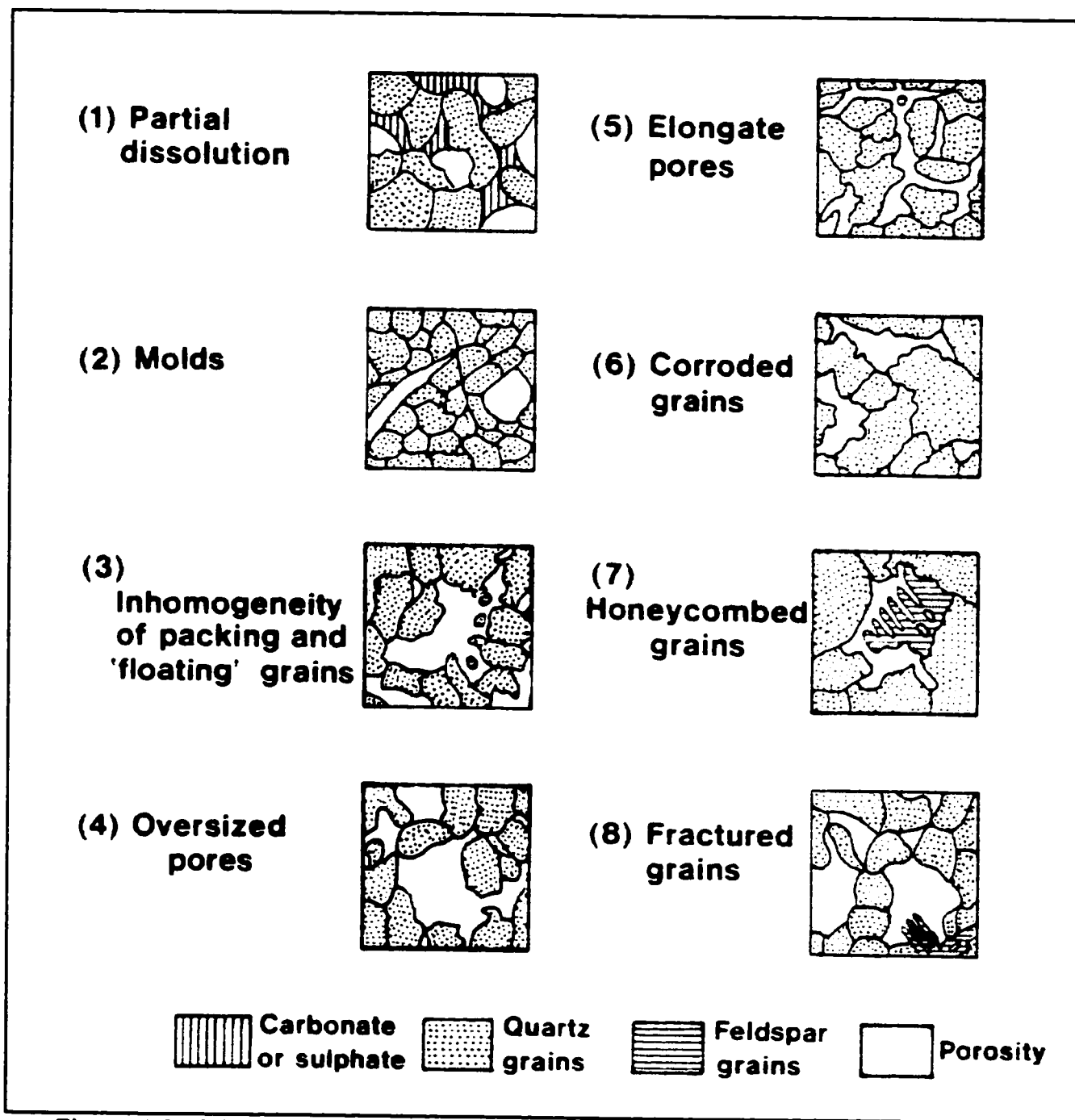


Figure 4-9: Criteria used for recognition of secondary porosity in the studied samples (After Schmidt and McDonald, 1979).

1. **Honeycomb grains or skeletal grains:** These are the most and obvious type of dissolution features observed in the studied samples. The partial dissolution of detrital grains creates honeycomb or skeletal shape. Most commonly detrital feldspar grains show skeletal or "honeycomb features (Figures 4-10 and 4-11).
2. **Inhomogeneity of packing:** This is a common criterion of large-scale dissolution. Sandstones displays marked packing inhomogeneity with areas of loosely packed grains and high intergranular porosity adjacent to areas of tightly packed grains. The dissolution of soluble calcite cement created the secondary porosity between the loosely packed grains. In the present study, an area of tightly packed grains with concavo-convex contact occur adjacent to an area where grains are loosely packed (Figure 4-12).
3. **Oversized Pores:** These have a significantly larger diameter than that of adjacent grains. In the studied sandstones, oversized pores occur as a result of feldspar grain dissolution leaving a larger than normal pore in the rock. In some samples, a rim around the oversized pore testifies the existence of grains that has been removed completely. (Figure 4-13).
4. **Partial dissolution:** It is the most conclusive criterion and it is also very common in the studied samples. Dissolution of soluble sedimentary and authigenic constituents is incomplete and patches of remnant material occur adjacent to pores. In the present study, calcite cements are completely or partially leached away generating extensive secondary porosity (Figure 4-14).



Figure 4-10: Honeycomb grain (arrow), sample # 394, Well A, depth 14394 feet, plane polarized light.



Figure 4-11: Close up photo of the previous Figure, plane polarized light.



Figure 4-12: Inhomogeneity of packing, sample # 373.6, Well A, depth 14373.6 feet, plane polarized light.

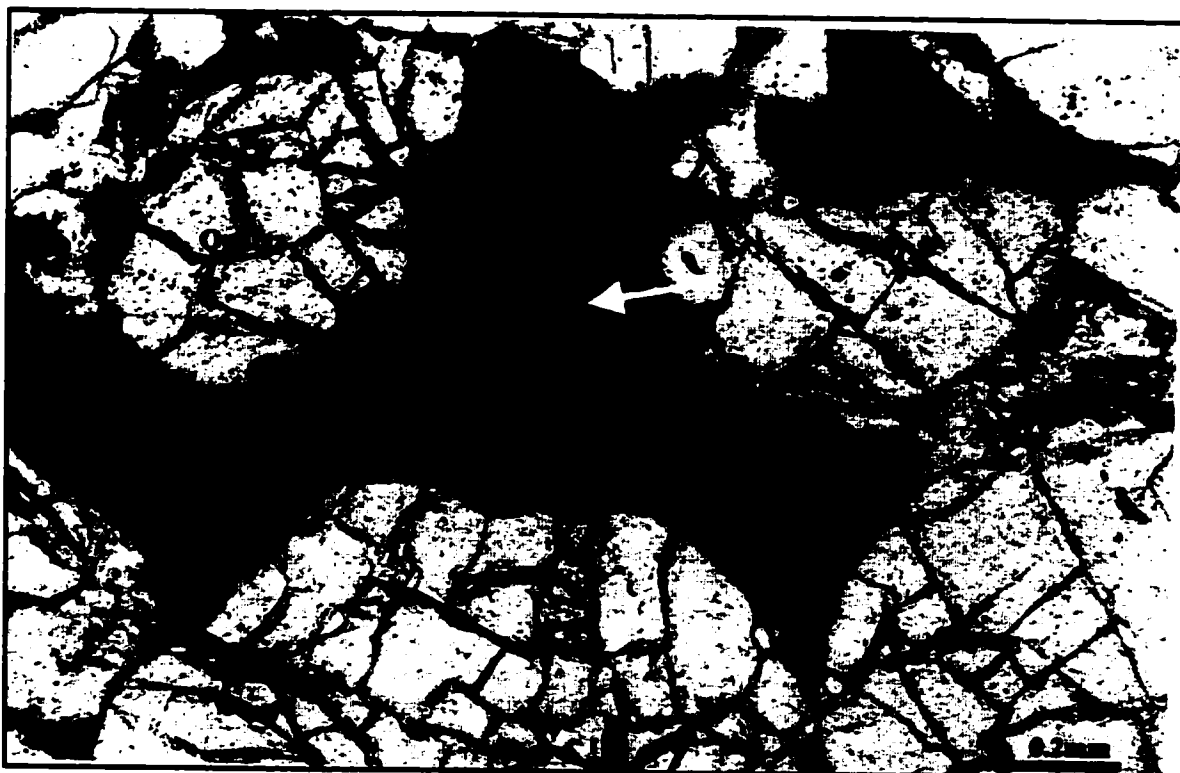


Figure 4-13: Oversized pores (arrow), sample # 523, Well A, depth 14523 feet, plane polarized light.



Figure 4-14: Partial dissolution of feldspar grains, sample #380, Well A, depth 14380feet, cross polarized light.

5. **Elongate Pores:** These indicate the presence of secondary porosity. If the replacive minerals are dissolved, the sandstone will exhibit a high incidence of elongate intergranular pores. In some studied samples, elongate pores are bounded by corroded grains (Figure 4-15).
6. **Corroded Grains:** These are useful criterion for secondary porosity recognition. These generally are associated with enlarged intergranular pores and result mainly from dissolution of soluble minerals that unevenly replaced the margins of sand grains. Corroded grains of quartz and feldspar are commonly observed in the studied samples (Figure 4-16).

Secondary Porosity Distribution in Well A and Well B

In Well A, secondary pores make up the major part of the pore system but primary pores are also important. The development of secondary pores appears to be more extensive. For example, sample from depth levels 14487, 14511 and 14538 feet have porosity values of 15%, 6% and 8%, respectively.

The degree of dissolution in the samples of Well B appears to be more extensive in the sandstone compared to Well A. Sandstone samples studied from depths of about 14035.9 feet (Sample 1), 14132 feet (Sample 4) and 14323.6 feet (Sample 11) show severe dissolution effect on its rock components and very large scale secondary porosity have been developed, i.e. thin section porosity of about 17% at 14035.9 feet, 15% at about 14132 feet and 12 % at about 14323.6 feet, respectively.

In both wells, most extensive secondary porosity has been generated by calcite cement dissolution. The evidences that very large-scale secondary pore developments are due to complete dissolution of feldspar and calcite cement include extensive

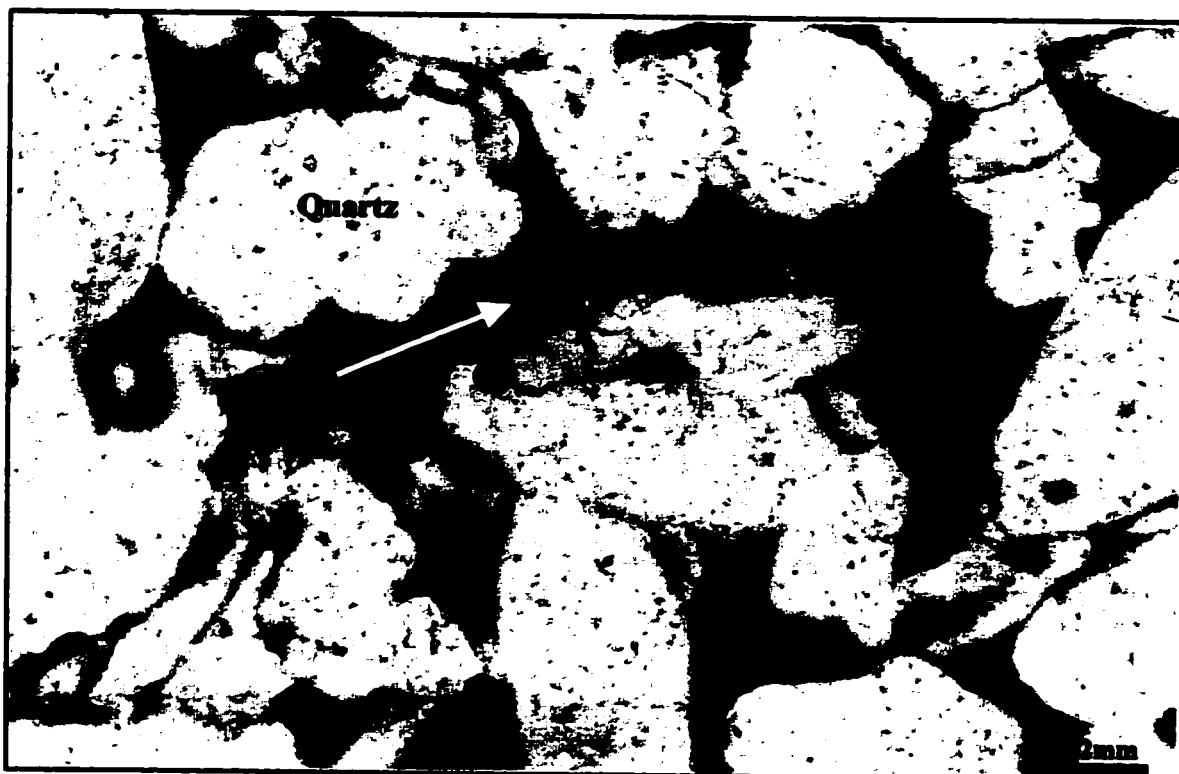


Figure 4-15: Elongate pore (arrow), sample # 365, Well A, depth 14365 feet, plane polarized light.



Figure 4-16: Corroded grain (arrows), Sample # 365, Well A, depth 14365 feet, plane polarized light.

honeycombed or skeletal grains and corroded grains (Figure 4-17). It can be observed that samples of high matrix contents have very low secondary porosity, if not completely absent.

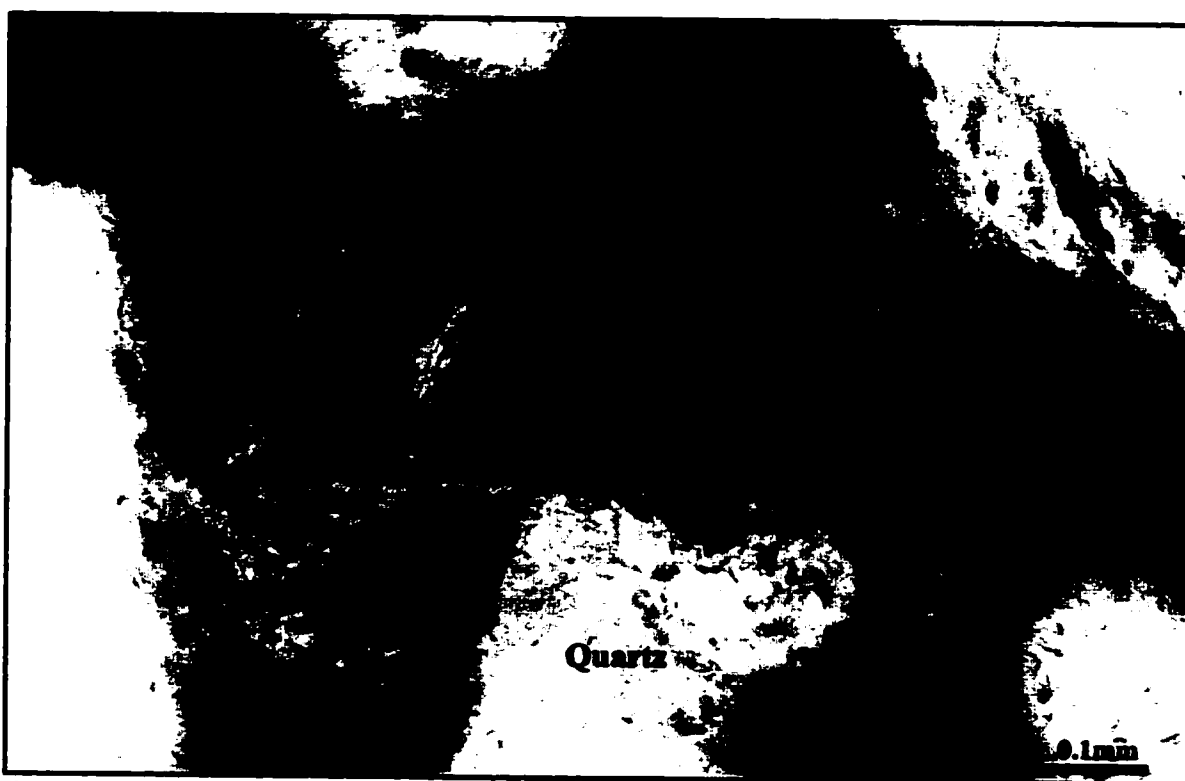


Figure 4-17: Photomicrograph showing secondary pores evidenced by skeletal grains (S), sample # 330, Well A, depth 14330 feet, plane polarized light.

4.4.1. Origin of Secondary Porosity

Many theories have been proposed for the origin of the secondary porosity. It is clear that the development of dissolution porosity needs a dissolving agent i.e. an acidic fluid and / or a fluid under saturated with respect to the minerals to be dissolved. The possible sources of pore fluid are as follows:

1. Meteoric-water penetration (Schmidt and McDonald, 1979)
2. Acidic fluids generate from CO₂ produced during the thermal maturation of organic matter (Schmidt and McDonald, 1979)
3. Carboxylic acids generated during the thermal maturation of organic matter (Surdam et al, 1984)
4. Acidic fluids generated by clay reactions in shales (Schmidt and McDonald, 1979)

A discussion on the role by the above mechanisms that might or might not have contributed to the development of secondary porosity in the studied Jauf Formation Sandstones reservoir is as follows.

Meteoric water can penetrate to considerable depth and its leaching capabilities depend on quantity of dissolved CO₂ and how much undersaturated it is with respect to the reactive minerals. It is unlikely in the studied samples that secondary porosity has been generated by meteoric water because the limestone of the younger formations will act as a barrier preventing the movement of the meteoric water from the surface to deeply buried Jauf Formation.

Acidic fluids generated from CO₂ may formed during the maturation of organic rich petroleum source rock in sedimentary sequence migrates out of shale into the sandstone reservoir may act as a dissolution agent (Schmidt and McDonald, 1979). It is suggested that underlying Qusaiba shales of Silurian age are the source of the hydrocarbon (Al-Hajri et al., 1999). Therefore, this mechanism for secondary porosity generation in the Jauf Formation Sandstones is the most possible mechanism.

From the above suggestion and discussion it might be concluded that none of the mechanisms convincingly explains extensive generation of secondary porosity in the studied Jauf sandstone reservoir. To conclude the discussion, statement may be referred to Giles and Marshall (1989) that secondary porosity in the subsurface is probably originated by some unknown process or processes, which have yet to be identified.

4.4.2. Importance of Secondary Porosity

In the present study, very large percentage of porosity in many samples is not primary porosity but is secondary porosity. Secondary sandstone porosity is of major geological significance. Its origin, stability, and distribution form important aspects of sandstone diagenesis. Also, the recognition of secondary porosity of is as important for production activities as it is for exploration.

Secondary porosity must be created before hydrocarbon migration through the sandstone to be the major reservoir porosity. The maturation of the hydrocarbon source rocks appears to be directly responsible for the generation of most secondary sandstone porosity. The majority of crude oil and natural gas in the present study has been generated in the source rocks after the intercalated sandstones had lost their primary porosity and after they had gained their secondary porosity. For this reason secondary sandstone porosity is a favorable habitat for crude oil and natural gas in present study.

CHAPTER 5

Discussion

The importance of diagenesis in controlling the quality of petroleum reservoir including its porosity-permeability has led geologists to pay attention on the processes of diagenesis. A petroleum reservoir has to have adequate porosity and permeability, which are essential for hydrocarbon production. Porosity is a key determinate of hydrocarbon volume, and permeability is a key factor in determining rate of production. Diagenesis is one of the most widely studied subjects in petroleum geology (Larsen and Chilingar, 1978; Blatt, 1979; Galloway, 1979; Hayes, 1979; Salem et al., 2000).

Diagenesis modifies the original porosity to the present day porosity of the potential reservoir (Hayes, 1979). Porosity may be reduced or enhanced by diagenetic processes. Thus, the ability of a reservoir to produce hydrocarbon is essentially related to its diagenetic events (Galloway, 1979). McDonald and Surdam (1984) provide a variety of papers that indicate the scope and importance of diagenesis. The processes in diagenesis include compaction, cementation, replacement and dissolution (Larsen and Chilingar, 1978).

Compaction is the reduction of bulk volume, which is induced by the overburden stress. Compaction is the first major factors that affect the sandstone reservoirs as it is buried under overburden sediment. The degree of compaction increases proportionally with the amount of ductile mica and soft grains like schist fragments and mudstone clasts (Blatt, 1979). As a result of compaction, original porosity may be reduced by plastic deformation of the ductile grains and as a result diagenetic fine-grained pseudomatrix is created (Hayes, 1974). Also, there is an inverse relationship between the compaction of the sandstone and its porosity (Blatt, 1979).

Cementation is the occlusion of intergranular volume by the precipitation of authigenic minerals. Cementation always results in the reduction of bulk volume (Blatt, 1979; Hayes, 1979; Larsen and Chilingar, 1978). The most common cements in sandstones are quartz, calcite, clay minerals, and hematite, although other minerals like anhydrite, pyrite, gypsum, and barite can also form cements under special geologic conditions (Worden et al., 2000). Cement may be early or late occurrence. The generation of cements depends on availability of elements in the pore water. This in term is dependent on composition of sandstone, fluid flow, sediment texture and composition of rocks above and below the reservoir (Hayes, 1979).

Dissolution results from chemical interaction between the minerals and aqueous solutions that fill the interstitial pores (Bjorkum, 1996). Secondary porosity may form due to the dissolution of feldspar, lithic grains, and carbonate minerals occurring as cement (Schmidt and McDonald, 1979)

Petrography of Jauf sandstone was done in detail and has been discussed in Chapter 3. The Jauf sandstone are dominantly composed of quartz with little to trace

amount of feldspar and lithic grains. The sandstones contain an average of 77% quartz, 2% feldspar and 0.1% lithic fragments. The sandstones are classified as quartz arenite and quartz wacke depending on matrix content (Figure 3-2 in Chapter 3).

Diagenesis, as recognized in the sandstone of Jauf Formation, is the result of several processes including compaction, cementation, replacement and dissolution of framework grains and cements. Since these processes overlap in time, it is difficult or impossible to define specific temporal relationships of diagenetic events precisely. On the basis of petrographic evidences especially mutual textural relationships, the sequence of major diagenetic events are suggested as follows (Figure 5-1):

1. Compaction
2. Early calcite cementation
3. Chlorite and illite coating of grains
4. Replacement of calcite cement.
5. Pressure Solution evidenced by concavo-convex contact.
6. Quartz overgrowths.
7. Late calcite cementation
8. Dissolution of framework grains.

In the present study, the degree of compaction is evidenced by point, long, concavo-convex and sutured contacts and by squashing of soft lithic grains (See Chapter 4). Compaction generally reduces pore space. Extensive sutured contact indicates high degree of compaction in the samples, which has significantly, reduces original porosity. However, because of very low to trace amount of lithic grains, plastic flow and generation

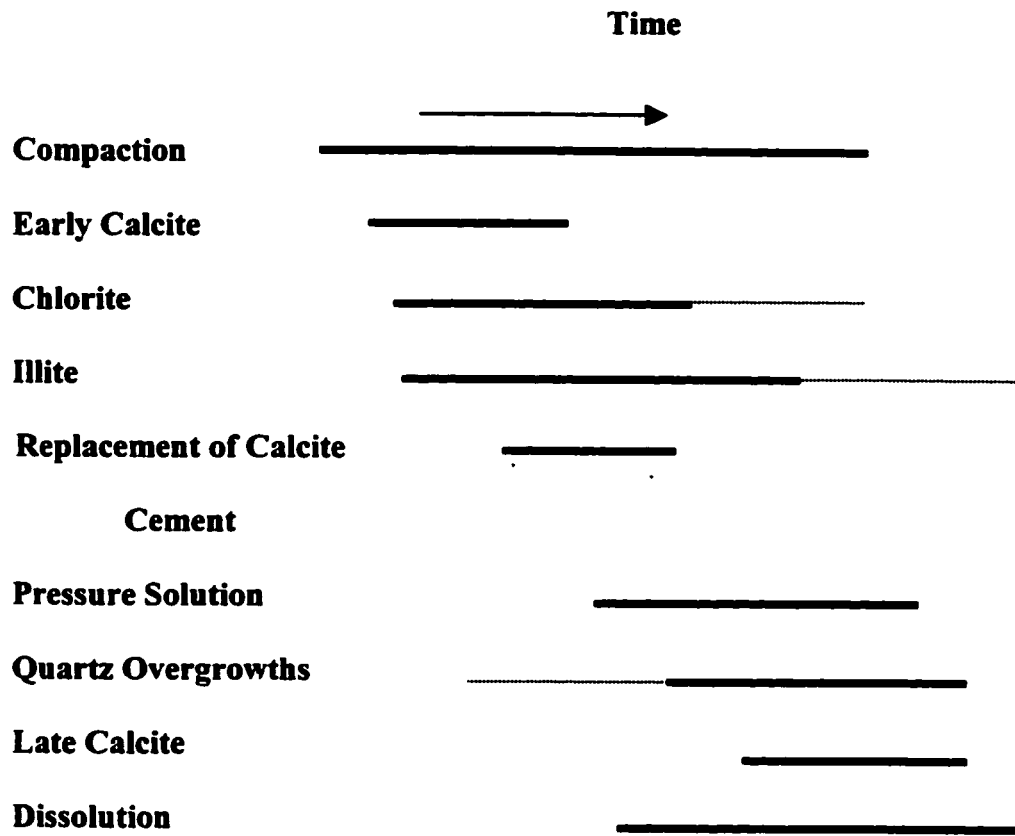


Figure 5-1: Paragenetic sequence of diagenetic events in the Jauf sandstone.

of pseudomatrix could not take place in Jauf sandstone and it did not play a major role in reducing porosity.

Extensive early cementation in the Jauf Formation has reduced reservoir quality. Three types of early cementation identified in the Jauf Formation sandstone samples include early pyrite, calcite, and clay coats.

Precipitation of the authigenic minerals began as early framboidal pyrite started to precipitate during sulfate reduction followed by the precipitation of calcite. The euhedral crystal faces of pyrite testify its earlier origin than calcite. Pyrite cements comprise 1% to 4% of the rock components and the amount of pyrite does not affect the reservoir quality in the sandstones.

Early calcite cements have occupied most of the pore spaces in some samples resulting in reducing the primary porosity. Early formation of calcite is indicated by the loose grain packing of calcite-cemented sandstones. Despite the fact that calcite has reduced the porosity, primary porosity has preserved due to the presence of scattered patches of calcite cement which prevent the compaction to play its role.

In the present study, it has been observed that authigenic, chlorite rims on quartz sand grains inhibited pressure solution though there are some quartz overgrowths. This is due to the occurrences of thin and discontinuous chlorite coating, which can not prevent quartz overgrowth. Also, the development of early grain coating chlorite helps to retain initial porosity and permeability at depths by retarding the development of quartz overgrowths. This preservation of porosity will allow pore fluids to attack feldspar grains and produce some secondary porosity, which in turn was partially clogged by late calcite

pore filling. In some samples, chlorite did not uniformly inhibit quartz cements because the chloritic grain coatings are discontinuous or absent in areas of significant porosity.

Clay minerals possess a high surface area to volume ratio. Consequently, clay minerals tend to react readily and rapidly with fluids introduced into a sedimentary rock. They react more rapidly and more vigorously than detrital grains of quartz, feldspar, etc., because of their smaller size and larger surface area. Authigenic chlorite has an economic significance because its coatings around the grains inhibit quartz cementation and prevent the destruction of reservoir properties (Imam, 1986). The presence of widely distributed diagenetic chlorite in the first diagenetic stage reduced the available area of free quartz surfaces for nucleation and growth of diagenetic quartz overgrowth cement. Imam (1986) noted that thick coatings of chlorite would allow only minute incipient growth of secondary quartz. This relationship has also been observed in Jauf sandstone.

The main engineering problem of chlorite cement is the acid sensitivity. The diagenetic chlorite in first interval of Well A is iron rich and if exposed to acid treatment, will dissolve and the iron liberated during dissolution will reprecipitate as a gelatinous ferric hydroxide as $\text{Fe}(\text{OH})_3$ when the acid has spent. This ferric hydroxide has a large crystal size. It is generally bigger than the pore throats and cannot pass through them. This possible iron precipitation problem can be avoided if an oxygen scavenger and iron-chelating agent are added to the acid and care is taken to recover all the acid introduced into the well.

The chlorite coatings are believed to be formed by the breakdown of ferromagnesium aluminosilicates and iron oxides during early burial (Galloway, 1979).

Sandstone samples in most of the intervals are characterized by illite pore coatings, which have a hairy-like structure. These illite hairs create large volumes of microporosity. This microporosity can bind water to the quartz grains and result in high irreducible water saturations. In the present study, hairy illite did not reduce the porosity too much but reduce the permeability dramatically. If these "hairy" illites are not dissolved prior to production, they may break during production, migrate to the pore-throats, and act as a check valve.

XRD data suggest that illite in the Jauf sandstone contain some expandable smectite interlayers and can swell to a small amount. Illite is dispersive clay and would be expected to disperse and migrate during production.

Quartz cement in siliciclastic sequences is commonly a major diagenetic phase that affects hydrocarbon reservoir quality. It is a major cause of porosity loss in many petroleum reservoirs in both moderately to deeply buried sandstones by narrowing pore throats and reducing pore size (Imam, 1986). In the present study, SEM photographs suggest that some quartz overgrowths continued to grow after chlorite precipitation. Quartz overgrowths have reduced the pore volume in the samples. These samples have high percentage of quartz cements and relatively low matrix content (As, for example, in samples 519 (Well A) and 9 (Well B)).

Subsequent water migration from nearby shale units might result in local precipitation of late calcite cement as small patches scattered between the grains and as isolated calcite cement which overlaps the previous authigenic minerals. This late calcite cement has not a profound effect on the samples because the invasion of acidic fluids

escaped from nearby shale units have resulted in partial dissolution of calcite cements and feldspar grains.

Incomplete dissolution of feldspars occurs quite commonly, but the material seems to have been reprecipitated very locally often in the form of clay minerals. Partially dissolved K-feldspar grains and pores, which outline feldspar grain shapes suggest that part of the secondary porosity resulted from feldspar dissolution.

The development of secondary porosity has greatly enhanced the reservoir quality of the Jauf sandstone. More than one mechanism for the development of secondary porosity is apparent. The invasion of acidic fluids released from organic matter maturation in the adjacent shale units has played a significant part upon the enhancement of the reservoir quality. Secondary porosity developed by dissolution in carbonate-cements (especially calcite) has greatly enhanced the reservoir quality of the Jauf sandstone.

The development of secondary porosity is directly related to the dissolution of feldspar grains and cements. It appears that remnant primary porosity is very important in the evolution of secondary porosity because some of the original pore was required for movement of pore fluids in order to initiate various dissolution reactions.

CONCLUSIONS

This research on the Jauf sandstone illustrates various diagenetic changes and their effect on reservoir properties. These may be summarized as follows:

1. Three major processes have dominated the diagenetic events: compaction, cementation and dissolution. All the three processes have affected the reservoir properties significantly.
2. Degree of compaction in Jauf sandstone is evidenced from different kind of grain contacts. Common concavo-convex and sutured contacts indicate high degree of compaction; long contact testifies moderate degree of compaction. Point contact is uncommon and actually represents remnant point left after dissolution of material remove part of original contacts.
3. The major authigenic cements present are calcite, chlorite, illite, and quartz. Cementation in the studied samples has both negative and positive effects on reservoir quality.
4. Early calcite cement is one of the major diagenetic cements in some of the Jauf Formation sandstones. This type of cement occupies most of the pore area and it has prevented the sandstones from the compaction. When these early calcite are present, porosity is severely reduced. On the other hand, when the early calcite suffers later dissolution, loose packing and good reservoir porosity is generated.
5. The clay mineralogy has important control on the porosity and permeability of the Jauf Formation. The grain coating illites in the studied samples mostly have hairy growth structure. Illite coatings generally develop microporosity at the expense of macroporosity. Hairy illite bridging between grains strongly reduce permeability.

6. The grain coating chlorites are seen as delicate platelet crystals standing more or less perpendicular to the grain surfaces. Also, chlorites are seen as rosettes pore filling. Thick chlorite coating prevented quartz overgrowths in some of the samples, retaining porosity at depths.
7. Authigenic quartz contributes to porosity reduction. Quartz cement has been promoted by pressure solution. Higher quartz cements are formed in more quartz rich sandstones.
8. Despite the loss of original primary porosity, subsequent dissolution event has led to the major development of secondary porosity in the Jauf Sandstone. In many sandstone samples secondary porosity is the main porosity type. The extensive development of secondary porosity in the deep gas reservoir has important implication in petroleum exploration in the country.

REFERENCES

- Al-Duaiji, AbdulAziz, 1991, Reservoir Characteristics of the Devonian Jauf Formation in Shedgum Area, Saudi Arabia. Master thesis, 132p.
- Al-Hajri, S. A., J. Filatoff, L. E. Wender and A. K. Norton, 1999, Stratigraphy and Operational Palynology of the Devonian System in Saudi Arabia. *GeoArabia*, v.4, p.53-68.
- Al-Laboun, A. A., 1993, Lexicon of the Paleozoic and Lower Mesozoic of Saudi Arabia. Part 1, lithostratigraphic units: Nomenclature review. Al-Hudhud publisher, 511p.
- Bjorlykke, K., and P. K. Egeberg, 1993, Quartz cementation in sedimentary basins: *Am. Assc. Petrol. Geol. Bulletin*, 77, 1538-1548.
- Bjorkum, P. A., 1996, How important is pressure in causing dissolution of quartz in sandstones? : *Journal of Sedimentary Research*, v.66, p.147-154.
- Blatt, Harvey, 1979, Diagenetic Processes in Sandstones: SEPM special Publication, v.26, p.141-157.
- Bramkamp, R. A., L. Ramirez, M. Steineke and W. Reiss, 1963, Geologic map of the Jawf-Sakakah quadrangle, Kingdom of Saudi Arabia. U.S. Geological Survey, Misc. Geol. Investig. Map I-201 A, Washington.
- Cagatay, M. N., Saner, S., Al-Saiyed, I., and Carrigan, W. J., 1996, Diagenesis of the Safaniya sandstone Member (mid-Cretaceous) in Saudi Arabia, *Sedimentary Geology*, v. 105, p. 221-239.
- Eslinger, E. and Pevear, D., 1988, Clay Minerals for Petroleum Geologists and Engineers: Society of Economic Paleontologists and Mineralogists.
- Galehouse, J. S., 1971, Sedimentation analysis, in: R. E. Carver (ed.), *Procedures in sedimentary Petrology*, Wiley Inter Science, New York, p.69-94.
- Galloway, W. E., 1979, Diagenetic control of reservoir quality in arc-derived sandstone: Implications for petroleum Exploration: SEPM Special Publication, v.26, p.251-262.
- Hayes, John B., 1979, Sandstone Diagenesis-The Hole Truth: SEPM Special Publication, v.26, p.127-139.

- Houseknecht, D. W., 1987, Assessing the relative importance of compaction processes and cementation to reduction of porosity in sandstones, *Am. Assoc. Petrol. Geol. Bulletin*, 71, 633-642.
- Imam, B., 1986, Scanning electron microscopy study of the quartz overgrowths within Neogene sandstones of Bengal basin, Bangladesh, *Journal Geological Society of India*, v. 28, p. 407-413.
- Larsen G. and Chililngar G., 1967: *Diagenesis in Sediments*, Elsevier Amsterdam, 551p.
- McDonald, D.A., and Surdam, R.C., 1984, *Clastic Diagenesis: Amer. Assoc. Petrol. Geol. Memoir 37*, p. 277-286.
- Pettijohn, F., Potter, P. and Siever, R., 1987: *Sand and sandstone*, Springer-Verlag, New York 533p.
- Pittman, Edward, 1979, Porosity, Diagenesis and Productive Capability of Sandstone Reservoir: *SEPM special Publication*, v.26, p.159-173.
- Powers, R. W., R. M. Ramirez, et al, 1966, *Geology of the Arabian Peninsula - Sedimentary Geology of Saudi Arabia*. U. S. Geological Survey, Professional Paper 560-D., Washington, p.1-147
- Salem, A., Morad, S., Mato, L. and Al-Aasm, I., 2000, Diagenesis and reservoir-quality evaluation of fluvial sandstones during progressive burial and uplift: evidence from the upper Jurassic Boipeba member, Reconcavo basin, northeastern Brazil: *AAPG Bulletin*, v. 84, p. 1015-1040.
- Saner, Saleh, 1998. *Geological Description of Jauf Formation cores in Well HWYH-206*, Research institute, KFUPM.
- Schmidt, Volkmar and McDonald, David A., 1979, The Role of Secondary Porosity in the Course of Sandstone Diagenesis: *SEPM Special Publication*, v.26, p.175-207.
- Schmidt, Volkmar and McDonald, David A., 1979, Texture and Recognition of Secondary Porosity in Sandstones: *SEPM Special Publication*, v.26, p.209-225.
- Schmidt, Volkmar and McDonald, David A., 1980, Secondary Reservoir Porosity in the Course of Sandstone Diagenesis: *AAPG Short course Series #12*, p.1-125.
- Surdam, R.C, Boese, S.W., and Crossey, L.J., 1984, The chemistry of secondary porosity, *in* MacDonald, D. A., and Surdam, R.C., eds., *Clastic Diagenesis: American Association of Petroleum Geologists Memoir 37*, p. 127-149.
- Tucker, M.E. 1991 (second edition) *Sedimentary Petrology*, Blackwells scientific publications, 260p.

Wender, L. E., J. W. Bryant, M. F. Dickens, A. S. Neville and A. M. Al-Moqbel 1998. Paleozoic (Pre-Khuff) Hydrocarbon Geology of the Ghawar Area, Eastern Saudi Arabia. *GeoArabia*, v.3, p.273-302.

Wilson, M.D. and E.D. Pittman, 1977, Authigenic clays in sandstones: recognition and influence of reservoir properties and paleoenvironmental analysis: *Journal of Sedimentary Petrology*, v. 47, p. 3-31.

Worden, R. H., Mayall, M. and Evans, I. J., 2000, The effect of ductile-lithic sand grains and quartz cement on porosity and permeability in Oligocene and lower Miocene clastics, South China Sea: prediction of reservoir quality: *American Association of Petroleum Geologists Memoir* v.84, no. 3, p. 345-359.